

**DEVELOPMENT AND INVESTIGATION OF
THE EFFICACY OF LAPATINIB LOADED
TARGETED DRUG DELIVERY
NANOSYSTEM FOR BREAST CANCER
TREATMENT**

**A Thesis Submitted to
the Graduate School of
İzmir Institute of Technology
in Partial Fulfillment of the Requirements for the Degree of**

MASTER OF SCIENCE

in Chemistry

**by
Ezgi ASLAN**

**July 2024
İZMİR**

We approve the thesis of **Ezgi ASLAN**

Examining Committee Members:

Prof. Dr. Gülşah ŞANLI MOHAMED

Department of Chemistry, Izmir Institute of Technology

Prof. Dr. Ali ÇAĞIR

Department of Chemistry, Izmir Institute of Technology

Prof. Dr. Şenay ŞANLIER

Department of Biochemistry, Ege University

12 July 2024

Prof. Dr. Gülşah ŞANLI MOHAMED

Supervisor, Department of Chemistry, Izmir
Institute of Technology

Prof. Dr. Gülşah ŞANLI MOHAMED

Head of the Department of Chemistry

Prof. Dr. Mehtap EANES

Dean of the Graduate School

ACKNOWLEDGMENTS

I would like to express my sincere gratitude to my supervisor, Prof. Dr. Gülşah ŞANLI MOHAMED, for her invaluable guidance and support throughout my master's program. Her constant encouragement and being with me was very important and valuable to me. This helped me to successfully complete my experiments and thesis.

I would like to express my deepest gratitude to Prof. Dr. Ali ÇAĞIR and Prof. Dr. Şenay ŞANLIER for being part of my thesis committee.

I would like to thank each and every member of the GSM Laboratory team, Derya METE and İbrahim Hanif NAZLI.

I would especially like to thank Sinem ŞAHİNOĞLU, who enlightened my path with her support and knowledge, for her contributions to the successful completion of this thesis. I am very grateful to her for always showing me my own light, comforting me with her professionalism, and igniting my desire to continue and succeed.

I would like to thank IZTECH - Integrated Research Centers (IZTECH IRC); Center for Material Research (MAM), Biotechnology and Bioengineering Application and Research Center (BIOMER), and Wind Energy Meteorology and Environmental Application and Research Center (RUZMER) specialists for their help and support during my analysis.

I am deeply thankful to my family and best friends for their love and support during this process. Without their encouragement and motivation, I would not have been able to complete this journey.

Finally, I would like to state that I received support within the scope of TUBITAK-BIDEB Scientist Support Programs Directorate 2210-A National Graduate (MSc/MA) Scholarship Program, which is a reward given for success. I would like to thank TUBITAK for this support.

ABSTRACT

DEVELOPMENT AND INVESTIGATION OF THE EFFICACY OF LAPATINIB LOADED TARGETED DRUG DELIVERY NANOSYSTEM FOR BREAST CANCER TREATMENT

Due to the limitations and side effects of current treatment methods, targeted drug delivery systems using chemotherapeutics in the treatment of breast cancer have been widely investigated in recent years.

The synthesis, characterization and biocompatibility studies of the cancer drug lapatinib (LAP) encapsulated in zeolitic imidazolate framework-8 (ZIF-8), one of the metal organic frameworks (MOF), were carried out and its cytotoxic effects were revealed in two different cancer cell lines. LAP encapsulated into ZIF-8 (LAP@ZIF-8) was synthesized with encapsulation efficiency of 72.42% and drug loading of 6.55%. Various characterization analyzes were used and evaluated to determine the particle size and images of LAP@ZIF-8, its hydrodynamic diameter, zeta potential, chemical content, functional groups/chemical bonds, crystallinity/structure, and finally its thermal properties. The release ability at pH 5.5 compared to pH 7.4 showed the controlled release of the drug in the acidic tumor microenvironment. While the serum protein binding study result showed that LAP@ZIF-8 was biocompatible, the hemolysis experiment showed that it was hemocompatible, harmless to fresh blood, and could be used in biologically practical applications. The IC_{50} value of LAP@ZIF-8 in SKBR-3 cell line was 9.38, 3.81, and 1.20 $\mu\text{g/mL}$ after 24 h, 48 h, and 72 h incubation time, respectively. The IC_{50} value of LAP@ZIF-8 in MCF-7 cell line was 22.05, 16.13, and 9.14 $\mu\text{g/mL}$ after 24 h, 48 h, and 72 h incubation time, respectively.

The developed LAP@ZIF-8 nanoparticle system is thought to have the potential to achieve optimal therapeutic effect for use in breast cancer treatment.

ÖZET

MEME KANSERİ TEDAVİSİNE YÖNELİK LAPATİNİB YÜKLÜ HEDEFLİ İLAÇ TAŞIYICI NANOSİSTEMİN GELİŞTİRİLMESİ VE ETKİNLİĞİNİN ARAŞTIRILMASI

Mevcut tedavi yöntemlerinin sınırlamaları ve yan etkilerinden dolayı, meme kanseri tedavisinde kemoterapötiklerin kullanıldığı hedefe yönelik ilaç taşıyıcı sistemler son yıllarda geniş çapta araştırılmaktadır.

Metal organik çerçevelerden (MOF) biri olan zeolitik imidazolat çerçeve-8 (ZIF-8) içinde kapsüllenen kanser ilacı lapatinibin (LAP) sentezi, karakterizasyonu, biyoyumluluk çalışmaları yapıldı ve sitotoksik etkileri iki farklı kanser hücre hattında ortaya çıkarıldı. ZIF-8 içerisine kapsüllenen LAP (LAP@ZIF-8), %72,42 kapsülleme verimliliği ve %6,55 ilaç yüklemesi ile sentezlendi. LAP@ZIF-8'in parçacık boyutunu ve görüntülerini, hidrodinamik çapını, zeta potansiyelini, kimyasal içeriğini, fonksiyonel grupları/kimyasal bağları, kristalliğini/yapısını ve son olarak termal özelliklerini belirlemek için çeşitli karakterizasyon analizleri kullanılmış ve değerlendirilmiştir. pH 7.4'e kıyasla pH 5.5'teki salım yeteneği, ilacın asidik tümör mikro ortamında kontrollü salımını gösterdi. Serum protein bağlama çalışması sonucu LAP@ZIF-8'in biyoyumlu olduğunu gösterirken, hemoliz deneyi hemouyumlu olduğunu, taze kana zararsız olduğunu ve biyolojik olarak pratik uygulamalarda kullanılabileceğini gösterdi. SKBR-3 hücre hattındaki LAP@ZIF-8'in IC₅₀ değeri, 24 saat, 48 saat ve 72 saatlik inkübasyon süresinden sonra sırasıyla 9,38, 3,81 ve 1,20 µg/mL idi. MCF-7 hücre hattındaki LAP@ZIF-8'in IC₅₀ değeri, 24 saat, 48 saat ve 72 saatlik inkübasyon süresinden sonra sırasıyla 22,05, 16,13 ve 9,14 µg/mL idi.

Geliştirilen LAP@ZIF-8 nanopartikül sisteminin meme kanseri tedavisinde kullanım için optimal terapötik etkiyi elde etme potansiyeline sahip olduğu düşünülmektedir.

*This thesis is dedicated to my dear mother Gülsün ALKAN,
and
To all female patients fighting with breast cancer...*

TABLE OF CONTENTS

LIST OF FIGURES	ix
LIST OF TABLES.....	x
LIST OF SYMBOLS	xi
LIST OF ABBREVIATIONS	xii
CHAPTER 1. INTRODUCTION	1
1.1. Cancer	1
1.1.1. Breast Cancer.....	2
1.1.1.1. HER2-Positive Breast Cancer.....	4
1.2. Tyrosine Kinase Inhibitors (TKIs)	5
1.2.1. Lapatinib (LAP)	6
1.3. Targeted Drug Delivery System and Nanoparticles	8
1.4. Metal Organic Frameworks (MOFs)	13
1.4.1. Zeolitic Imidazolate Framework (ZIF)	17
1.4.1.1. ZIF-8	19
1.5. Encapsulation of Lapatinib in Literature	23
1.6. Encapsulation of Lapatinib into ZIF-8 (LAP@ZIF-8)	25
1.7. The Aim of This Thesis	26
CHAPTER 2. MATERIALS AND METHODS.....	27
2.1. Materials	27
2.2. Methods.....	27
2.2.1. Synthesis of ZIF-8 and LAP@ZIF-8	27
2.2.1.1. The Synthesis Yield of ZIF-8.....	28
2.2.2. Characterization of ZIF-8 and LAP@ZIF-8	28
2.2.2.1. Encapsulation Efficiency and Drug Loading	28
2.2.2.2. Structural Analysis	30
2.2.2.3. Drug Release Study.....	32
2.2.2.4. Biocompatibility Assays	33
2.2.2.4.1. Serum Protein Binding	33

2.2.2.2.2. Hemocompatibility (Hemolysis)	35
2.2.3. <i>In Vitro</i> Investigation of Cancer Activity	35
2.2.3.1. Cell Lines and Culture Medias	35
2.2.3.2. Passaging (Subculturing) Cells.....	37
2.2.3.3. Freezing and Thawing Cells	37
2.2.3.4. Cell Counting and Checking Their Viability	38
2.2.3.5. Determination of Cell Viability by MTT Assay.....	38
2.2.4. Statistical Analysis.....	39
CHAPTER 3. RESULTS AND DISCUSSION	40
3.1. Synthesis of ZIF-8, LAP@ZIF-8 and Yield of ZIF-8	40
3.2. Characterization of ZIF-8 and LAP@ZIF-8.....	40
3.2.1. Encapsulation Efficiency and Drug Loading.....	40
3.2.2. Structural Analysis.....	41
3.2.3. Drug Release Study	50
3.2.4. Biocompatibility Assays.....	52
3.2.4.1. Serum Protein Binding	52
3.2.4.2. Hemocompatibility (Hemolysis)	53
3.3. <i>In Vitro</i> Investigation of Cancer Activity	55
3.3.1. Coefficient of Variation for Cell Viability	59
CHAPTER 4. CONCLUSION.....	60
REFERENCES	62
APPENDICES	
APPENDIX A. SOLUTIONS.....	88
APPENDIX B. ENCAPSULATION EFFICIENCY AND DRUG LOADING.....	89

LIST OF FIGURES

<u>Figure</u>	<u>Page</u>
Figure 1.1. The chemical structure of lapatinib.....	6
Figure 1.2. Passive and active targeting of nanoparticles.....	10
Figure 1.3. The stick diagram and as a tiling of ZIF-8. The largest cage in ZIF-8.....	20
Figure 1.4. Applications of ZIF-8 as nanocarrier in drug delivery.....	21
Figure 2.1. The calibration curve of lapatinib.....	29
Figure 2.2. Schematic representation of the dialysis membrane method.....	32
Figure 2.3. BSA standard calibration curve.....	34
Figure 2.4. Morphological appearance of SKBR-3 cells.....	36
Figure 2.5. Morphological appearance of MCF-7 cells.....	36
Figure 3.1. SEM images of (a) ZIF-8 and (b) LAP@ZIF-8.....	41
Figure 3.2. DLS measurements of (a) ZIF-8 and (b) LAP@ZIF-8.....	42
Figure 3.3. Zeta potentials of ZIF-8 and LAP@ZIF-8.....	43
Figure 3.4. EDX analysis of ZIF-8 and LAP@ZIF-8.....	44
Figure 3.5. FTIR spectra of LAP, ZIF-8 and LAP@ZIF-8.....	46
Figure 3.6. XRD of LAP, ZIF-8 and LAP@ZIF-8.....	47
Figure 3.7. TGA curves of LAP, ZIF-8 and LAP@ZIF-8.....	48
Figure 3.8. Drug release profile of LAP@ZIF-8 in media of different pH for (a) 60 min and (b) 96 h.....	51
Figure 3.9. Hemolysis percentages of LAP, ZIF-8 and LAP@ZIF-8.....	54
Figure 3.10. <i>In vitro</i> cytotoxicity profile of LAP, ZIF-8, LAP@ZIF-8 against SKBR-3 cell line at various concentrations.....	56
Figure 3.11. <i>In vitro</i> cytotoxicity profile of LAP, ZIF-8, LAP@ZIF-8 against MCF-7 cell line at various concentrations.....	56
Figure 3.12. Coefficient of variation of average cell viabilities for different concentrations and incubation times of samples in (a) SKBR-3 and (b) MCF-7 cell lines.....	59

LIST OF TABLES

<u>Table</u>	<u>Page</u>
Table 3.1. The calculated EE% and DL% of different samples of LAP@ZIF-8.....	41
Table 3.2. Protein binding percentages of LAP, ZIF-8 and LAP@ZIF-8.....	52
Table 3.3. The IC ₂₅ and IC ₇₅ values of LAP, ZIF-8, and LAP@ZIF-8 for SKBR-3 and MCF-7 cell lines.....	57
Table 3.4. The IC ₅₀ values of LAP, ZIF-8, and LAP@ZIF-8 for SKBR-3 and MCF-7 cell lines.....	57

LIST OF SYMBOLS

h	Hour/Hours
nM	Nanomolar
mg	Milligram
mL	Milliliter
%	Percentage
°C	Degrees Celsius
nm	Nanometer
µg/mL	Microgram per Milliliter
C	Concentration
mV	Millivolts
µL	Microliter
cm ²	Square Centimeter
mg/mL	Milligram Per Milliliter
cm ⁻¹	Wavenumber(s)
a.u.	Arbitrary Unit
θ	Theta
°	Degree
~	Approximately
v/v	Volume per Volume
µm	Micrometer

LIST OF ABBREVIATIONS

MOF	Metal Organic Framework
ER	Estrogen Receptor
PR	Progesterone Receptor
HER2	Human Epidermal Growth Factor
TNBC	Triple-Negative Breast Cancer
EGFR	Epidermal Growth Factor Receptor
ErbB	Erythroblastic Leukemia Viral Oncogene Homolog
FDA	Food and Drug Administration
TKI	Tyrosine Kinase Inhibitor
ATP	Adenosine Triphosphate
LAP	Lapatinib
IC ₅₀	Half Maximal Inhibitory Concentration
NP	Nanoparticle
EPR	Enhanced Permeability Retention Effect
PBS	Phosphate Buffered Saline
ZIF	Zeolitic Imidazolate Framework
2-MeIm	2-Methylimidazole
MTT	Methyl Thiazolyl Tetrazolium
LAP@ZIF-8	Encapsulation of Lapatinib into ZIF-8
SEM	Scanning Electron Microscope
EDX	Energy Dispersive X-ray
FTIR	Fourier-Transform Infrared
XRD	X-ray Diffraction

TGA	Thermal Gravimetric Analysis
DLS	Dynamic Light Scattering
UV-vis	Ultraviolet-visible
DMSO	Dimethyl Sulfoxide
min	Minute or Minutes
rpm	Revolutions Per Minute
EE	Encapsulation Efficiency
DL	Drug Loading
FBS	Fetal Bovine Serum
BCA	Bicinchoninic Acid
BSA	Bovine Serum Albumin
Concn	Concentration
Abs	Absorbance
PDI	Polydispersity Index
SD	Standard Deviation

CHAPTER 1

INTRODUCTION

1.1. Cancer

Cancer is a global health problem whose seriousness increases day by day as it is among the causes of death in the world. According to 2020 global cancer statistics, approximately 19.3 million new cancer cases and 10.0 million cancer-related deaths have been recorded worldwide. Breast cancer has become the most diagnosed cancer type in women, surpassing lung, colorectal, prostate and stomach cancers (Sung et al. 2021).

Cancer alters cell functions and creates dysfunctions in vital genes due to mutations in genes; affects the cell cycle and causes abnormal (uncontrolled) proliferation. Proto-oncogenes responsible for cell division become oncogenes by genetic mutation. Abnormal cell division is also caused by a deficiency of tumor suppressor genes such as p53 (Hassanpour and Dehghani 2017).

Exposure to environmental mutagens, tobacco smoke containing various carcinogenic chemical compounds, as well as viral infection (virus and bacteria) and carcinogenesis factors such as UV-light cause gene mutations and these are among the important causes of human cancer (Hassanpour and Dehghani 2017; Poon et al. 2014). The fact that cancer is a diverse disease at the tissue level makes it difficult to diagnose and treat (Meacham and Morrison 2013).

Common cancer treatments include chemotherapy, surgery, and radiation therapy. Chemotherapy works with the logic of a drug delivery system used to prevent and kill cancer cell proliferation. New treatments that continue to be developed in addition to hyperthermia, photodynamic therapy, immunotherapy, and photothermal therapy include angiogenesis inhibitor therapy, biological therapies, and targeted cancer therapies. The main purpose of these therapies is to reduce drug toxicity with nanostructures and to increase effectiveness by targeting the tumor (Arruebo et al. 2011).

Chemotherapy is based on inhibiting the growth and division of cancer cells. Chemotherapy is still a preferred therapeutic method despite its known side effects. However, it has been observed that high doses of chemotherapeutic drugs cause many

side effects and damage to healthy cells (Anand et al. 2022). Various treatment strategies such as surgery, chemotherapy and radiotherapy against cancer have been widely applied, but the results have been found to be unsatisfactory. As some small molecule drugs that suffer from non-specific biodistribution damage normal cells, there is an increasing need to develop alternative treatments to replace traditional treatment modalities (L. Zhang et al. 2022).

The fact that it is necessary to develop drugs and pharmaceuticals for the treatment of increasing deaths due to different types of cancer makes this subject worth continuing to research. Over the last 20 years, studies on small molecule-based inhibitor drugs, the approval of new ones, and ongoing development studies have shown that they are promising cancer drugs. Delivery vehicles such as peptides and peptide-drug conjugates, metal organic framework (MOF) and many other nano-devices have been investigated (Chhikara and Parang 2022).

1.1.1. Breast Cancer

Breast cancer is a type of cancer that is due to the presence of malignant tumors in the mammary glands and is the result of uncontrolled growth of epithelial cells in the ducts or breast lobules. Compared to phyllodes tumors and angiosarcomas, carcinoma constitutes the majority of breast cancer. Breast cancer is divided into three main groups: non-invasive (or in situ), invasive, and metastatic breast cancers. About 5-10% of breast cancer is genetic, the rest is caused by epigenetic and environmental factors (Y. Feng et al. 2018).

Breast cancer, which covers 11.7% of cancer, surpasses lung cancer and ranks first as the most frequently diagnosed cancer with approximately 2.3 million new cases in both genders in 2020. It represents 25% of cancer cases in women and 16% of cancer deaths (or 1 in 6 deaths). It has been recorded that approximately 685,000 women died from breast cancer in 2020 (Sung et al. 2021; Arnold et al. 2022) .

Treatment is usually with combinations of surgery, chemotherapy, and radiotherapy. The limitations of current targeted therapy methods, such as various side effects and drug resistance, have triggered new method development and research efforts. Searches for new methods continue to improve survival and reduce side effects (Anastasiadi et al. 2017).

Specific subtypes of breast cancer are characterized by morphological features and some biomarkers such as the hormone estrogen receptor (ER), progesterone receptor (PR), and human epidermal growth factor receptor 2 (HER2). Differences in the expression of receptors are called heterogeneity of biomarkers. PR-positive tumors are generally more aggressive than ER-positive ones. Breast tumors are divided into several subtypes based on hormone receptor expression and the amount of cellular proliferation marker Ki67 such as Luminal A, Luminal B, HER2 (non-luminal) and triple-negative breast cancer (TNBC, Basal-like breast cancer).

Despite responding to anti-HER2-targeted therapy, HER2-positive carcinomas are the most aggressive subtype in the hormone receptor-positive breast cancer group. Breast carcinomas that do not express ER, PR, HER2 are classified as TNBC. It is known that some subtypes of TNBC, which is a highly heterogeneous cancer, are more aggressive, have a poor prognosis and respond poorly to treatment, while other types have a better prognosis and respond well to treatment. ER and PR-positive tumors are characterized as Luminal carcinomas. Luminal A type is ER-positive, PR-positive, HER2-negative and Ki67<14%. Luminal B type is ER-positive, PR-positive and is divided into two subgroups. While the first one is HER-negative and Ki67 is high, the second one is HER2-positive and Ki67 is absent. In the HER2 type is ER-negative, PR-negative and HER2-positive. In TNBC, it is ER-negative, PR-negative, and HER2-negative (Januškevičienė and Petrikaitė 2019).

Luminal subtype A is the most common among the intrinsic subtypes and defined by expression of hormonal receptors, ER-positive and PR-positive. It is associated with a better prognosis (Carey et al. 2006). Luminal subtype B is defined by ER-positive, PR-positive, and HER2-positive or HER2-negative. It is associated with higher tumor grade and worse prognosis compared to luminal A (Creighton 2012). HER2 overexpressed type is defined by ER-negative and PR-negative and HER2-positive. Triple-negative (basal-like) breast cancer is defined by immunohistochemical staining being negative for ER, PR and HER2, and a high expression of myoepithelial markers like CK 5/6 (cytokeratin 5/6). Both are associated with a worse prognosis (Yersal 2014).

1.1.1.1. HER2-Positive Breast Cancer

The epidermal growth factor receptor family having tyrosine kinase activity consists of epidermal growth factor receptor (EGFR, erythroblastic leukemia viral oncogene homolog 1 (ErbB 1) and HER1), HER2 (ErbB2), HER3 (ErbB3), and HER4 (ErbB4). One of these family members, HER2, is an oncogene whose purpose is to control cell growth, survival, differentiation, and migration through multiple signal transduction pathways, and is a 1255 amino acid, 185 kilodalton (kD) transmembrane glycoprotein located in the long arm of human chromosome 17 (Iqbal and Iqbal 2014).

ErbB, another name for these members, refers to its origin in the Erb-b gene responsible for avian erythroblastosis virus. HER2 (also known as ErbB2 or p185) was discovered by scientists at Massachusetts Institute of Technology, Rockefeller, and Harvard University (Padhy et al. 1982; Schechter et al. 1984). In half of all ductal carcinomas in situ, amplification of the HER2 gene occurs without any evidence of invasive disease (K. Park et al. 2006), and HER2-positive breast cancer resulting from this amplification is resistant to some cytotoxic chemotherapeutic and hormonal agents and tends to metastasize to the brain (Gabos et al. 2006).

HER2-positive breast cancer accounts for 20-25% of all breast cancers, with approximately 360,000 new cases per year worldwide. Breast cancer resulting from the overexpression of HER2 is aggressive and associated with a poor prognosis resulting from an increased level of metastasis. Various HER2-targeted agents have been approved for treatments for HER2 over the past five years (Schlam and Swain 2021).

HER2-positive breast cancer is an unfavorable prognostic feature, and it has been reported that patients have shorter disease-free survival and overall survival times compared to patients with HER2-negative tumors (Opdam et al. 2012).

The fact that 30-40% of HER2-positive breast cancers have high ER hormone levels causes the resistance of anti-hormone therapy in this type of breast cancer. FDA (Food and Drug Administration) approved drugs have been developed for the treatment of HER2-positive breast cancer. However, at the end of treatment, cancer cells develop resistance to the drug. HER2 therapy includes specific monoclonal antibodies (trastuzumab and pertuzumab) and small molecule inhibitors (lapatinib, neratinib, and pirotinib) (Fedorova et al. 2020).

The aim of HER2-positive breast cancer with metastatic HER2-positive tumor, which worsens the cancer by developing resistance, is to increase the number of patients recovering and to prevent possible recurrence of the cancer with treatment. Monoclonal antibodies, tyrosine kinase inhibitors, and antibody-drug conjugates are methods that target HER2. The hopeful clinical activity results and the presence of HER2 signal-dependent tumors highlighted the need for the development of new targeted therapies (Swain, Shastry, and Hamilton 2023).

1.2. Tyrosine Kinase Inhibitors (TKIs)

Tyrosine kinases are enzymes that catalyze the transfer of the gamma phosphate group of adenosine triphosphate (ATP) to the hydroxyl group of tyrosine residues in target proteins. Tyrosine kinase enzymes are part of many cell functions, including cellular processes such as cell signaling, growth, division, cell migration, motility, differentiation, and apoptosis. These enzymes are activated or may be present at high levels in human tumors (Schaeper and Grossmann, n.d.). Blocking these may help prevent the growth of cancer cells. Tyrosine kinase inhibitors (TKIs) work by blocking tyrosine kinase enzymes. TKIs are a type of targeted therapy.

TKI refers to a series of oral small molecular drugs that are active in promoting apoptosis and inhibiting the proliferation of cancer cells. There are five drugs officially approved by the FDA for the treatment of HER2-positive breast cancer, known as trastuzumab, pertuzumab, trastuzumab emtansine (TDM-1), lapatinib, and neratinib. Additionally, China's State Drug Administration has authorized a new TKI, pyrotinib. Due to the homologous structure of ATP, they inhibit tyrosine kinase phosphorylation by binding to the intracellular ATP binding sites of the EGFR family and stopping the signaling pathways. Compared with intravenous monoclonal antibodies, TKIs have the advantage of oral administration, multiple targets, and less cardiotoxicity (Xuhong et al. 2019).

1.2.1. Lapatinib (LAP)

Small molecules, especially TKIs, are currently used as targeted therapy agents in various malignancies. Lapatinib (GW 572016; Tykerb, Glaxo Smith Kline), the first dual inhibitor of EGFR / HER1 and HER2/ ErbB2 tyrosine kinases, was approved by the US FDA in 2007. Lapatinib is an orally active small molecule and dual tyrosine inhibitor of EGFR and HER2, which can inhibit the growth of cancer cells and induce cell apoptosis (Tevaarwerk and Kolesar 2009). Lapatinib (GW2016, also known as GW572016) (Figure 1.1) was shown in cell-free biochemical kinase assays to have concentration that inhibits 50% of cell growth (IC_{50}) values of 10.2 and 9.8 nM against EGFR and ErbB2, respectively (Rusnak et al. 2001) .

Lapatinib, a hydrophobic compound with a water solubility of approximately 0.007 mg/mL, is synthesized from the quinazoline core found in other TKIs (Blair et al. 2007). They are heterocyclic aromatic compounds containing a quinazoline moiety substituted with one or more amine groups. Additionally, lapatinib is the strong base compound (acid dissociation constant at logarithmic scale, $pK_a = 7.20$) (Shprakh, Poskedova and Ramenskaya 2022).

Lapatinib is an oral small molecule derivative of 4-anilinoquinazoline that targets the C-terminus tyrosine kinase domain of these two oncogene receptors and inhibits their activity. Lapatinib is better at inducing apoptosis of tumor cells than monoclonal antibodies targeting EGFR or HER2 previously used for this purpose. (Xia et al. 2002).

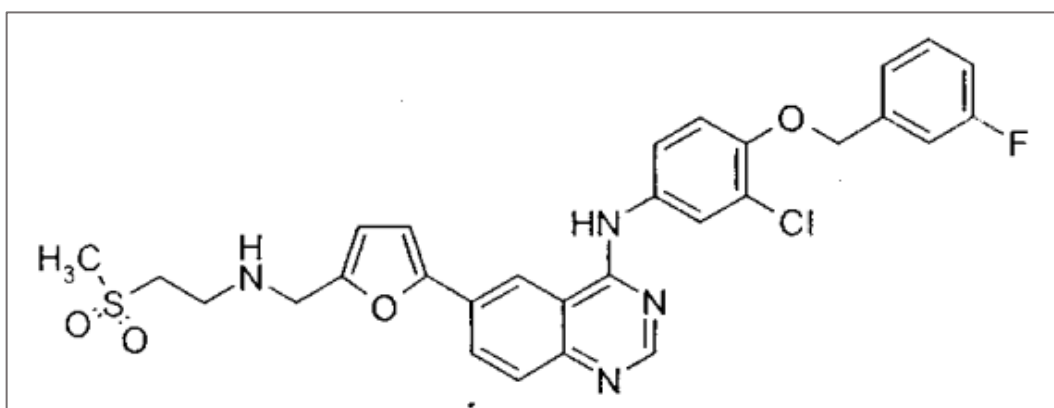


Figure 1.1. The chemical structure of lapatinib
(Rusnak et al. 2001)

It is a potent, reversible, and selective inhibitor and exerts its effect through competitive binding by competing with ATP at the intracellular ATP binding site of the receptor. This results in downstream blockade of the mammalian target of mitogen-activated protein kinase and phosphatidylinositol 3-kinase, Akt, and rapamycin-dependent transduction pathways, resulting in growth arrest or apoptosis of tumor cells (Xia et al. 2002; Ahn and Vogel 2012).

Lapatinib has been used in combination with other drugs in several studies. FDA-approved for use with capecitabine for HER2-positive metastatic breast cancer after pretreatment with anthracycline, taxane, and trastuzumab-containing regimens. In 2010, it was approved for use with letrozole for hormone receptor positive HER2-positive metastatic breast cancer (Rana and Sridhar 2012). Trastuzumab, the first HER2-targeted agent approved by the FDA in 1998 to enter clinical practice, is a selective monoclonal antibody with antitumor activity that targets the extracellular domain of the HER2 receptor. Trastuzumab is the first registered anti-HER2 agent to improve longer time to disease progression, higher response rate, longer duration of response and improved overall survival when combined with chemotherapy (Slamon et al. 2001). Unlike trastuzumab, lapatinib is oral, has less cardiotoxicity and may penetrate the central nervous system (CNS) better (Rana and Sridhar 2012). The combination of lapatinib with other chemotherapeutic drugs increases the effectiveness of lapatinib in breast cancer metastasis (Basuli et al. 2011), while it penetrates cells faster and crosses the blood-brain barrier more easily than trastuzumab in the treatment of brain metastasis (S. Chen et al. 2016). In addition, the combination of lapatinib and capecitabine has been used effectively in patients with HER2-positive breast cancer that is trastuzumab-resistant and has brain metastases (Chintalaramulu et al. 2020).

The efficacy of lapatinib in other malignancies overexpressing EGFR and/or HER2 continues to be evaluated (Medina and Goodin 2008). As treatment strategies continue to evolve, it is hoped that the clinical management of patients with HER2-positive breast cancer will continue to improve and translate into greater survival benefits in both adjuvant and metastatic settings (McArthur 2009). Although it is an effective drug, lapatinib is poorly water-soluble, which reduces its absorption in the intestine, reduces its bioavailability and damages the gastrointestinal structure. This does not allow it to be used as an injectable drug. Its low solubility in water has highlighted the application of lapatinib with nanoparticles (NPs) (H. Gao, Wang, et al. 2014). Lapatinib, which is also approved in tablet form, must be taken at a dose of 1250 mg per day due to

its poor oral bioavailability; this causes side effects such as diarrhea and rash. Therefore, it requires the development of an injectable dosage form and the design of a delivery system (Huo et al. 2015).

1.3. Targeted Drug Delivery System and Nanoparticles

Nanotechnology has recently attracted more and more attention in the diagnosis and treatment of tumors. In addition, nanotechnology is widely used in the biomedical field to develop nano-sized particles. The use of traditional drug delivery systems by anticancer drugs poses problems such as poor specificity, high toxicity, and induction of drug resistance, resulting in reduced therapeutic effect of drugs (Din et al. 2017).

Nanotechnology is the creation of useful materials and synthesis used to manipulate matter on an extremely small scale of 1 to 100 nm. Most anticancer drugs do not make a clear distinction between cancerous and normal cells, causing systemic toxicity and adverse effects. This results in greatly limiting the maximum allowable dose of the drug. Administration of large amounts of the drug for rapid elimination and widespread distribution to targeted organs and tissues is uneconomical and results in undesirable toxicity. For these reasons, nanoparticles have attracted great attention recently and their use in cancer treatment is becoming a growing industry. Pharmacologically, cancer drugs in chemotherapy reach the tumor tissue with low specificity and dose-dependent toxicity. Classical drug administrations are oral and intravenous, and they have some disadvantages. Oral intake of tablets or capsules results in erratic pharmacokinetics due to metabolic pathways. Therefore, it is necessary to apply a higher amount than the required dose, but this causes increased toxicity. It is known that intravenously administered drugs also cause problems because their specificity is low, and they damage healthy tissues. Direct delivery of anticancer drugs to tumor tissue prevents the drug from circulating in the body and participating in metabolism through various systems (Sinha et al. 2006).

Chemotherapy, which is frequently used for cancer, has disadvantages such as poor bioavailability, high dose requirements, adverse side effects, low therapeutic indices, development of multi-drug resistance and non-specific targeting. Conventional drug delivery system limits clinical applications in terms of untargeted and poor drug release. Problems such as high toxicity, drug resistance, and preventing specificity result from the

use of anticancer chemotherapeutics with conventional drug delivery systems (Senapati et al. 2018). These limitations can be overcome by applying nanotechnology approaches with the drug release mechanism of nanocarriers (Patra et al. 2018). Targeted drug delivery systems increase the treatment effectiveness of the drug in specific organs and reduce the possible side effects of the drug in other organs. Researchers have extensively studied the development of carrier-based drug delivery systems, nanocarriers with targeted properties to prevent drug degradation, resistance, and drug side effects (Majumder, Taratula, and Minko 2019). Effectively treating disease with minimal side effects is the overall goal of utilizing nanocarriers in targeted drug delivery (Mishra, Patel, and Tiwari 2010).

There is an increasing demand for nanocarriers targeting various diseases, which have optimized efficacy, reduced side effects and improved stability compared to conventional drug forms due to their small size, huge surface area and applicable targetability. There are several types of nanocarriers synthesized for drug delivery. Examples of these are dendrimers, liposomes, solid lipid nanoparticles, polymersomes, polymer–drug conjugates, polymeric nanoparticles, peptide nanoparticles, micelles, nanoemulsions, nanospheres, nanocapsules, nanoshells, carbon nanotubes and gold nanoparticles (Alshawwa et al. 2022).

As a result of nanotechnological research, nanoparticles have revolutionized the pharmaceutical industry in the way drugs are formulated and delivered. In the pharmaceutical field, the production of nanoparticles has attracted a lot of attention due to their properties such as entrapment and targeting. Due to the small size and large surface area of drug delivery systems, drug nanoparticles show enhanced bioavailability with increased solubility. Nanoparticles are made from natural and synthetic polymers (biodegradable and non-biodegradable). They enable the targeted delivery of drugs, improve bioavailability, and enable controlled drug release from a single dose (Rizvi and Saleh 2018). Nanoparticles can be categorized as liposomal, polymer, metal, carbon, protein-based, and mesoporous silica. Nanoparticles used in cancer treatment have advantages such as solving the problem of poor solubility by increasing the bioavailability of the loaded drug, providing slow release by facilitating the permeability of the drug to cancer cells, and being able to load cancer drugs (Liyanage et al. 2019). Nanoparticles improve the stability and solubility of drugs, increase the efficiency of transport between membranes and extend circulation times (Mitchell et al. 2021).

Accumulation of nanoparticles in cancer cells occurs by passive and active targeting. In passive targeting, NPs accumulate near the tumor site as a result of the permeability of tumor blood vessels. This situation is also known as the enhanced permeability retention (EPR) effect and allows NPs to passively accumulate in solid tumors and/or metastatic sites through properties such as size, shape, and superficial charge. Active targeting takes advantage of biofunctionalization of the NP surface using overexpressed receptors and molecules, or ligands (with a strong affinity and specificity for secreted proteins in the tumor microenvironment) on tumor cells. Passive and active targeting that can occur simultaneously do not interfere with each other (Figure 1.2) (Sanità, Carrese, and Lamberti 2020).

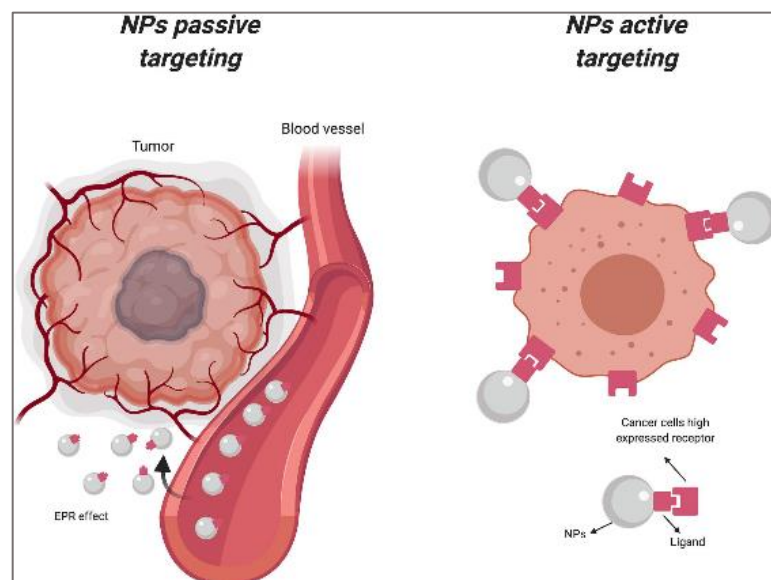


Figure 1.2. Passive and active targeting of nanoparticles (Sanità, Carrese, and Lamberti 2020)

Passive targeting is defined as a system in which drug delivery nanoparticles can deliver the drug to the target site based on the selective properties of tumor tissues compared to healthy tissues. Tumors are highly permeable and lack functional lymphatic circulation. As a result of these pathophysiological conditions of tumor tissues, appropriately designed “drug delivery systems” easily penetrate and retain abnormal types of cells. By utilizing this mechanism, known as the EPR effect, it can be aimed to deliver low molecular weight chemotherapeutics to the tumor site. This type of drug targeting is called “passive targeting” because it is based on the pathophysiological specificity of the targeted tissue. However, the physicochemical properties of the vector,

such as its charge, size and surface, also play an important role in passive targeting with the EPR effect (Matsumura and Maeda 1986). Passive targeting is achieved by the characteristics of the tumor microenvironment with increased EPR effect. The nanoparticle enters the cell via simple diffusion. Angiogenic blood vessels in tumor tissues, unlike those in normal tissues, have gaps of 600 – 800 nm in size. These vascular structures induce the EPR effect by allowing nanoparticles to enter through these gaps and accumulate within tumor tissues (Mohanraj and Chen 2007). In passive targeting, the encapsulated anticancer agent can be released from the nanoparticle upon specific stimulation. The release of anticancer drug into the target tissue can be achieved with the pH-sensitive nanoparticle system. The accumulation of nanoparticle in tumors depends on the particle size, surface characteristics and circulation half-life, as well as the degree of angiogenesis of the tumor. It is known that nanoparticles with a diameter of less than 200 nm and a positive surface charge tend to accumulate more in the tumor tissue and their residence time in the tumor tissue is longer than neutrally charged or negatively charged nanoparticles. Accumulation of the tumor drug in the tumor tissue more than the free drug form can be achieved by loading the drug into nanoparticles and the EPR effect in the tumor tissue. The accumulation of nanoparticles in tumor tissue is not homogeneous. Nanoparticles may accumulate in high concentrations in one part of the tumor tissue and less in another, and the reason is not yet fully understood. In passive targeting, when nanoparticles are transported to the target diseased organ or tissue, they must enter the cell of interest and release the anticancer agent they carry into the sub-cellular organelles. For this purpose, a non-specific cell penetration strategy must be adopted. Non-specific uptake of nanocarriers into the cell occurs through the endocytotic process, where the nanoparticles form an envelope around the membrane and form a vesicle called endosome. Endosomes transport their contents to lysosomes, which are highly acidic organelles and rich in degrading enzymes. Endocytosed nanocarriers generally move in a specific direction and fuse with the nuclear membrane (Ganta et al. 2008).

Cancer nanotherapeutics are being developed to solve various limitations of traditional drug delivery systems. To improve the biodistribution of cancer drugs, nanoparticles are designed with optimum size and surface properties to increase their circulation time in the bloodstream. They can deliver their drugs to cancer cells by taking advantage of the pathophysiology of tumors, such as enhanced permeability and retention effect and tumor microenvironment. It appears that nanoparticles' anticancer drugs can

pass through barriers in the body and reach the desired tumor tissues with minimal loss of volume or activity in the bloodstream, and that the drugs can selectively kill tumor cells without affecting normal cells with controlled release. In order to deliver the drug to the targeted tumor tissue, nanoparticles must have the ability to remain in the bloodstream for a long time without being eliminated. The size of nanoparticles used in a drug delivery system must be large enough to prevent rapid infiltration into blood capillaries, but small enough not to be captured by resident macrophages (liver and spleen) in the reticuloendothelial system. This shows that the size of nanoparticles must be up to 100 nm in order to reach tumor tissues. Nanoparticles that meet the size and surface properties requirements to evade reticuloendothelial system capture can circulate in the bloodstream for longer periods of time and reach targeted tumor tissues. Thanks to the unique pathophysiological properties of tumor vessels, nanoparticles enable their selective accumulation in tumor tissues. This is called the increased permeability and retention effect. Another factor contributing to passive targeting is the unique microenvironment surrounding tumor cells, which differs from normal cells. Fast-growing, hyperproliferative cancer cells display a high metabolic rate, and the supply of oxygen and nutrients is often not sufficient to maintain it. Therefore, the acidic environment occurs when tumor cells use glycolysis to obtain additional energy. As tumor cells obtain energy through glycolysis, the pH value of the tumor microenvironment becomes acidic. By taking advantage of this feature, pH-sensitive systems can be designed that can release drugs at low pH values when targeting the tumor (Cho et al. 2008). Nanoparticles are of interest to support the release of anticancer drugs targeting the tumor microenvironment to target sites and to increase intra-tumor accumulation (Mo and Gu 2016).

Anticancer agents encapsulated in the nanoparticles inhibit the development of drug resistance. It owes this to its inability to be recognized by cellular flow mechanisms. In recent years, with the understanding of tumor biology, new targeted drug delivery approaches provide optimism in developing successful cancer therapy (Vasir and Labhasetwar 2005).

Nanotechnology aims to ensure that the drug is targeted to the site of action. It also works on the formulation of therapeutic agents in biocompatible nanocarriers such as nanoparticles, nanocapsules, micelle systems and dendrimers, and develops new methods. While nanocarriers enable the transport of targeted drugs to the tumor structure, research makes it possible to diagnose and treat diseases, especially cancer. With efficient

drug delivery, nanotechnology can foster innovative use of manufactured existing drugs. Nanotechnology has become more and more common in many disciplines, especially in healthcare, showing that the process of replacing conventional drugs has begun and will accelerate over time (Parveen, Misra, and Sahoo 2012).

1.4. Metal Organic Frameworks (MOFs)

Targeted therapies often inhibit the proliferation of cancerous cells (cytostatic), while conventional chemotherapy drugs kill tumor cells (cytotoxic) (Tran et al. 2023). Most biomolecules have insufficient stability, solubility, poor pharmacokinetics, biocompatibility and/or off-target activities. Scientists have developed MOFs that work by surrounding active cargoes and directing them to specific tissues to address pharmacokinetic issues (Williams et al. 2021).

MOFs were first proposed by Hoskins and Robson in 1989 (Hoskins and Robson 1989). With over 20,000 variants available, biomaterials called MOFs are created by combining metal clusters or metal ions with organic ligands via coordinative bonds. Ultimately, it results in a two- or three-dimensional structure (Furukawa et al. 2013).

Chemotherapeutic drugs are not specific, and usually cause toxicity in normal cells. Nanoscale MOFs are versatile and important drug carriers for chemotherapy. Drugs are readily incorporated within the MOF porosity, while the MOF replaceable surface can provide extended circulation capabilities, targeting, and controllable drug release. To go a step further, attention has recently been drawn to personalized medicine that uses MOF nanoparticles for cancer treatment, rather than traditional radiotherapy and chemotherapy, which cause a lot of pain to patients. MOFs are synthesized using various metal ions and organic linkers such as carboxylates, phosphonates, and sulfonates. Repetitive metal ions act as knots to bind organic binders, and it creates a lattice-like structure. In recent years, MOFs have been studied in drug delivery system because of their biocompatibility, tunable composition, editable surface, and exceptionally high drug loading capabilities. Drugs can be enclosed in cages with MOF matrices. These drugs can circulate *in vivo* with good stability within MOFs without interacting with healthy tissues (Ding, Liu, and Gref 2022). MOFs have attracted attention in various fields, especially in the field of medicine. They owe this to their high drug storage capacities and porosity, variable pore sizes, and easy modification as drug delivery systems. They have a crystal structure, high

porosity and a certain surface area. They can be composed of different metal ions and organic bridging ligands and have easy-to-design structures. The σ single bond in the organic ligand structure gives MOFs a certain degree of flexibility to have characteristic functions and the structure is easy to change. MOFs have come to the forefront with their performance in adsorption, separation, catalysis, sensing and drug delivery, and wide application prospects. These properties have been used to design MOFs that minimize non-specific distribution of drugs, reduce toxicity in healthy cells, and increase treatment efficacy. Divalent metal ions such as Mn^{2+} , Co^{2+} , Cu^{2+} and Zn^{2+} are often used to form MOFs. Generally, when drug-loaded MOFs are stimulated with a certain pH or temperature, the weaker coordination bond is broken, and the drug is released. Monovalent ions such as Cu^+ , Ag^+ and K^+ are also used to form MOFs. They are very sensitive to light, heat or water and this weakens their stability. MOFs formed with trivalent metal ions such as Cr^{3+} , Fe^{3+} , Al^{3+} and oxygen-containing ligands (mainly carboxylic acids) generally have high chemical and thermal stability. The preparation of these MOFs usually requires acid and very high reaction temperature. Tetravalent metal ions such as Zr^{4+} and common oxygen-containing ligands form coordination bonds with more covalent components and the reaction conditions are more severe. Given the stability of the coordination bond between metal ions and organic ligands and the designability of organic ligands, carboxylate and pyridine ligands are often used to synthesize MOFs. Polyazole molecules such as imidazole and pyrazole, which can remove a proton to form an anionic multi-terminal ligand, have the advantages of carboxylate and pyridine ligands (Q. Wang et al. 2020).

Common nanoMOFs studied were designed using Materials of the Institute Lavoisier (MIL), Zeolitic Imidazolate Frameworks (ZIFs), Porous Coordination Networks (PCNs), and University of Oslo (UIO) materials. In terms of toxicity, the currently most investigated nanoscale MOFs are MIL-100(Fe), ZIF-8 (Zn), and UiO 66 (Zr) (Ettliger et al. 2022).

Various synthesis methods that allowed the formation of different MOFs affected their drug loading capacity. Various techniques have been developed and employed, such as the solvothermal synthesis approaches, the sonochemical method, microwave-assisted chemistry, electrochemical synthesis, mechanochemistry, and flow chemistry method (Huiyuan Zhang et al. 2018; Abánades Lázaro, Wells, and Forgan 2020; Pang et al. 2020; J. Lu et al. 2021; Yang et al. 2021). Various strategies have been proposed to encapsulate drugs within MOFs. While drugs act as organic binders of MOFs, they can be

encapsulated into MOFs by solvent impregnation or solvent-free methods, such as the one-step method, multi-step method, high-pressure encapsulation method, and mechanochemical method. In addition to drugs, amino acids, peptides, proteins, nucleobases, saccharides, porphyrins were also used as constructive organic binders. These have coordination functions with metal ions to form MOFs. A variety of nanosized MOFs were engineered from non-toxic metals (Fe, Zn, K, etc) and organic ligands (carboxylates, phosphonates, sulfonates, etc) and displayed controlled size distribution, high porosity, biocompatibility, and biodegradability. Besides the above-mentioned intrinsic advantages, various drugs and imaging contrast agents can be (co)loaded in the porous MOF structures, thus expanding their applications in drug delivery system. Nanoscale MOFs attract growing interest in the drug delivery area, due to their flexible composition, large surface areas, degradability, and versatile surface properties (Ding, Liu, and Gref 2022).

The one-step encapsulation method, also called the one-pot method, is the simple strategy to achieve simultaneous drug loading and MOF synthesis (Paseta et al. 2015). In 2012, Liédana et al. was mixed 2-methyl imidazole (2-MeIm), zinc nitrate and caffeine in methanol and water using one-step encapsulation method for MOF synthesis. The drug was loaded with high efficiency due to hydrogen bonds and van der Waals interactions. This study highlighted the advantage of the one-step encapsulation method (Liédana et al. 2012).

Once the drug molecules are incorporated within their MOF carriers, they experience host (drug) - guest (MOF) interactions such as, with increasing intensity, van der Waals forces, hydrogen bonding, coulombic forces, and coordination bonds (H. Cai, Huang, and Li 2019). The host-guest interaction can be affected by environmental factors such as temperature, light, or competitive guest binding (Antoniuk and Amiel 2016).

The host MOF must degrade in the biological environment to release its cargo to the target site, and the drug release process depends on the stability of the host MOFs, the solubility of the guest molecules, and their localization and aggregation within the MOF (di Nunzio et al. 2014; Bruneau et al. 2019; X. Li et al. 2021; Velásquez-Hernández et al. 2021).

Drug-responsive release triggered by endogenous (ie, pH, redox) and exogenous (ie, light, temperature, magnetic field) stimuli was studied (Bruneau et al. 2019; W. Cai et al. 2019). The pH-triggered mechanism is the most studied. Leveraging the acidic tumor microenvironment and the acid sensitivity of MOFs, drug delivery system is

designed to release the drug specifically at the tumor site (Mura, Nicolas, and Couvreur 2013). Zheng et al. reported that doxorubicin (DOX) release is closely related to the degradation of ZIF-8 (H. Zheng et al. 2016). Drug release and degradation are closely related to the size and surface properties of the nano-MOFs. The study confirmed that the release of DOX under acidic conditions is associated with the dissolution of the upper layers of ZIF-8, which acts as the protective shell around DOX@ZIF-8 (Ding, Liu, and Gref 2022).

In other studies, it was demonstrated that not only pH, but drug loading can play an effect on drug release (di Nunzio et al. 2014). It was encapsulated in MIL100 (Fe) nanoMOFs at different payloads. Release was very low at the highest loading, whereas it was fast at the lowest loading. In contrast to the situation described as the cause of drug aggregation within MOF lattices and forming aggregates, aggregates were found to stabilize the MOF matrix upon degradation. It forms aggregates in DOX and similar results were obtained with MIL 100(Fe) (Qiu et al. 2021). The stability of MOFs is affected by several variables, including pH, temperature, humidity, solvents, metal ions, and biological molecules (Awasthi et al. 2022). According to studies, ZIF-8 and PCN-222 were found to be stable in water and to degrade in phosphate buffered saline (PBS) and at pH 6, MIL-100, MIL-88, and UiO-66 (Zr) were stable in water and acidic conditions but degraded in PBS and basic environments (N. Singh, Qutub, and Khashab 2021).

MOFs, whose backbones can be organic (polymeric, liposomal, or proteinaceous) or inorganic (metal, non-metallic, or biomimetic), are multifunctional nanostructures. Traditional cancer therapeutic approaches have many limitations. The creation of MOFs has overcome their limitations such as low aqueous solubility, low selectivity, high lethality, and multidrug resistance. A wide range of MOFs can be fabricated for critical applications, including separations, gas storage, analytical chemistry, catalysis, sensing, energy, imaging, and biomedicine. Recently, MOFs have been developed as nanocarriers of drugs for cancer therapy. These allow tumor detection, screening, and management to improve cancer treatment. It leads to an increase in the amount of MOFs that are taken up by cells with their large specific surface area and a high porosity that allows it to come into contact with cell membranes. The biofunctionalization of MOFs is an important research topic in the field of nanomedicine basic research. In the last decade, progress has been made in biomolecule-metal-organic framework composites, both in the identification and treatment of cancer. The development strategies of MOF-based

materials for cancer treatment will make it possible to improve survival and quality of life and reduce the cost of treatment. In addition, their biocompatibility, large drug payloads, and the ability to hybridize with a wide range of functions still make MOFs desirable for targeted drug delivery (Tran et al. 2023).

1.4.1. Zeolitic Imidazolate Framework (ZIF)

The biocompatibility of both the metal and the bridging ligand must be considered in the development of MOFs, the aim of which is to design carriers that are as less toxic as possible in the human body. Some metals such as chromium and nickel are highly toxic. The human body contains iron (in plasma), zinc, copper, manganese, and nickel (in tissues). It facilitates the selective delivery of anticancer drugs to cancer cells while reducing the dose-limiting side effects of most anticancer chemotherapeutics (Huxford, Della Rocca, and Lin 2010).

Conventional drug delivery systems are made from organic or inorganic based materials. These systems have problems such as uncontrolled drug release, biocompatibility, and cytotoxicity. ZIF hybrid materials may be involved in solving these problems (Adhikari, Das, and Chakraborty 2015). Other systems have negative properties such as low drug loading capacity, poor biocompatibility, undesirable biodegradability, and complex synthesis procedures. Such porous materials, on the other hand, have attracted attention to obtain a controllable drug release (K. Lu et al. 2018; W. Cai et al. 2019).

ZIFs, a subfamily of MOFs, have properties such as adjustable pore size, large surface area, high thermal stability, and biodegradability/biocompatibility. These properties make ZIFs excellent candidates for many applications. These applications include gas capture, separation, chemical sensors, drug delivery and catalysis. In addition, their ability to encapsulate high volumes of therapeutic drugs, proteins or imaging cargoes into drug delivery systems makes them attractive for applications in the field of biomedicine, drug delivery and biomineralization. The pore size of ZIFs is easily adjustable, resulting in tunability of molecular diffusion/mass transfer and loading of large cargoes. This property has positively impacted drug delivery. There are various ZIFs created. ZIF-8 (2-MeIm and Zn^{2+}), ZIF-67 (2-MeIm and Co^{2+}), ZIF-4 (Zn^{2+} -Im), ZIF-7 (Zn^{2+} -benzimidazole) and ZIF-90 (Zn^{2+} -imidazole-2-carboxaldehyde) can be given as an

example. ZIF-based drug delivery systems have been developed for use in biomedical applications such as chemotherapy (CT), photothermal therapy (PTT), photodynamic therapy (PDT), antimicrobial applications, development of theranostic nanomedicines, and biomimetic mineralization (Maleki et al. 2020). ZIFs consist of tetrahedral coordinated transition metal ions such as Fe^{2+} , Co^{2+} , Cu^{2+} , Zn^{2+} , which are connected by imidazolate linkers (K. S. Park et al. 2006).

Structurally, ZIFs are formed by coordination between M^{2+} cations and imidazole (Im) anions. Im acts as a linker between the metal centers of the $\text{M}(\text{Im})_4$ tetrahedral units (Kaneti et al. 2017). Zn^{2+} , an endogenous metal ion, is widely used to form MOFs.

The ZIF is a metal-organic framework composed of Zn^{2+} and imidazole or its derivatives, the most widely used drug carrier in Zn-based MOFs. The solution reaction method at room temperature, solvothermal method, electrodeposition-solvothermal method and microfluidic synthesis method are the synthesis methods of Zn-MOFs (Q. Wang et al. 2020). The type of solvent and metal salt during synthesis, the ratio of metal salt to Im binder, mixing order of ZIF precursors, and addition of surfactants make the crystal size and morphology of ZIFs controllable (Yao, He, and Wang 2015). The green and sustainable production of ZIFs under mild synthesis conditions and the use of non-toxic solvents (Pan et al. 2011) and solvent-free methods (Tanaka et al. 2013; Y.-R. Lee et al. 2015) are very important for environmental protection. In 2017, a fast and scalable method for the synthesis of hierarchical ZIFs, such as ZIF-8 and ZIF-67, and one-pot encapsulation of dyes or proteins cargoes using an organic base trimethylamine (TEA) was reported by Zou and colleagues. The addition of TEA into the solution of $\text{Zn}(\text{NO}_3)_2 \cdot 6\text{H}_2\text{O}$ promoted the formation of ZnO NPs, which rapidly transformed to ZIF-8 NPs after the addition of the 2-MeIm as a binder (Abdelhamid et al. 2017).

pH-sensitive MOFs are the most widely investigated. This is due to the acidic tumor microenvironment (TME) and the sensitivity of coordination bonds in MOFs to external pH. These are termed MOF nanocarriers triggered by external stimuli, single stimulus sensitive MOFs or pH sensitive MOFs (Angelos et al. 2009). Developing stimuli-sensitive drug delivery systems, especially pH-sensitive drug delivery systems, has formed the core of studies to develop sensitive nanosystems for cancer therapy. This is due to the pH of the tumor tissue (pH 5.5-6.0), which is more acidic than blood and normal tissues (pH 7.4) (J. Liu et al. 2014).

Among MOFs, ZIFs are most frequently studied as drug delivery systems due to their biocompatibility at low concentrations, ease of synthesis, and pH response

properties. They are of particular interest as pH-sensitive drug carriers due to their high drug loading ability and biodegradability. While ZIFs can remain stable in water and aqueous NaOH, their frameworks rapidly degrade in acidic solutions and therefore their pH sensitivity may contribute to the development of ZIF-based drug delivery systems.

Cancer cells have more acidic microenvironments compared to normal cells, making ZIF nanosystems containing anticancer drugs suitable for the realization of tumor-specific target therapy. This specificity in targeting cancer cells is due to the unique ability of zeolite to break down under acidic conditions created by the tumor microenvironment. ZIF-8, formed by copolymerization of Zn with 2-MeIm, is frequently used in studies on the transport of DNA, proteins, and drugs.

Recently, interest in investigating the effectiveness of zeolites and ZIFs in pre-existing anticancer drugs has increased, and numerous studies have been and continue to be conducted. Various studies show that ZIFs have great potential for targeted and controlled delivery of anticancer drugs to tissues and organs and can be achieved successfully. For this reason, it is recommended to use ZIFs containing anticancer drugs as a treatment option to increase the effectiveness of cancer treatment by reducing the disadvantages of drugs within the scope of traditional treatment options (Hao et al. 2021). ZIFs, particularly ZIF-8, have been investigated for cancer ablation both *in vitro* and *in vivo* as nanocarriers (Sun et al. 2012; Zheng et al. 2015; M. Gao et al. 2019).

1.4.1.1. ZIF-8

ZIF-8 is an important subgroup of ZIF nanomaterial, which is formed by the coordination of Zn^{2+} and nitrogen (N) atom on the 2-MeIm ring, with features such as high porosity, easy modification, certain thermal and chemical stability, low toxicity, and excellent biocompatibility. In Figure 1.3, ZIF-8 is shown in a framework type sodalite (SOD) structure. Black dots represent carbon atoms, green dots represent nitrogen atoms, blue polyhedrons represent Zn ions, and the yellow sphere represents the largest van der Waals sphere at the center of ZIF-8 (K. S. Park et al. 2006).

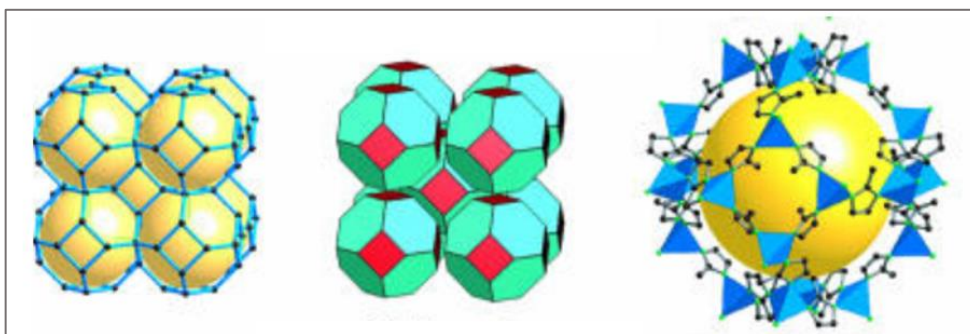


Figure 1.3. The stick diagram (left) and as a tiling (center) of ZIF-8. The largest cage (right) in ZIF-8 (K. S. Park et al. 2006)

ZIF-8 can be used as a pH sensitive drug delivery system of small molecules, anti-cancer and antibacterial drugs. The reason why ZIF-8 is pH sensitive is that acidic conditions can protonate organic ligands, leading to cleavage of the Zn^{+} -imidazolium ion coordination bond and cleaving its skeleton to release the drug. This property allows ZIF-8 to release drugs in the acidic environment of the tumor (Q. Wang et al. 2020). Decreased drug efficacy results from poor drug stability and non-specific targeting. These are associated with the direct use of therapeutic drugs. Generally, high doses of drugs cause side effects. The main goals and tasks of nanomaterial drug delivery are to stabilize the drug by encapsulation or surface binding, to promote cellular internalization, and to control the release of the drug at the designated target. ZIF-8 nanoparticles (ZIF-8 NPs) have properties such as the nanoparticles remain firm under neutral conditions and undergo rapid degradation in low pH environments due to the effects of drug-releasing protonation in the tumor with pH between about 5.0 - 6.5. These features allow ZIF-8 to be considered as a suitable delivery vehicle (X. Chen et al. 2018). The pH-triggered activation of ZIF-8 is attributed to the protonation of imidazole, resulting in the disassembly of ZIF-8 (K. S. Park et al. 2006). ZIF-8 is widely used for pH-sensitive drug release. Its enhanced drug loading capacity and pH sensitive drug release ability are due to its acid sensitivity and pores (Ren et al. 2014).

The size of ZIF-8 particles is also important for drug release. Research by Velásquez-Hernández et al. showed that the rate of degradation of ZIF-8 particles in PBS is related to their size, indicating that the smaller the size, the faster the degradation rate of ZIF-8 particles and the faster the release of the charged drug (Velásquez-Hernández et al. 2019). For N-donor ligands, which provide high thermal and chemical stability, one of the most stable bonds is the bond between imidazole (Im) and Zn^{2+} . Besides the high

structural stability, ZIF-8 has a high specific surface area of about $1630 \text{ m}^2\text{g}^{-1}$ and micropore volume of $0.636 \text{ cm}^3\text{g}^{-1}$ with large micropores (11.6 \AA in diameter) connected through small apertures (3.4 \AA) (Y. J. Kim et al. 2021). Various applications of ZIF-8 as a nanocarrier in drug delivery systems are shown in Figure 1.4 (S. Feng et al. 2021).

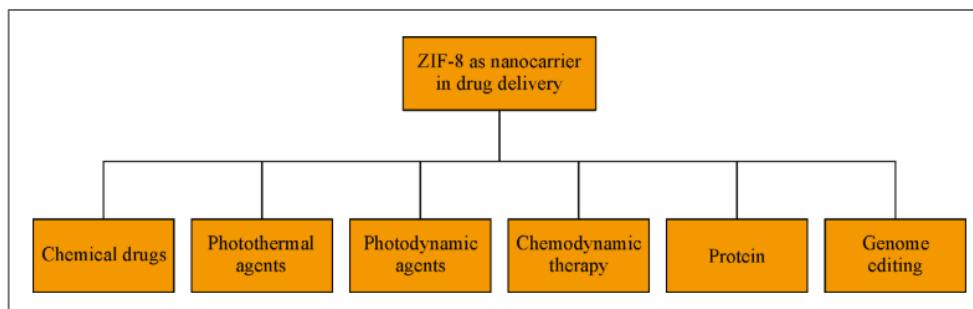


Figure 1.4. Applications of ZIF-8 as nanocarrier in drug delivery (S. Feng et al. 2021)

Studies have been conducted and published on the successful encapsulation of various drugs into ZIF-8. According to their solubility, drugs are divided into hydrophobic drugs, hydrophilic drugs, and amphiphilic drugs. A simple one-pot method for encapsulating hydrophobic drugs into ZIF-8 was proposed by Zheng group (H. Zheng et al. 2016). As shown by various studies in the literature, ZIF-8 can encapsulate hydrophobic, hydrophilic, and amphiphilic drugs.

Physcion is a natural hydrophobic compound that was successfully encapsulated into ZIF-8 by the one-pot method with high drug loading (11.49%) and encapsulation efficiency (88%). Physcion@ZIF-8 showed high antibacterial activity against gram-positive and gram-negative bacteria and loading of Physcion onto ZIF-8 proved to be beneficial in drug delivery (Soomro et al. 2019). The hydrophobic zinc(II) phthalocyanine (ZnPc) molecule is encapsulated in the pores of ZIF-8. ZnPc@ZIF-8 nanoparticles, whose synthesis is carried out in a single step, have excellent luminescence intensity and photodynamic activity against the HepG-2 cancer cell line (Xu et al. 2018). Encapsulation of curcumin (CCM), a hydrophobic drug, into ZIF-8 exhibits high drug encapsulation efficiency (88.2%) while possessing good chemical stability and rapid drug release in the tumor environment (Zheng et al. 2015).

Sun et al. have studied the *in vitro* delivery of anticancer drugs in ZIF-8. The first example of the application of ZIFs in drug delivery systems, the anticancer drug 5-Fluorouracil (5-Fu), was loaded into the drug delivery system ZIF-8. *In vitro* experiments

were carried out. It showed that 5-Fu loaded ZIF-8 provided faster drug release in acetate buffer and was able to release more than 85% within 12 h (Sun et al. 2012).

Biological research and studies were continued with the encapsulation of molecules such as DOX, rhodamine B, methyl orange and methylene blue into ZIF-8, which was synthesized by the one-pot method (H. Zheng et al. 2016). Caffeine, an amphiphilic compound, was encapsulated in ZIF-8. One-step encapsulation successfully resulted in controlled release of caffeine over 27 days and high drug loading of approximately 28% by weight (Liédana et al. 2012).

Other molecules are cytochrome c (Cyt c) enzyme (C. Zhang et al. 2017), 3-methyladenine (3-MA) (X. Chen et al. 2018), insulin (Duan et al. 2018), and protein (Liang et al. 2018), CpG oligodeoxynucleotides (ODNs) (Huijie Zhang et al. 2017), melittin (MLT) (Y. Li et al. 2018), ceftazidime (Sava Gallis et al. 2019), in addition to these, anticancer molecules such as camptothecin (CPT) (Zhuang et al. 2014), and 6-Mercaptopurine (6-MP) (Kaur et al. 2017) were also encapsulated in ZIF-8.

Although there are extensive studies on its applications in cancer diagnosis and treatment, the most interest in the research area has been to ZIF-8. The various applications of ZIF-8 are mainly due to the easy polymerization of Zn^{2+} and 2-MeIm around various objects. Drugs, nanoparticles, and bio-macromolecules can be incorporated into these objects, making them multifunctional while maintaining the structural crystallinity and porosity of the ZIF shell (Maleki et al. 2020). The poor biodegradability of some materials limits their development. For this reason, more biodegradable and biocompatible ZIF-8 materials need to be developed (Q. Wang et al. 2020).

Zn ions released from ZIF-8 can increase the regulatory efficiency of gene expression while acting as a cofactor for the enzymatic cleavage reaction. Zn is considered a highly biocompatible metal ion. The toxic effect of ZIF-8 in cancer cells is more pronounced than in normal cells. The toxicity of ZIF-8 is due to released Zn ions, whereas cancer cells take up more Zn ions due to increased permeability. Zn ions have been reported to have a Fenton-like reaction with highly expressed hydrogen peroxide (H_2O_2) in cancer cells, resulting in increased Reactive Oxygen Species (ROS) production and a stronger killing effect on cancer cells (Xie et al. 2022).

TP53 (or p53), the most frequently mutated gene in human cancers, is critical in preventing cancer development. The p53 gene is a tumor suppressor that plays a role in maintaining genome integrity by regulating cell cycle progression, apoptosis, senescence,

DNA repair and cell metabolism in mammals. Approximately 30% of all breast cancers, and for HER2-positive subtypes, the rate of p53 gene mutations reaches 70% (Fedorova et al. 2020). Zn forms a functional component of various proteins that contribute to gene expression and regulation of genetic activity. It protects against UV, improves wound healing, contributes to immune and neuropsychiatric functions, and reduces the risk of cancer and cardiovascular disease. Zn inhibits the oxidation of the oxidized inactivated p53 tumor suppressor gene. In other words, it prevents p53, an antioncogenic and apoptotic gene, from being inactivated as oxidized (Belgemen and Akar 2004).

There are studies showing that a certain level of Zn is important in the treatment of breast cancer during the formation of cancerous cells and that Zn accumulates in cancerous areas in the breast tissue and reduces the progression and risk of cancer (Kaczmarek et al. 2012). One article was reported that Zn enhances the pro-survival signal *in vitro* (Y.-M. Kim et al. 2006). In addition, Zn has been reported to inhibit caspases *in vitro* (Velázquez-Delgado and Hardy 2012). Caspases is a family of endoproteases that link in cell regulatory networks that control inflammation and cell death (McIlwain, Berger, and Mak 2013).

Zn is an essential mineral and is a cofactor for more than three hundred enzymes. It is involved in numerous signaling pathways important for cell proliferation and differentiation, cell cycle regulation, apoptosis, and redox regulation. There are reports in the literature about Zn and the risk of breast cancer. However, the effect of Zn on breast cancer survival and its role are not clearly known, and possible biochemical mechanisms are still discussed (Bengtsson et al. 2022).

1.5. Encapsulation of Lapatinib in Literature

There are successful examples of encapsulation of lapatinib in different drug delivery systems in the literature. In the study investigating polymer-lipid hybrid nanoparticles for lapatinib delivery in breast cancers, it was noted that the nanoparticles effectively killed MCF-7 cancer cells and triggered their apoptosis, compared to free lapatinib. Lapatinib-loaded hybrid nanoparticles have been shown to have great potential to achieve therapeutic effect in breast cancer treatment (Huo et al. 2015).

In the study aiming to evaluate lapatinib-loaded polymeric micelles for breast cancer treatment, Lyophilized lapatinib-loaded polymeric micelles exhibited sustained

drug release and high cytotoxicity against SKBR-3 breast cancer cells. Moreover, it induces effective inhibition of tumor growth *in vivo* compared to free lapatinib, indicating the great potential of lapatinib-loaded polymeric micelles for breast cancer treatment (Gunjan Vasant et al. 2020).

The development of lapatinib-loaded human serum albumin nanoparticles with nanoparticle albumin-bound technology offers the opportunity to use lapatinib in the treatment of brain metastases of TNBC. Results such as effective inhibition effects of lapatinib-loaded human serum albumin nanoparticles in treatment, anti-tumor activity, and significantly prolonging the median survival of brain metastatic mice clearly revealed that lapatinib-loaded human serum albumin nanoparticles may be a promising candidate for clinical applications against brain metastasis of TNBC (Wan et al. 2016).

In the study in which lapatinib was loaded into exosomes as a nanocarrier, it was observed that lower doses significantly reduced the cellular proliferation of SKBR-3 cells compared to free lapatinib treatment. As a result of the analysis, lapatinib-loaded exosomes showed a high apoptotic rate, increasing the effectiveness of the drug. As a result of the study, it was noted that the use of exosomes in drug delivery approaches is an effective treatment method and can increase the therapeutic index of chemotherapeutic drugs (Değirmenci et al. 2022).

In the study where dextran sulfate-chitosan nanoparticles were used as drug carriers, lapatinib encapsulated nanoparticles were developed. Methyl-thiazolyl-tetrazolium (MTT) assay showed that the drug-loaded nanoparticles have effective anticancer activity, while dextran sulfate-chitosan nanoparticles can retain and release lapatinib in a controlled manner and act as a suitable drug carrier in cancer treatment (Mobasseri et al. 2017).

Self-assembled nanocolloidal lapatinib-loaded polymeric micelles were produced. Encapsulation of lapatinib into micelles increased its cytotoxicity against SKBR-3 breast cancer cells. Study findings demonstrate the increasing potential of nanocolloidal polymeric micelles as promising carriers for delivery of lapatinib to tumors (Bonde et al. 2020).

Another study showed that in multidrug-resistant breast cancer, the production of chitosan-coated PLGA nanoparticles providing the combination of paclitaxel and lapatinib had effective cytotoxicity against BT-474/TR cells. This suggests that it may be one of the promising formulations in the treatment of MDR1-mediated chemoresistance in HER2-positive breast tumors (Pitchika and Sahoo 2022).

Lapatinib-loaded gold nanorods, synthesized to combine photothermal and pharmacological activities, showed photothermal activity. The combined application of laser irradiation and lapatinib-loaded nanorods yielded higher anticancer activity against HER2-positive SKBR-3 breast cancer cells compared to monotherapies (Papaioannou et al. 2023).

Lipid-based nanoparticles were designed to combine lapatinib with siRNA directed against the apoptosis inhibitor protein Survivin (siSurvivin) in an injectable form. It is a nanosystem consisting of chitosan grafted via transacylation reaction and lipid nanocapsules coated with a cationic polymeric shell. Cytotoxicity studies confirmed that lipid-based nanoparticles was not toxic to cells at the concentrations tested. The findings suggested that the developed lipid-based nanoparticles could potentiate the anti-cancer activity of anti-Survivin siRNA and lapatinib (Eljack et al. 2022).

1.6. Encapsulation of Lapatinib into ZIF-8 (LAP@ZIF-8)

Lapatinib, a TKI, is limited in use for some toxicity reasons. These reasons are due to its extensive albumin binding capacity, poor aqueous solubility, poor bioavailability, high binding affinity to blood proteins, and high dose. The fabrication of delivery systems such as nanoparticles, micelles, nano capsules, nanochannels and liposomes contribute to solving these challenges. The development of active/passive targeting via non-oral routes and the formulation of a nanocarrier drug system with fewer side effects due to the side effects of conventional lapatinib therapy are needed in the pharmaceutical field in breast cancer treatment (Bonde et al. 2018).

Various study results show that, thanks to its pH sensitivity, ZIF-8 can selectively release small molecule drugs in an acidic environment, thereby providing controlled release of drugs, indicating that ZIF-8 is an excellent drug delivery system (Q. Wang et al. 2020).

One of the MOFs, ZIF-8, is a potential carrier for anticancer drugs. The pore opening of ZIF-8 is 3.4 Å in diameter and the pore gap is 11.6 Å in diameter. Therefore, large molecules cannot enter the pores. However, post-synthesis approaches result in low loadings and rapid or poorly controlled release of molecules. Various post synthetic approaches have been developed, such as preparing hollow ZIFs and adsorbing molecules to outer surfaces. These approaches are meant to overcome limitations. The method that

enables the incorporation of the molecule and nanoparticles into the MOF crystal at the same time is the one-pot method. This method is an approach combining MOF synthesis and molecule encapsulation. High loading is obtained with the one-pot synthesis method (H. Zheng et al. 2016).

A pH sensitive drug delivery system that releases drugs only in the cancer/tumor region, not in the general circulation, that is, in a healthy environment, will reduce the systemic side effects of chemotherapy and will continue to be desirable for cancer treatment (Helmlinger et al. 1997).

1.7. The Aim of This Thesis

The aim of this thesis is to develop and characterize a biocompatible, biodegradable, pH-sensitive, cytotoxic nanoparticle system for the treatment of breast cancer and to examine the in vitro biological effects of the developed nanosystem. The nanoscale size of the system to be created will ensure effective drug transport into the cells. At the same time, this study aims to improve lapatinib's low water solubility, its effectiveness decreasing before reaching the relevant area, and many side effects it causes in biological systems. It is aimed to make the treatment more economical and reduce the side effects of the drug, thanks to the less use of lapatinib, which has a high cost.

For these purposes, LAP@ZIF-8 nanoparticle will be synthesized by encapsulating the drug lapatinib, a small chemotherapeutic molecule, into the ZIF-8, a member of the metal organic framework family, as a drug delivery material. ZIF-8, which is used in the literature to encapsulate different drug active ingredients such as DOX, 5-FU and 6-MP, will be used as the carrier system in which lapatinib is encapsulated for the first time in this study. The synthesized LAP@ZIF-8 nanoparticle will be characterized by measuring Scanning Electron Microscope (SEM), Energy Dispersive X-ray spectrometer (EDX), Fourier-Transform Infrared (FTIR) spectroscopy, X-ray Diffraction (XRD), Thermal Gravimetric Analysis (TGA), Dynamic Light Scattering (DLS) and Zeta potential, and measurements will be taken using ultraviolet-visible (UV-vis) spectrometer to determine the amount of lapatinib loaded on ZIF-8. Cytotoxic effects of LAP, ZIF-8 and LAP@ZIF-8, for which biocompatibility and release experiments will be performed, will be investigated on breast cancer cell lines SKBR-3 (HER2-positive breast cancer cell line) and MCF-7 (HER2-negative breast cancer cell line).

CHAPTER 2

METHODS AND MATERIALS

2.1. Materials

All chemicals used in the experiments are presented in parentheses for each chemical in the method sections. Additionally, details of the preparation of the solutions used are presented in Appendix A.

2.2. Methods

2.2.1. Synthesis of ZIF-8 and LAP@ZIF-8

ZIF-8 ($C_8H_{10}N_4Zn$) nanoparticles were synthesized by one-pot method and this synthesis was carried out with Zn^{2+} :2-MeIm: H_2O molar ratio of 1: 70: 1238 (Pan et al. 2011; Kaur et al. 2017). 58.5 mg of $Zn(NO_3)_2 \cdot 6H_2O$ (zinc nitrate hexahydrate) was weighed (Radwag AS 82/220.X2 analytical balance) into a vial and dissolved with 0.4 mL of deionized water. 1135 mg of 2-MeIm ($C_4H_6N_2$, Sigma-Aldrich) was weighed into another vial and dissolved with 4 mL of deionized water. The linker solution was stirred (DLAB MS-H-S-10 stirrer) magnetically until completely dissolved in deionized water, and then 0.6 mL of dimethyl sulfoxide (DMSO, HoneyWell) was added into it. Zinc nitrate solution was then added to the linker solution, immediately forming a milky white solution. The mixture was stirred at room conditions for approximately 15 min. At the end of mixing, the solution was transferred to eppendorfs and centrifuged (DLAB D2012Plus centrifuge) at 13500 rpm for 15 min to form a white precipitate. For unreacted substances, the solution was washed three times with 30% ethanol (TekkimLab). At the end of washing, the solution was allowed to dry and ZIF-8 nanoparticles, which appeared as white powder, were obtained.

For the synthesis of LAP@ZIF-8, similar synthesis steps were applied with the ZIF-8 nanoparticle synthesis method. It was prepared using various amounts (0.75 – 1.5

– 3 – 5 mg of lapatinib) for the optimization of LAP@ZIF-8. In this study, lapatinib is used in the form of lapatinib ditosylate. It was purchased from Xi'an Ruixi Biotechnology Co., Ltd (Xi'an, China). Lapatinib was dissolved in DMSO and added to 2-MeIm solution. Afterwards, this mixture was added to the dissolved zinc nitrate and the solution was stirred. Other steps were performed as in ZIF-8.

2.2.1.1. The Synthesis Yield of ZIF-8

The yield of ZIF-8 was defined as the ratio of the amount of solid product obtained from synthesis mixture to the maximum possible amount of ZIF-8 that can be produced from synthesis mixture if all limiting reactant is consumed. The synthesis yield value of the ZIF-8 was calculated using the amount obtained as a result of the synthesis, and the following formation reaction of ZIF-8:



2.2.2. Characterization of ZIF-8 and LAP@ZIF-8

2.2.2.1. Encapsulation Efficiency and Drug Loading

The nanoparticles were synthesized, and encapsulation efficiency and drug loading were determined by gravimetric method using UV-vis spectrometer (Shimadzu-UV-2550, Japan and PekinElmer LAMBDA Bio+). Supernatants were collected during the washing step of the synthesis of LAP@ZIF-8. To determine the drug loading efficiency, the supernatant was analyzed by UV-vis spectrometer at a wavelength of 270 nm (max absorbance of lapatinib) (Taskar et al. 2012).

The calibration curve shown in the Figure 2.1 was drawn using the absorbance values at 270 nm obtained as a result of the measurement and 2.5 - 80 $\mu\text{g/mL}$ lapatinib concentrations in DMSO by using UV-vis spectrometer. The equation obtained from the calibration curve was used to calculate the amount of lapatinib encapsulated.

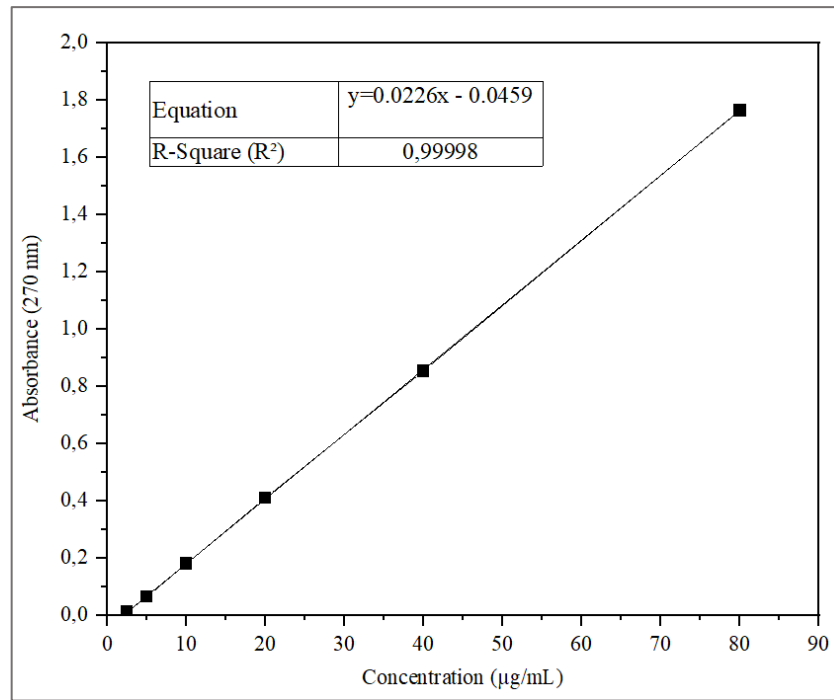


Figure 2.1. The calibration curve of lapatinib

The amount of lapatinib encapsulated into the nanoparticle was determined by an indirect method. Free lapatinib was determined by the UV-vis spectrophotometric method in the supernatant after three wash cycles. Supernatant concentration calculation was calculated using Equation 2.1 and 2.2.

$$Y_{(\text{absorbance})} = 0.0226 \times X_{(\text{concentration})} - 0.0459 \quad (2.1)$$

Equation 2.2 (C_s : supernatant concentration, V_1 : taken volume of lapatinib supernatant, C_2 : concentration found by using Equation 2.1 - $X_{(\text{concentration})}$, V_2 : taken DMSO volume to dilute it) was used to determine the concentration of the supernatant used with the $X_{(\text{concentration})}$ value found using supernatant absorption. The concentration of the prepared solution was calculated by using Equation 2.3, where C_1 is lapatinib stock concentration (mg/mL), V_1 is the lapatinib volume taken for synthesis, C_2 is prepared solution concentration and V_2 is total synthesis volume. The amount of lapatinib encapsulated was calculated using Equation 2.4.

$$C_{(\text{supernatant})} \times V_1 = X_{(\text{concentration})} \times V_2 \quad (2.2)$$

$$C_1 \times V_1 = C_{(\text{prepared solution concentration})} \times V_2 \quad (2.3)$$

$$\text{Amount of lapatinib encapsulated} = C_{(\text{prepared solution concentration})} - C_{(\text{supernatant})} \quad (2.4)$$

Encapsulation efficiency (EE%) and drug loading (DL%) were calculated based on Equations 2.5 and 2.6, respectively (Levit, Yang, and Tang 2020).

$$EE \% = \frac{\text{Amount of lapatinib encapsulated}}{\text{Amount of the prepared solution of lapatinib}} \times 100 \% \quad (2.5)$$

$$DL \% = \frac{\text{Amount of lapatinib encapsulated}}{\text{Total amount of nanoparticle}} \times 100 \% \quad (2.6)$$

2.2.2.2. Structural Analysis

The shape, size, size distribution, structure and crystallinity, composition, and surface charge of the nanoparticles to be used in the study were analyzed and their characterization properties were determined. Colloidal size and surface (DLS and Zeta potential), microscopic (SEM), spectroscopic (EDX, ERD, FTIR) and thermodynamic (TGA) characterization techniques were used.

DLS (DLS Nano Particle Size Analyzer, Particulate Systems – NanoPlus) analysis is based on the diffusive motion of particles in solution, where larger particles move slower and smaller particles scatter more light. The hydrodynamic diameter measured by DLS shows how the particle moves in the liquid.

Zeta potential (ζ -potential) occurs between the particle and the liquid in which the particle is located. It is affected by the surface structure of the particle and the content of the liquid it is in. The charge on the nanoparticle surface depends on the solution pH, and since the hydrogen ion (H^+) is the potential determining ion in many systems, the zeta potential varies with the pH of the liquid in which the particle is located. While the numerical magnitude of the zeta potential indicates the stability of the sample, its sign indicates whether positive or negative charges predominate on the surface. Nanoparticles with a zeta potential value of 0-5 mV tend to cluster or come together, while nanoparticles with a zeta potential value of 5-20 mV are minimally stable. Nanoparticles with a zeta

potential value of 20-40 mV are moderately stable, while nanoparticles with a zeta value potential of 40 mV and above are extremely stable. The size distribution and potential of the nanoparticle in the aqueous environment was determined by using Zeta Potential Analyzer (Particulate Systems - NanoPlus).

The dimensions of the nanoparticles were determined by SEM (FEI QUANTA 250 FEG) measurement. Based on the principle of scanning the particle surface with high-energy electrons focusing on a very small area, information about the particle size and arrangement of the particles is obtained from the images obtained at both micro and nano scales in SEM. The images obtained by SEM analyzes gave information about the structural properties of the nanoparticle (such as porosity, layer thickness, morphology) (Ateş 2018).

EDX (FEI QUANTA 250 FEG) spectroscopy was used to determine the elemental composition of nanoparticles. EDX is based on the creation of characteristic X-rays that provide information about the presence of elements in the samples to be examined. EDX is used together with SEM. Near-surface element contents of nanoparticles can be determined quantitatively and qualitatively, and mapping can be done by analyzing their amounts in different locations (Scimeca et al. 2018).

The degree of crystallinity and impurity of the nanoparticles were determined by XRD (Philips X'Pert Pro diffractometer - Royal Philips Electronics, Amsterdam, The Netherlands) device measurement. It is an analytical technique that provides information about various crystal forms or phases in the structures of solid and powder samples. In the XRD device, the produced X-rays are refracted after being directed to the sample and the refracted rays are determined and counted. The sample is not destroyed in the analysis performed using a very small amount of sample.

Functional groups in nanoparticles were examined by FTIR (PerkinElmer Spectrum Two FTIR Spectrometer), spectroscopy analysis. The bonds and functional groups in the nanoparticle structure are characterized by FTIR, which is based on the principle of vibrational movement of the bonds in the structure due to the interaction of infrared light with a substance with a dipole moment (Ateş 2018).

Thermal stability of nanoparticles was examined by TGA (Perkin Elmer Diomand TG/DTA). In TGA, changes in the mass of the sample are measured as the temperature is increased.

2.2.2.3. Drug Release Study

Tumor cells have an acidic pH due to their rapid metabolism and anaerobic respiration. ZIF-8 has been shown to dissociate in acidic buffer by Xin-Long Wang and colleagues (Sun et al. 2012). This encourages current drug release kinetics to control at pH 5.5, which mimics the inner environment of tumor cells; where, controlled decomposition of ZIF-8 supported by acidic pH liberates lapatinib. In addition, release studies were performed at physiological pH 7.4. Dynamic membrane dialysis method was used to investigate the *in vitro* release properties of the nanoparticle. The dialysis membrane technique is a widely used technique to evaluate drug release from nanosized carriers, as summarized in Figure 2.2.

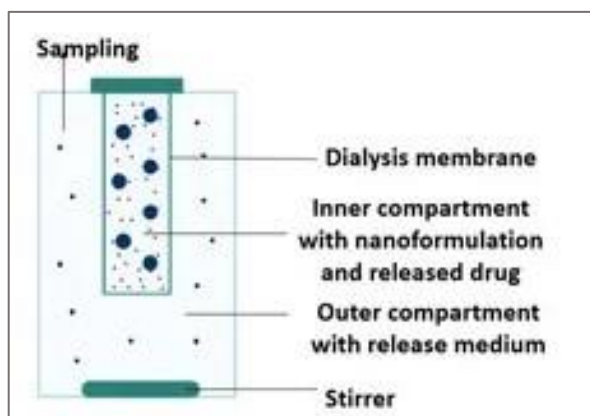


Figure 2.2. Schematic representation of the dialysis membrane method (Gómez-Lázaro et al. 2024)

This technique is based on placing a free drug in a dialysis container that acts as a dialysis membrane and release medium, passing a free drug through the membrane while nanoparticles are retained and determining the drug released from there. Generally, the dialysis membrane volume (usually 1-10 mL) must be smaller than the release medium (usually 40-500 mL) to ensure diffusion of the drug under sink conditions (Gómez-Lázaro et al. 2024). Dialysis membrane (MWCO 14000 Dalton, 34mm, TX0111, BioBasic) was used in the release study. Consequently, the release kinetics were investigated in PBS at pH = 7.4 and 5.5 at physiological temperature (37°C). Firstly, 6 mg of the LAP@ZIF-8 was dispersed in 2 mL of PBS (pH 5.5 or 7.4) by using sonicator (Elma - Ultrasonic Cleaners - Elmasonic S). The solution was transferred into the dialysis membrane and immersed in container containing 40 mL pH 5.5 or pH 7.4 of PBS. Then,

shaking was performed with a stirrer at 37°C. Samples were taken at certain time intervals and lapatinib concentration was measured at 270 nm (maximum absorbance peak given by the drug) on a UV-vis spectrometer (PekinElmer LAMBDA Bio+). The cumulative release % of lapatinib was calculated according to the following formula (Equation 2.7) (X. Feng et al. 2022):

$$\text{Cumulative Drug Release \%} = \sum_{i=1}^n M_i / M_0 \times 100 \% \quad (2.7)$$

where M_i is the amount of lapatinib released from LAP@ZIF-8 at time i and M_0 is the total amount of loaded drug in LAP@ZIF-8.

2.2.2.4. Biocompatibility Assays

2.2.2.4.1. Serum Protein Binding

Possible binding of samples to serum proteins was evaluated by analysis using the bicinchoninic acid (BCA) Protein Assay Kit (The Pierce, Thermo Fisher Scientific). To determine protein binding rates to the drug carrier system, the method applied by Cole et al. (Cole et al. 2011) and Semete et al. (Semete et al. 2012) were modified and used. Protein standards were prepared using the guidance included in the

Protein Assay Kit. Absorbance values were read at 595 nm against blank (distilled water). Using these absorbance and protein standard values, the bovine serum albumin (BSA) standard calibration curve in the Figure 2.3 was drawn.

Fetal bovine serum (FBS, Gibco): samples were prepared at various ratios (50:50; 60:40; 70:30; 80:20; 90:10 (v/v - volume per volume) with a total volume of 1000 μ L. Samples were incubated at 37°C (body temperature) water bath and 150 rpm for 2 h. Since it is known that drugs are eliminated from the body in approximately 2 h, the incubation period was 2 h. After incubation, the samples were centrifuged at 13500 rpm for 15 min.

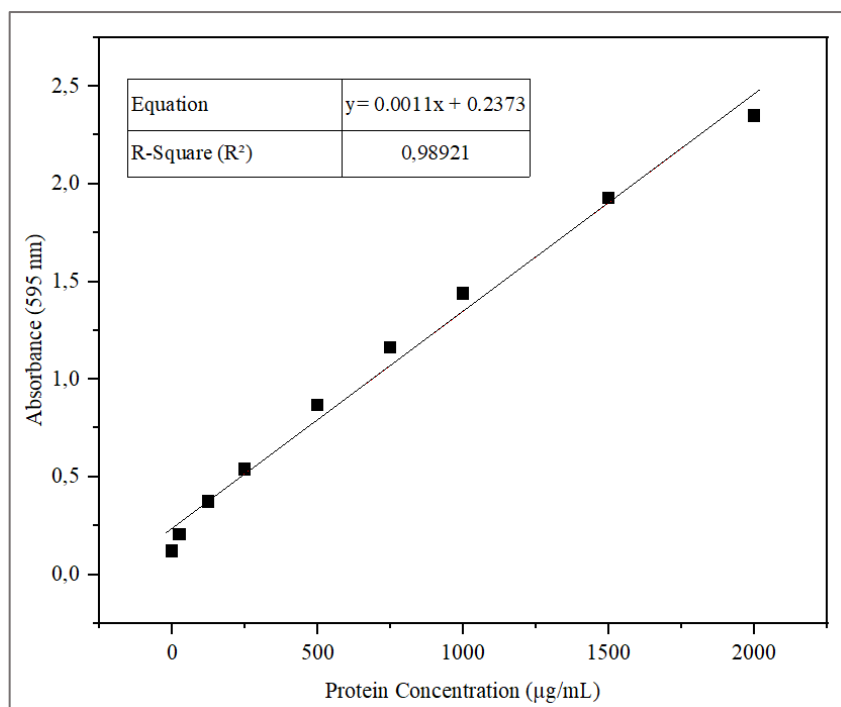


Figure 2.3. BSA standard calibration curve

Reagent A, a carbonate buffer containing BCA reagent, and Reagent B, a cupric sulfate solution, which were mixed to make a green colored working solution. After centrifugation, 1800 μL of BCA reagent (reagent A + reagent B) (working solution that will turn purple after 30 min at 37°C in the presence of protein) was added into 200 μL of samples. Samples containing BCA reagent were mixed in water bath at 37°C for 30 min. Absorbance values were read at 595 nm against blank. Protein determination was performed in the supernatant according to the Bradford method (Bradford 1976), and the percentage of binding to serum proteins was calculated based on the remaining unbound protein in the supernatant. Using the prepared BSA standard calibration curve, the amounts of initially added protein and the amount of unbound protein were calculated. The amount of unbound protein was subtracted from the amount of initially added protein and the amount of bound protein was obtained. The protein binding percentages were calculated using Equation 2.8.

$$\text{Protein Binding \%} = \frac{\text{Concn (Initial protein)} - \text{Concn (unbound protein)}}{\text{Concn (initial protein)}} \times 100\% \quad (2.8)$$

2.2.2.4.2. Hemocompatibility (Hemolysis)

The damage caused by nanoparticles on erythrocytes was determined by *in vitro* hemolysis assay. To determine the amount of hemolysis, the study of Mayer et al. (Mayer et al. 2009) and the method applied by Yallapu et al. (Yallapu et al. 2015), were used.

Hemolysis caused by samples was evaluated photometrically. Two tubes of blood taken into EDTA tubes were centrifuged at 13500 rpm for 15 min to remove plasma and leukocytes. This process was repeated three times. The pellet consisting of erythrocytes was washed two times with 1x PBS (pH 7.4). Erythrocytes were washed with PBS and suspended in PBS to a final concentration of 2%. Samples of varying concentrations (2 µg/mL, 10 µg/mL ve 20 µg/mL) and erythrocyte suspension were prepared in a 1:1 ratio and incubated at 37°C and 100 rpm for 4.5 h. As positive (100% hemolysis) and negative (0% hemolysis) hemolysis controls suspensions of erythrocytes in 1% Triton X-100 (non-ionic surfactant, Amresco) and PBS were used, respectively. After incubation, all samples were centrifuged (NÜVE NF 800R) at 4100 rpm for 10 min and the supernatants were used for measurement.

Free hemoglobin in the supernatant was measured photometrically at 540 nm. Hemolysis percentage was calculated using Equation 2.9 (Yallapu et al. 2015).

$$\text{Hemolysis \%} = \frac{\text{Abs (sample)} - \text{Abs (negative control)}}{\text{Abs (positive control)}} \times 100\% \quad (2.9)$$

2.2.3. *In Vitro* Investigation of Cancer Activity

2.2.3.1. Cell Lines and Culture Medias

SKBR-3 (Figure 2.4), one of the important cancer cell models for HER2-positive breast cancers, is one of the most studied breast cancer cell lines in basic research and preclinical applications. The SKBR-3 (HER2-positive breast cancer cell line) was chosen in this study, as the SKBR-3 genome contains many features of cancer changes such as a set of gene fusions and oncogene amplification (Nattestad et al. 2018).

MCF-7 (Figure 2.5), a breast cancer cell line isolated from a woman in 1970, is named after the Michigan Cancer Foundation. The number 7 in MCF-7 represents Soule's

seventh attempt to create a cancer cell line. MCF-7 cancer cell line is frequently used in breast cancer research (A. V. Lee, Oesterreich, and Davidson 2015).

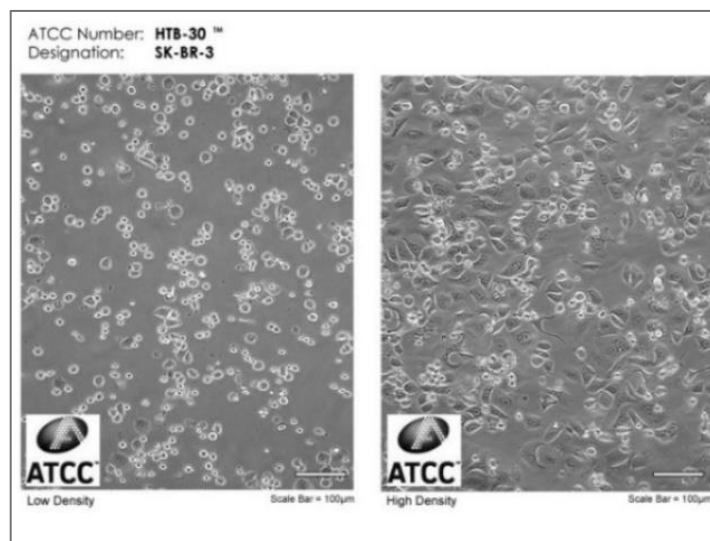


Figure 2.4. Morphological appearance of SKBR-3 cells (“SK-BR-3 [SKBR3] - HTB-30,” n.d.)

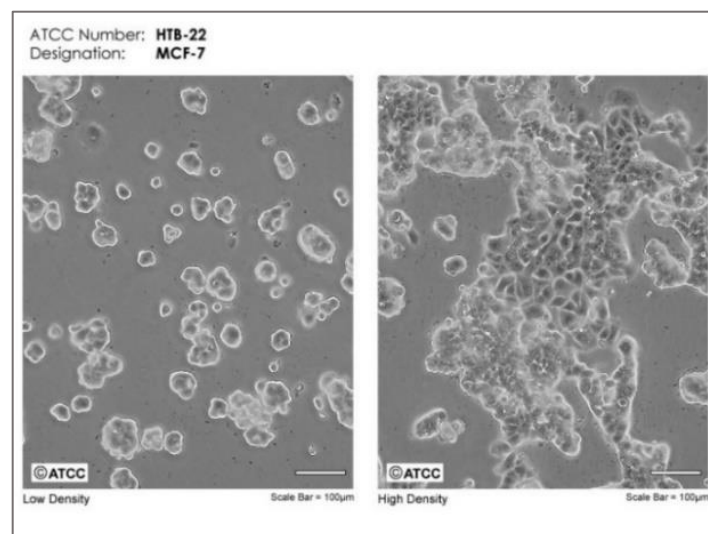


Figure 2.5. Morphological appearance of MCF-7 cells (“MCF7 - HTB-22,” n.d.)

This study was performed using breast cancer cell lines SKBR-3 and MCF-7, and they were obtained from Izmir Institute of Technology - Molecular Biology and Genetics department. SKBR-3 and MCF-7 cells were grown in Dulbecco's Modified Eagle's Medium (DMEM, Gibco) supplemented with 10% FBS, 1% L-glutamine (Biological Industries) and 1% Penicillin-Streptomycin (Biological Industries). Cell culture media

are nutrient solutions that provide the microenvironment necessary for cells to maintain their normal metabolic activities in a laboratory environment. All cells were cultured at 37°C with 5% CO₂ in a humidified incubator (NÜVE EC 160 CO₂ incubator).

2.2.3.2. Passaging (Subculturing) Cells

Sterilization of the cell culture cabinet (NÜVE MN 090 biosafety cabinet) before use was achieved by wiping the interior with the UV light in the cabinet and the prepared 70% ethanol solution. Growth medium and trypsin were heated in a 37°C water bath to be ready for use. The culture medium was changed every time the flask surface reached 80% confluence, the cells were collected with 0.25% (v/v) Trypsin-EDTA (Gibco) and passaged or, in other words, subcultured. To passaging, the old medium was first aspirated, and the cells were washed with sterile PBS (amount depends on cell growth flask size) to remove Ca and Mg salts. Cells adhering to the surface were removed by adding 0.25% (v/v) Trypsin-EDTA (amount depends on cell growth flask size) and incubating for 3-4 min at 37°C and 5% CO₂. The lifted cells were washed by adding some medium, collected in a sterile falcon and centrifuged at 800 rpm for 5 min for the cell pellet. After centrifugation, the supernatant was discarded, and the cells were taken with new medium and placed in a new flask. This flask was then placed in a 5% CO₂ at 37°C incubator for growth.

2.2.3.3. Freezing and Thawing Cells

During the centrifugation phase of the cell passaging process, after the cell pellet was suspended, 10% FBS and 10% DMSO were added, respectively, and transferred to cryotubes. The freezing process was carried out gradually. Cryotubes were frozen at -20°C for 1-2 hours and then frozen at -80°C.

The frozen cells in the cryotube were carefully thawed in a 37°C water bath and transferred to a sterile falcon. 3-4 mL of cell medium was added and centrifuged at 800 rpm for 5 min to remove the DMSO it contained. The supernatant was discarded and resuspended with 4–5 mL of fresh medium. Suspended cells were transferred to a 25 cm² cell culture flask and incubated in a 5% CO₂ at 37°C incubator.

2.2.3.4. Cells Counting and Checking Their Viability

Trypan blue dye (NutriCulture) test was used to determine the viability and number of cultured cells. 100 μ L of dye was added to 100 μ L of suspended cells. Viability and cell number were evaluated under a light microscope using a hemocytometer. For this purpose, areas consisting of 4x4 squares on the hemocytometer were counted. Since trypan blue dye cannot pass through the living cell membrane, it stains dead cells while not staining living cells. Cells that absorbed the dye and appeared blue were considered dead, while cells that did not absorb the dye were considered alive. The Equation 2.10 was used to calculate the number of cells in 1 mL.

$$\text{Viable cells/mL} = \text{average viable cell count/square} \times \text{DF} \times 10^4 \quad (2.10)$$

(DF: Dilution Factor)

2.2.3.5. Determination of Cell Viability by MTT Assay

Cytotoxicity of LAP@ZIF-8 against SKBR-3 and MCF-7 cells using MTT (GoldBio) was investigated. The MTT test, developed by Mosmann in 1980, is frequently used to determine cell viability and proliferation. MTT, the tetrazolium salt used for the test, detects live cells but not dead cells. Reduction of tetrazolium salts by gaining electrons causes them to transform into a structure called formazan, resulting in a color change. The tetrazolium ring can only be broken by active mitochondria, and thus only living cells can produce the color reaction. The advantages of the test, which can be used to measure cytotoxicity, are that it is fast and accurate and does not contain any radioisotopes (Mosmann 1983). The MTT compound is yellow in color, while the formed formazan is purple in color and insoluble in water and must be dissolved in a suitable solvent to measure the absorbance. It has been shown that it is appropriate to use DMSO to dissolve the formazan formed in the MTT test (Denizot and Lang 1986). The MTT (3-[4,5-dimethylthiazol-2-yl]-2,5 diphenyl tetrazolium bromide) assay, which determines mitochondrial activity and is based on its conversion to formazan crystals by living cells, is a calorimetric assay. MTT, yellowish tetrazolium dye, gives a water insoluble (lipid soluble) violet-blue formazan solution when reduced by reducing agents present in metabolically active cells. The amount of MTT formazan, which is directly proportional

to the number of viable cells, can be estimated by spectrophotometry. The absorbance of this colored solution can be measured with a spectrophotometer, usually between 500 and 600 nm (van Meerloo, Kaspers, and Cloos 2011).

For this purpose, cells at a concentration of 1×10^4 cells/well were seeded into 96-well cell culture plates. These cells were incubated for 24 h at 37°C, with 95% humidity and 5% CO₂. After 24 h, cells were treated with various concentrations of LAP, ZIF-8, and LAP@ZIF-8. They were dissolved in DMSO using a sonicator. Then, they were diluted in various proportions and added to the plate. After 24-, 48-, and 72-h incubation, 10 µL of MTT solution (5 mg/mL PBS) was added and incubated at 37°C for 4 h. After 4 h, the plates were centrifuged at 1800 rpm for 10 min and the supernatant was removed. Then the formazan crystals were dissolved in 100 µl of DMSO and shaken (IKA KS250 basic orbital shaker) 150 rpm for 15 min to homogenize. They were measured at 570 nm by using microplate reader (Thermo Fisher Scientific Multiskan GO). Cell viability was calculated according to the formula (Equation 2.11) (Mi et al. 2021):

$$\text{Cell Viability \%} = \frac{\text{Abs (sample)} - \text{Abs (blank)}}{\text{Abs (control)} - \text{Abs (blank)}} \times 100\% \quad (2.11)$$

2.2.4. Statistical Analysis

All data were given as mean \pm standard deviation (SD). All experiments were repeated at least three times (n=3). Statistical analysis was done with Excel and GraphPad Prism 9.0.0. MTT analysis results were evaluated by two-tailed paired t-test (for two-group comparison) and one-way ANOVA followed by Tukey multiple comparison test for multiple comparisons (more than two groups). Statistical significance for all analyzes was set at $\alpha = 0.05$. In addition, the results were evaluated by calculating the coefficient of variation for the MTT results. The graphs created to visualize results (except MTT results by GraphPad Prism 9.0.0) were drawn using OriginLab Pro 2024 (OriginLab Corporation, USA).

CHAPTER 3

RESULTS AND DISCUSSION

3.1. Synthesis of ZIF-8, LAP@ZIF-8 and Yield of ZIF-8

ZIF-8 and LAP@ZIF-8 were produced by the one-pot method. The yield of ZIF-8 synthesis was calculated as a percentage by considering the amount of substance synthesized and the synthesis reaction. As a result of the calculation, the yield was determined as 58.52 ± 2.44 %. This result is shown as mean percentage and standard deviation.

3.2. Characterization of ZIF-8 and LAP@ZIF-8

3.2.1. Encapsulation Efficiency and Drug Loading

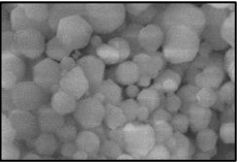
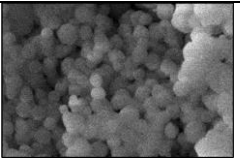
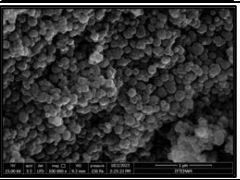
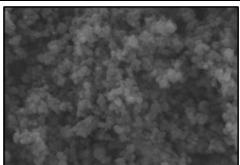
Syntheses were performed using various amounts of lapatinib to optimize the amount of drug to be used for LAP@ZIF-8 synthesis. The synthesized LAP@ZIF-8 was examined in terms of drug loading and encapsulation efficiency and are shown in the Table 3.1.

The results in trial 1 showed that the drug was not loaded. In addition to encapsulation efficiency and drug loading, the SEM images of the samples were examined structurally. Considering the encapsulation efficiency and drug loading, although the highest results were found in the trial 4, the SEM image could not be examined, and the diameter calculation could not be made. Among the structurally examined trials, trial 3 was found to have the best SEM image and optimal encapsulation efficiency and drug loading. It was decided that the most suitable one in terms of both structural, encapsulation efficiency and drug loading was the LAP@ZIF-8 synthesized using 3 mg of lapatinib. It was decided to use this synthesis material for further studies.

According to these result, LAP@ZIF-8 (trial 3) showed a high encapsulation efficiency of 72.42% with a drug loading of 6.55%. This indicates that 2.173 mg of

lapatinib was loaded into LAP@ZIF-8. The calculation of encapsulation efficiency and drug loading was shown in detail in Appendix B.

Table 3.1. The calculated EE% and DL% of different trials of LAP@ZIF-8 (additionally, SEM images of trials). The concentration of $Zn(NO_3)_2 \cdot 6H_2O$ and 2-MeIm remained same in all the synthesis.

	Amount of lapatinib used in sythesis (mg)	EE %	DL %	Images of SEM
Trial 1	0.75	-	-	
Trial 2	1.5	50.24	2.20	
Trial 3	3	72.42	6.55	
Trial 4	5	85.30	12.15	

3.2.2. Structural Analysis

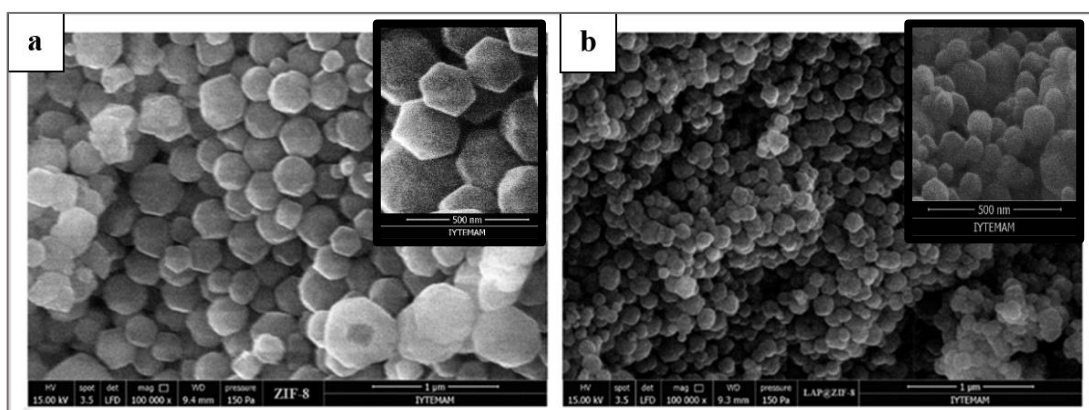


Figure 3.1. SEM images of (a) ZIF-8 and (b) LAP@ZIF-8

The surface morphology and particle size of ZIF-8 and LAP@ZIF-8 were observed by SEM, as shown in Figure 3.1. The size of ZIF-8 was found to be 155.7 ± 54 nm, while LAP@ZIF-8 was 132.3 ± 30.7 nm, and the diameter of 100 nanoparticles was measured using the Image J program for this average particle size analysis. The size values calculated for ZIF-8 as a result of SEM were found to be comparable to similar results in the literature (Schejn et al. 2014). It can be clearly seen that the ZIF-8 and LAP@ZIF-8 nanocrystals are hexagonal in shape, which is the typical ZIF-8 morphology (S. Liu et al. 2011). The average particle size of ZIF-8 and LAP@ZIF-8 was found to be 263.5 ± 4.8 nm and 236.1 ± 2.4 nm, respectively, from DLS analysis (Figure 3.2). The polymer dispersion index (PDI) of ZIF-8 and LAP@ZIF-8 were obtained as 0.230 ± 0.016 and 0.173 ± 0.015 , respectively. Size measurement is carried out with particles in dry form by SEM, while the hydrodynamic size is determined in aqueous medium by DLS. SEM cannot be compared with DLS, which gives higher values due to various non-covalent interactions of nanoparticles with solvent molecules. In the literature, the difference between the average dimensions obtained due to the procedures of DLS and SEM analysis has been observed and shown. PDI refers to the variance of the size distribution of nanoparticles. The results showed that LAP@ZIF-8 gave a lower PDI value reflecting more consistent and equal-sized particles than ZIF-8. Therefore, LAP@ZIF-8 was observed to be more monodisperse and have greater particle stability compared to ZIF-8 (Vasić et al. 2020).

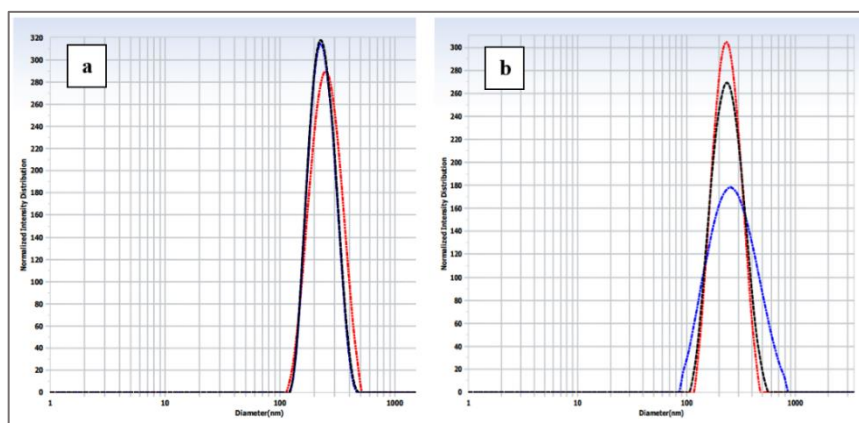


Figure 3.2. DLS measurements of (a) ZIF-8 and (b) LAP@ZIF-8

This decrease in size was also confirmed by SEM images. This may be because lapatinib limits crystal growth upon encapsulation into the system (N. Wang et al. 2022).

In another study, the hydrodynamic dimensions after lapatinib loading were lower than those of empty nanoparticles; this demonstrated that encapsulating a hydrophobic drug into the internal hydrophobic cavity of the nanostructure resulted in smaller particles (S. Y. Lee and Cho 2019). In addition, it is thought that the positively charged ZIF-8 surface may have been attracted to the negatively charged groups of lapatinib and clustering may have occurred between the two, causing a decrease in diameter. In the literature, it is seen that the sizes of nanoparticles containing lapatinib vary widely below 200 nm. It has been reported in various articles that particle sizes below 200 nm are suitable for cancer cell uptake, while nanoparticles between 100-200 nm accumulate in cancerous tissues due to the EPR effect (Huo et al. 2015). This shows that the particle size of LAP@ZIF-8 is compatible with the literature. Zeta potential of the ZIF-8 and LAP@ZIF-8 was $+32.13 \pm 1.18$ and $+29.49 \pm 0.75$ mV respectively (Figure 3.3). The positive surface charge of ZIF-8 is attributed to the metal components (Zn^{2+}) on its outer surface (Oh et al. 2023). Insignificant difference between zeta potential values; it shows that lapatinib molecules coordinate with Zn^{2+} and are located within the nanoparticle. It is thought that the reason for the decrease in zeta potential is due to the negatively charged elements in the structure of lapatinib. This decrease also confirms the presence of lapatinib in the nanoparticle. It has been shown in the literature that the zeta potential values of nanoparticles obtained by encapsulating the chemical into ZIF-8 are similar to the value decrease after encapsulation (Jiang et al. 2018), and that ZIF-8 synthesized in another article also has similar value (M. Wang et al. 2022; Jongert et al. 2024). In addition, studies in the literature have observed that the zeta value obtained as a result of nanoparticle encapsulation of lapatinib is a positive value (H. Gao, Chen, et al. 2014; Wan et al. 2016). Based on the zeta potential values of the synthesized nanoparticles, it can be said that the particles have a stable structure.

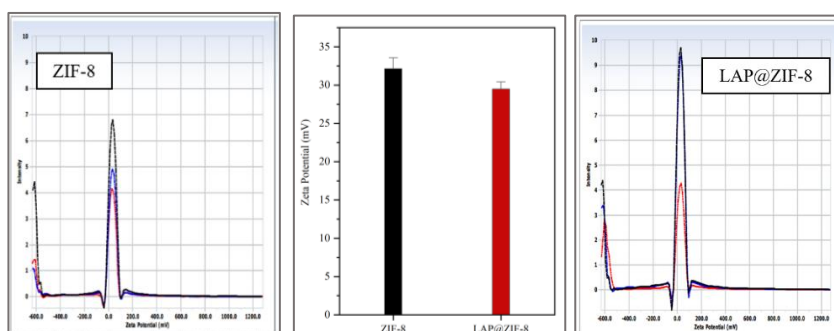


Figure 3.3. Zeta potentials of ZIF-8 and LAP@ZIF-8

Nanoparticles show a high affinity for the cell membrane, mainly due to electrostatic interactions. Cancer cell surface become negatively charged in the case of cancer, when negatively charged components such as phosphatidylserine, anionic phospholipids, glycoproteins and proteoglycans in the inner layer of the cell membrane settle on the cell surfaces. Cell membrane are known to have large negatively charged areas that should repel negatively charged nanoparticles. After adsorption of nanoparticles to the cell membrane, uptake occurs through several possible mechanisms, such as pinocytosis, nonspecific or receptor-mediated endocytosis, or phagocytosis. Positively charged nanoparticles are preferentially taken up by tumors. Studies show that positively charged nanoparticles bind to the negatively charged surface on tumor endothelial cells through electrostatic interactions. It was showed that a higher cellular uptake, where electrostatic interactions between the negatively charged membrane and positively charged nanoparticles facilitate uptake (Honary and Zahir 2013).

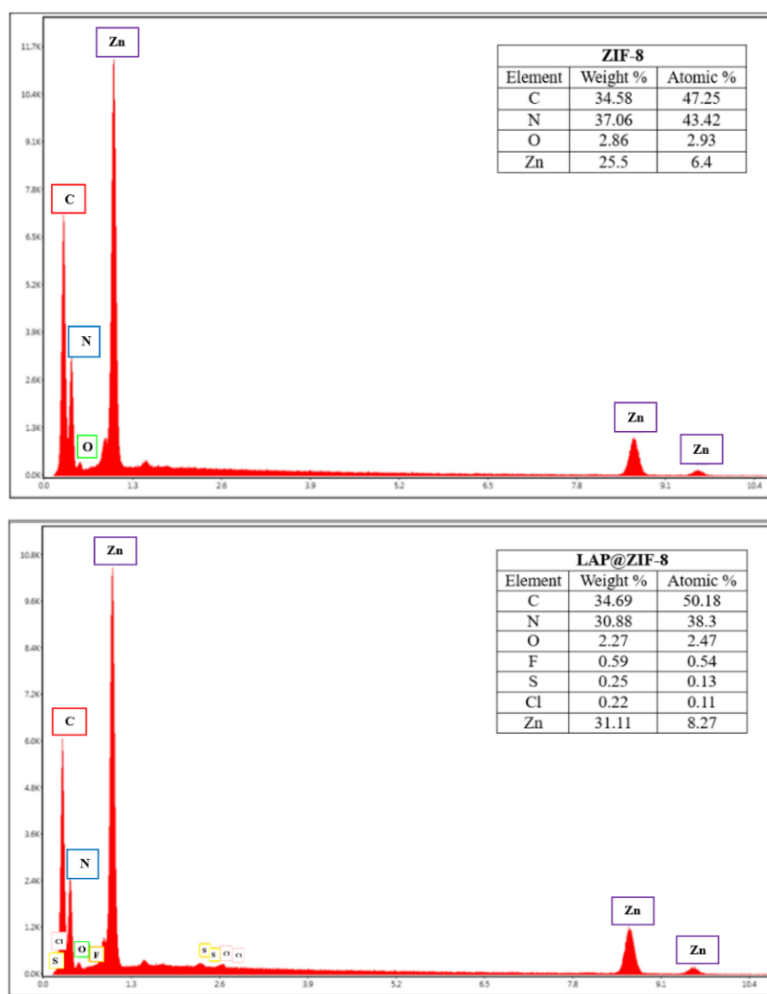


Figure 3.4. EDX analysis of ZIF-8 and LAP@ZIF-8

The EDX analysis of ZIF-8 and LAP@ZIF-8 are shown in Figure 3.4. While characteristic elements such as carbon (C), oxygen (O), nitrogen (N) and zinc (Zn) were seen in the EDX spectrum of ZIF-8, the presence of fluorine (F), sulfur (S) and chlorine (Cl) elements found in lapatinib was also seen in LAP@ZIF-8. The EDX spectra of the LAP@ZIF-8 confirmed the incorporation of lapatinib into ZIF-8, as shown by the detection of F, S and Cl elements. The existence of C, N, O and Zn indicates that the nanomaterial contains ZIF-8, while the lapatinib component in the nanoparticle is proved by the presence of F, S, and Cl. The existence of all used elements in the nanoparticles and also the absence of any impurity was proved by EDX analysis. These results showed that the absence of contaminants with confirmation of the elemental composition of lapatinib in formulated LAP@ZIF-8.

The measurement of FTIR was performed for LAP, ZIF-8 and LAP@ZIF-8. The FTIR spectrum of the samples on the 400-4000 cm^{-1} absorption band is shown in Figure 3.5. The LAP peaks were observed at 3150-3050 cm^{-1} (N-H stretch), 3017 cm^{-1} (aromatic -CH stretch), 1690 cm^{-1} (C=N stretch), 1312 cm^{-1} (S=O stretch), 1264 cm^{-1} (C-O stretch), 1160 cm^{-1} (furan C-O-C stretch), 1250-1120 cm^{-1} (C-SO₂ stretch), 1031 cm^{-1} (C-F stretch), 679 cm^{-1} (C=C bend) and 564 cm^{-1} (C-Cl stretch). The characteristic aromatic C=C stretch peaks at 1620 and 1440 cm^{-1} were also visible in FTIR spectrum of LAP (Khan et al. 2021; Mane, Wakure, and Wakte 2022). It presented remarkable bands at 3136, 2932, 1635, 1584, 1456, 1425, 1383, 1311, 1146, 995, 759, 694 and 420 cm^{-1} for ZIF-8 sample. The peaks were observed at 3136, 2932, 1635 and 1584 cm^{-1} corresponding to aromatic C-H asymmetric stretching, aliphatic C-H asymmetric stretching, C=C stretching and C=N stretching vibrations of imidazole respectively. The bands in the spectral region of 1460-1300 cm^{-1} (1456, 1425, 1383 and 1311 cm^{-1}) were associated for the ring stretching, whereas band at 1146 cm^{-1} associated from aromatic C-N stretching mode. The peak at 995 cm^{-1} could be assigned as C-N bending (in-plane ring bending) vibration. The peak at 759 and 694 cm^{-1} were associated as C-H bending mode and ring out-of-plane bending vibration of the 2-MeIm, respectively. Combination of Zn and N to form the imidazolate was confirmed by observing the Zn-N stretching vibration band at 420 cm^{-1} . The results match studies in the literature and demonstrate successful synthesis of ZIF-8 (Y. Zhang, Jia, and Hou 2018).

Several peaks such as 564 cm^{-1} of LAP disappeared in the spectrums of LAP@ZIF-8, indicated the peaks were covered by other components. On the other hand, some LAP peaks broadened, shifted, or disappeared but were still present, indicating the

formation of LAP@ZIF-8. Several peaks in the nanoparticle was shifted in the spectrum, suggesting there was interaction among components in the formation of LAP@ZIF-8.

When the spectra obtained for ZIF-8 were compared with LAP@ZIF-8, it was noticed that the spectra of the two samples were very similar. When the LAP@ZIF-8 spectrum is examined carefully, it can be said that the intensity and sharpness of the peaks have increased. Considering the FTIR spectra, LAP@ZIF-8 overlaps with the spectra of ZIF-8 but does not completely overlap with the spectra of LAP. This result suggests the successful incorporation of LAP into ZIF-8 molecules. Due to the encapsulation within the ZIF-8 framework, the characteristic peaks of LAP are masked, and this encapsulation also protects the drug from degradation caused by the environment (Kaur et al. 2017).

These results confirm that the synthesized nanoparticle contains both ZIF-8 and LAP and, LAP was successfully loaded in ZIF-8.

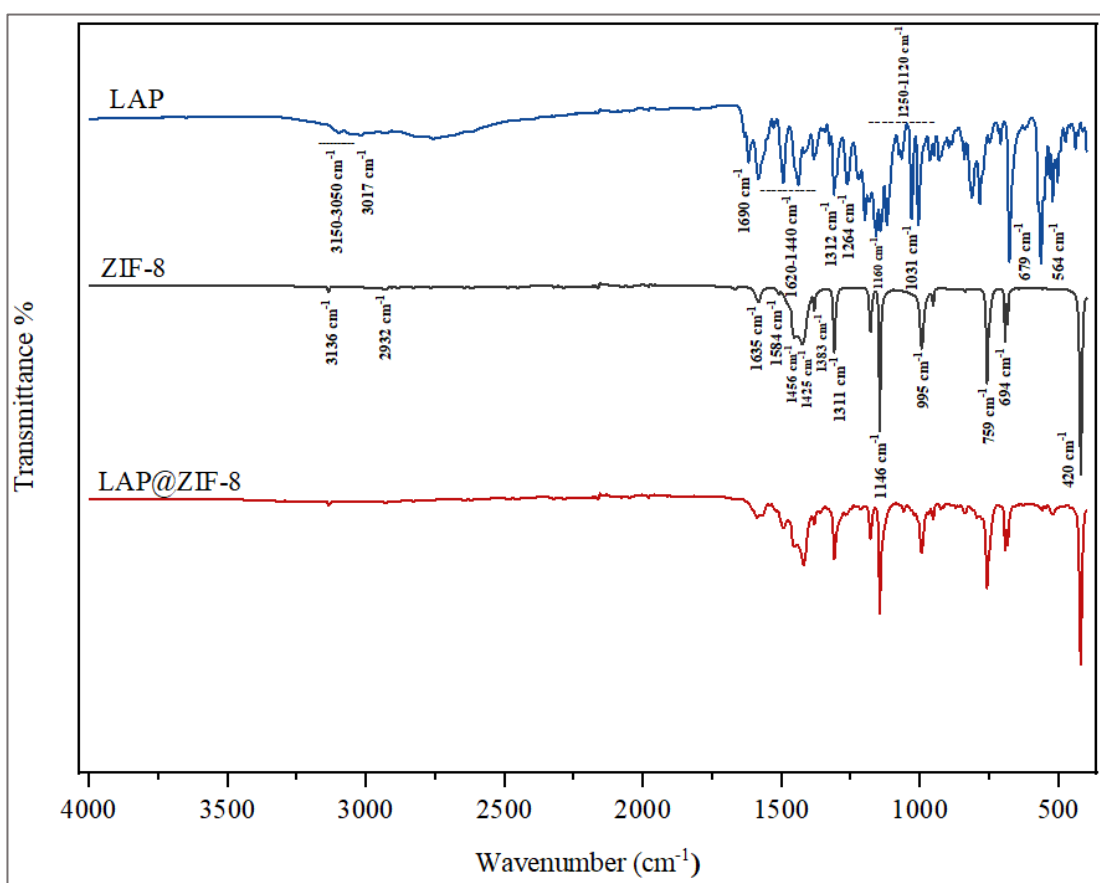


Figure 3.5. FTIR spectra of LAP, ZIF-8 and LAP@ZIF-8

The crystal structures of the synthesized ZIF-8 and LAP@ZIF-8 were identified by XRD and the results are shown in the Figure 3.6. Peak positions and sharp diffraction peaks of ZIF-8 crystals were illustrated between 2θ values of 5 and 40° . A very sharp peak 7.28° was observed in the XRD pattern of the ZIF-8, indicating that a highly crystalline material was achieved. The characteristic diffraction peaks at $2\theta = 7.28^\circ$, 10.34° , 12.68° , 14.67° , 16.40° , 18.00° , 22.12° , 24.48° , 26.67° and 29.66° for ZIF-8 sample were observed, which can be assigned to (011), (002), (112), (022), (013), (222), (114), (233), (134) and (044) planes respectively (Y. Zhang, Jia, and Hou 2018). ZIF-8 nanoparticles showed strong peaks which are in good agreement with previously reported findings (K. S. Park et al. 2006). The other weak peaks at $2\theta = 25.58^\circ$, 30.59° , 31.52° ve 32.38° for ZIF-8 sample were observed, which can be assigned to (224), (334), (244), (235) planes respectively (Gross, Sherman, and Vajo 2012).

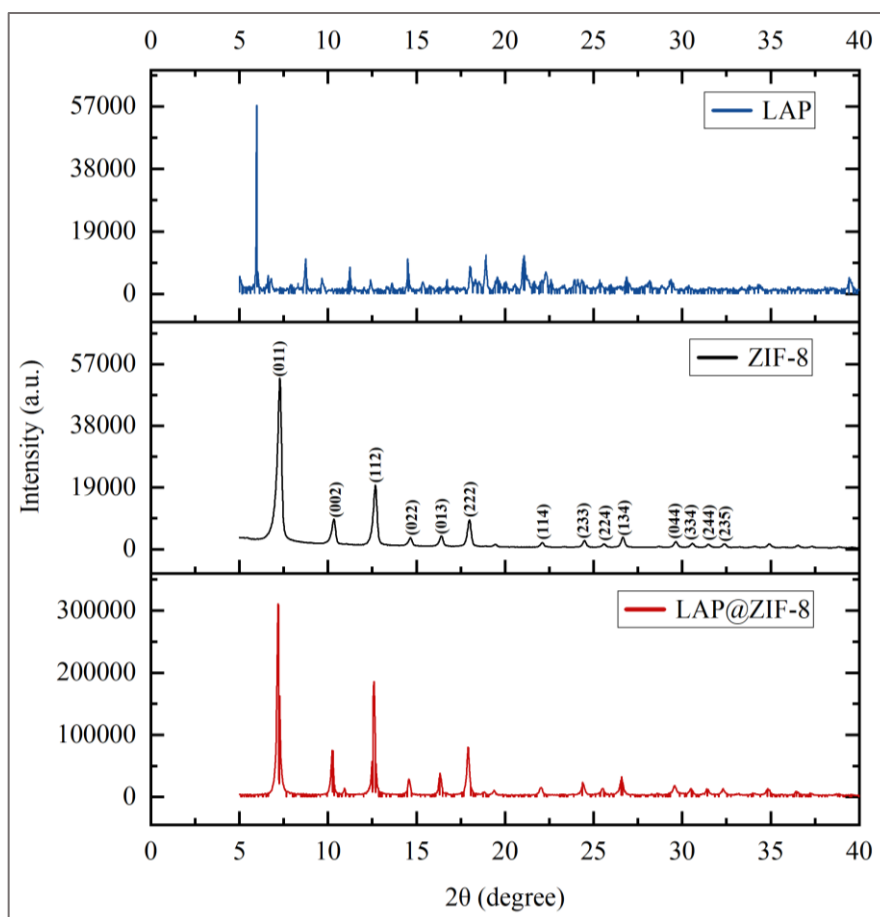


Figure 3.6. XRD pattern of LAP, ZIF-8 and LAP@ZIF-8

It was observed that after LAP loading, the characteristic diffraction peaks of ZIF-8 were weakened, but the main characteristic peaks were essentially unchanged. Solubility is an important criterion for the absorption and effect of drugs. Compared to the crystalline form, the metastable or amorphous drug form dissolves faster due to greater internal energy as well as molecular motion (Prabhu et al. 2021). The observation of the solubility difference between LAP and LAP@ZIF-8 during the experiments proves this. The XRD result of LAP showed much more frequent sharp peaks at higher intensity, while LAP@ZIF-8 showed sharp but less intense peaks. This demonstrated that the crystalline form of LAP was converted to its amorphous form by encapsulation into ZIF-8. This is thought to increase the solubility and bioavailability of the nanoparticle.

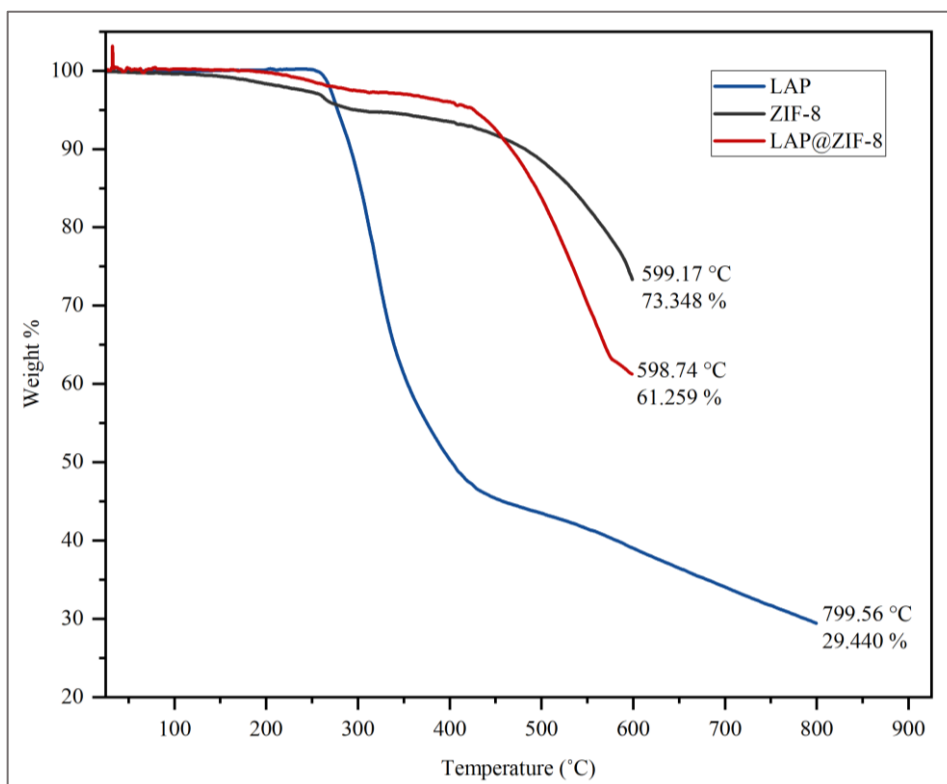


Figure 3.7. TGA curves of LAP, ZIF-8 and LAP@ZIF-8 (LAP: Heat from 25°C to 810°C at 10°C/min, ZIF-8 and LAP@ZIF-8: Heat from 25°C to 610°C at 10°C/min)

The TGA method is used to identify the composition of nanoparticle, evaluate thermal stability and to investigate the loss of material mass due to oxidation, decomposition, or loss of volatile matter. This method results in temperature versus weight percentage. For all samples, the initial weight loss occurs due to physical adsorbed of water. It is thought that the initial weight loss is due to the evaporation/disappearance

of the adsorbed surface water/wetness, while other subsequent weight losses may be due to the evaporation and combustion of organic species in the sample (Rami et al. 2021). Figure 3.7 exhibits the TGA curves of LAP, ZIF-8, and LAP@ZIF-8. Analysis was performed in between 25-800 °C at a constant heating rate of 10 °C/min under air atmosphere. TGA analysis showed that LAP, ZIF-8, and LAP@ZIF-8 samples were stable below ~100 °C. It was observed that the thermal decomposition of LAP started at 245°C and the maximum weight loss was 70.56% at 799.56°C, while the thermal decomposition of ZIF-8 started at 250°C and the maximum weight loss was 26.652% at 599.17°C. It was observed that the thermal decomposition of LAP@ZIF-8 started at 420°C and the maximum weight loss of 38.741% occurred.

In the TGA curve for thermal degradation process of LAP has five stages. In the first point, starting at 25°C and ending at 245 °C, this weight loss is 0.27%. In the second point, starting at 245°C and ending at 285 °C, this weight loss is 7.444 %. The third stage of decomposition, starting at 290 to 350 °C, this weight loss is 36.832 %, which is weight loss steadily decreased could be due to the volatilization and combustion of organic species in the sample. The fourth stage of decomposition, starting at 350 to 470 °C, this weight loss is 12.165 %. The fifth stage of decomposition, starting at 470 to 799.56 °C, this weight loss is 15.1%.

In the TGA curve for thermal degradation process of ZIF-8 has three stages. In the first point, starting at 25°C and ending at 250 °C, this weight loss is 2.692%. This value may be related to the loss of water molecules in cavities or on the surface of ZIF-8. The second stage of decomposition, starting at 250 to 275.5 °C, this weight loss is 1.533%. The loss of only 7.02% of the initial mass at 420 °C proves the high thermal stability of ZIF-8. This value can also indicate the exit of water molecules connected to the ZIF-8 network. The third stage of decomposition, starting at 275.5 to 599.17 °C, this weight loss is 19.578%. The weight loss above 400 °C is due to the decomposition of 2-MeIm molecules. Decomposition of ZIF-8 crystals occurs between 420-599.17 °C and a sudden mass loss is observed. In this range, it was possible to observe a significant mass loss, related to the molecule organic portion degradation, the imidazolate. This situation of ZIF-8, which exhibits a slow degradation, is caused by the thermal decomposition of the inorganic part until zinc oxide is formed. These results are in accordance with previous studies (de Moura Ferraz et al. 2020).

In the TGA curve for thermal degradation process of LAP@ZIF-8 has three stages. The LAP@ZIF-8 was stable up to 420°C and had very minor changes in weight

loss, which is 4.625%. The second stage of decomposition, starting at 420 to 560 °C, this weight loss is 27.814%. The third stage of decomposition, starting at 560 to 598.74 °C, this weight loss is 6.265%. The situation after the loss of water molecules of ZIF-8 indicates the loss of LAP molecules because there is no weight loss of ZIF-8 in this temperature range. The weight loss can be attributed to the decomposition of LAP that is encapsulated in ZIF-8 frameworks. The latter degradation state is due to the thermal degradation of LAP and ZIF-8 along with their carbonization. This weight loss may have caused by the release of water molecules and other absorbed unreacted molecules, such as 2-MeIm, from the pore structure. Subsequently, with the increase of temperature, the skeleton structure of the sample collapses and decomposes, and the structural integrity of the crystal is destroyed. ZIF-8 and LAP@ZIF-8 samples decompose, and zinc oxide is formed. Encapsulation of LAP in the ZIF-8 is clearly evident from the thermal curve of LAP@ZIF-8. The decreased weight loss of LAP suggests that LAP interacts with ZIF-8 through electrostatic interactions and coordination reactions. All these results illustrate that the LAP@ZIF-8 sample has good thermal stability.

3.2.3. Drug Release Study

The ability of the nanocarrier to efficiently release the drug at the desired site is an important feature of delivery system. In Figure 3.8 represents the release of lapatinib from LAP@ZIF-8 in pH 5.5 and pH 7.4. LAP@ZIF-8 showed a controlled release profile in the release environment. In the pH 5.5 environment, 54.92% and 68.43% of lapatinib were released, while in the pH 7.4 environment, 33.52% and 35.99% of lapatinib were released at 24 h and 48 h, respectively. At the end of 96 h, 76.99% and 42.75% of lapatinib was released in pH 5.5 and pH 7.4, respectively. This revealed that the release of lapatinib was greater in acidic pH than in neutral pH. Lapatinib was released continuously for up to 96 h, indicating that lapatinib was encapsulated in the hydrophobic core of the nanoparticle, leaving almost nothing on the surface.

Release of lapatinib from LAP@ZIF-8 after internalization may result in enhanced cytotoxic activity against cancer cells. The slower release at pH 7.4 compared to that at pH 5.5 is beneficial for cancer cell targeting and higher tumor cell inhibition. The slow and relatively low release of lapatinib at the body's physiological pH of pH 7.4 also helps reduce its toxicity on normal tissue. The release state can be considered as

imidazolate protonation in the acidic state, where the coordination link between Zn^{2+} ions and imidazolate is broken, leading to increased lapatinib release from ZIF-8.

Based on the findings, it is hypothesized that lapatinib release can be controlled at pH 7.4 and remain stable in ZIF-8 frameworks; on the other hand, faster release of drugs tends to occur under acidic conditions. Additionally, the solubility of lapatinib increases at pH 5.5 due to increased protonation of the amino groups in lapatinib molecules (El-Bindary et al. 2020). This slow release in pH 7.4 indicated that the hydrophobic pores of ZIF-8 had assisted slow release of hydrophobic lapatinib. The fast release in pH 5.5 was due to the disintegration of the ZIF-8 structure in acidic pH. In general, sustained release exposes cancer cells to the drug continuously, providing an increased likelihood of cell death. This can also reduce drug dose and dosing frequency and increase therapeutic effectiveness in cancer treatment (Huo et al. 2015).

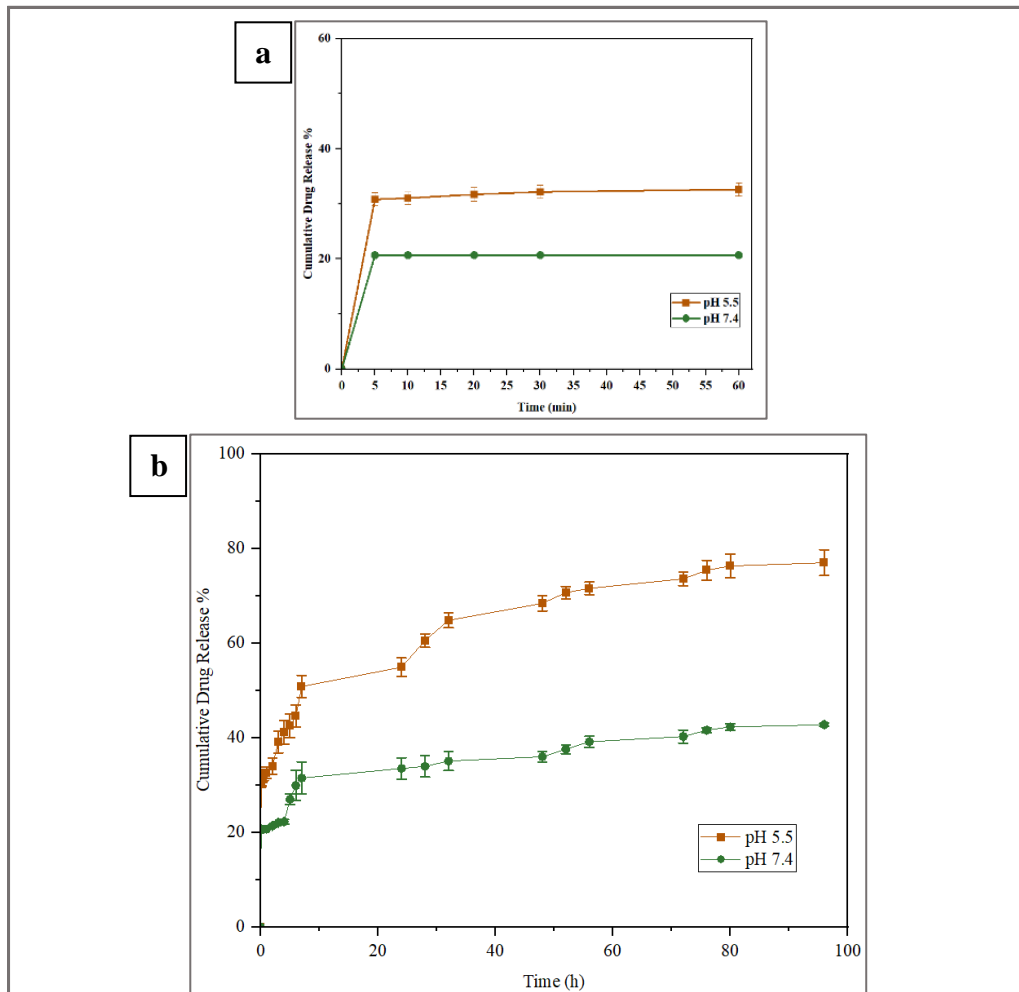


Figure 3.8. Drug release profile of LAP@ZIF-8 in media of different pH for (a) 60 min and (b) 96 h

3.2.4. Biocompatibility Assays

3.2.4.1. Serum Protein Binding

Serum albumin is the most abundant in blood, human serum albumin (HSA) and BSA are the most studied proteins. The interaction of drugs with serum albumin may affect their pharmacokinetic and pharmacodynamic properties, distribution in the body, passage through biological membranes, severity of pharmacological effect and elimination rate. Drugs can be present in the circulatory system either bound to plasma protein or in a free/unbound state. The drug bound to plasma protein is not pharmacologically active. Drugs with strong binding affinity to serum albumin may cause undesirable effects, such as causing a longer half-life of a drug in the body, thus reducing its value as a therapeutic. The unbound drugs interact with their therapeutic targets and exert their effects. (Siddiqui et al. 2021).

Table 3.2. Protein binding percentages of LAP, ZIF-8, and LAP@ZIF-8 (n.d.: not determined)

Sample	$V_{FBS}:V_{Sample}$	Protein Binding % (Mean±SD)
LAP	10:90	n.d.
	20:80	n.d.
	30:70	n.d.
	40:60	n.d.
	50:50	5.36±0.57
	60:40	9.45±2.80
	70:30	15.99±0.44
	80:20	12.26±1.94
	90:10	11.53±0.62
ZIF-8	10:90	n.d.
	20:80	n.d.
	30:70	n.d.
	40:60	n.d.
	50:50	10.46±7.01
	60:40	19.26±3.44
	70:30	15.55±5.54
	80:20	14.11±5.89
	90:10	14.48±8.45
LAP@ZIF-8	10:90	n.d.
	20:80	n.d.
	30:70	n.d.
	40:60	n.d.
	50:50	6.50±2.10
	60:40	6.87±1.65
	70:30	10.39±1.47
	80:20	8.32±2.79
	90:10	5.57±0.90

In the serum protein binding study, the samples were centrifuged with FBS and the binding percentages to serum proteins were calculated based on the unbound protein remaining in the supernatant. Since the amount of plasma protein may vary from person to person, experiments were carried out using different serum and sample concentrations. Table 3.2 shows protein binding percentages. It is seen that the binding percentages with serum proteins change between 5.36 - 19.26%. It appears that there is no linear increase or decrease according to serum/sample ratios and the increase in serum ratio does not have a significant effect on protein binding. When the study by Semete et al. (Semete et al. 2012) was examined, serum protein binding to nanoparticles was around 40%, and in this study, the highest binding was found to be 10.39% in LAP@ZIF-8. Based on the literature information and the obtained trial data, it is expected that the drug will have good pharmacokinetic distribution and accumulate concentratedly in the targeted tissues. It is thought that the nanoparticle can be delivered to the target tissue at high rates due to its non-protein binding or low binding results. When the results are evaluated; it is thought that the samples, especially the LAP@ZIF-8 is biocompatible since the protein binding percentages are low.

3.2.4.2. Hemocompatibility (Hemolysis)

Hemolysis is the breakdown (lysis) of red blood cells and the release of their contents (cytoplasm) into the surrounding fluid. Nanoparticles can easily reach the circulation due to their size and route of administration, and red blood cells (erythrocytes) may be the first biological entity they come into contact with. Hemolysis assay is used to evaluate nanoparticle toxicity resulting from the interaction of nanoparticles with red blood cells. This assay aims to determine the interaction of nanoparticles with the red blood cell membrane and the percentage of released hemoglobin (Hb) (Martinez et al. 2015). Evaluation of the ability of nanoparticles to integrate with blood is described as nanoparticle compatibility. Hemolytic activity (% hemolysis) is calculated by dividing the released hemoglobin concentration by the total hemoglobin concentration in exposed red blood cells. Accordingly, 0%–2% hemolysis is nonhemolytic, 2%–5% is slightly hemolytic, and more than 5% is hemolytic (Malehmir et al. 2023).

An *in vitro* hemocompatibility study was performed. *In vitro* study of hemolysis detects plasma-free hemoglobin derivatives spectrophotometrically following incubation

of particles with blood. Then, undamaged cells are separated by centrifugation and the percentage of hemolysis is evaluated. The percentages of *in vitro* hemolysis results in the experimental groups remained below 2%, which is lower than the 5% acceptable hemolysis limit reported for biomaterials in contact with blood (Figure 3.9). This research showed that the samples showed that in case of blood contact, blood hemolysis did not exceed 5% of the positive control and there was no hemolytic effect.

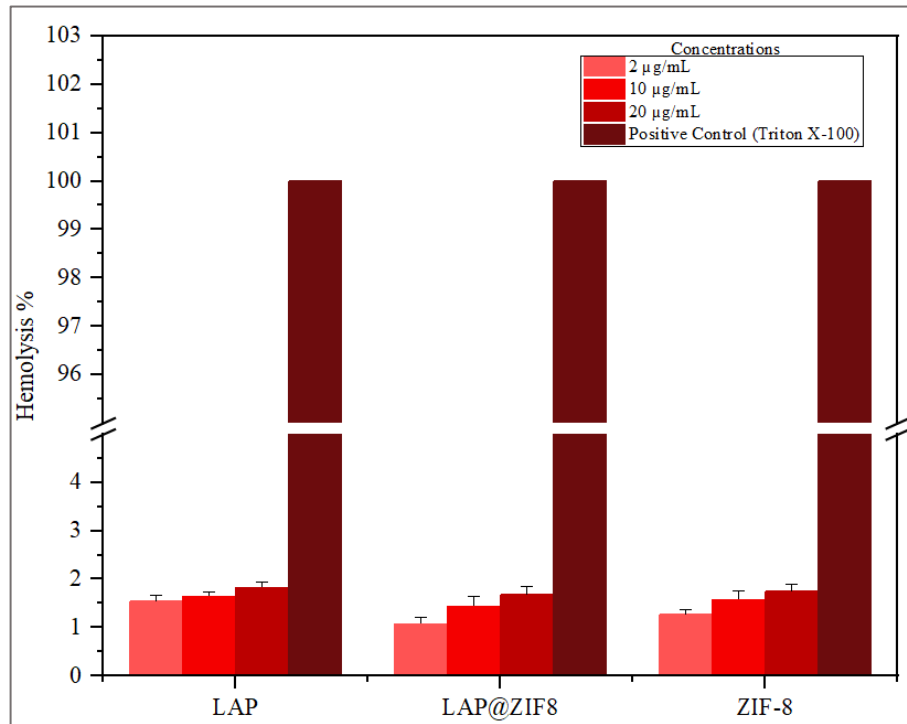


Figure 3.9. Hemolysis percentages of LAP, ZIF-8, and LAP@ZIF-8

The experimental result showed that LAP@ZIF-8 is hemocompatible, harmless to fresh blood (does not show any damage to the red blood cell membrane) and can be used in practical applications related to biological aspects. The hemolytic value of LAP@ZIF-8 was determined as 1.08, 1.44, and 1.68% according to the increasing concentration value, indicating that the hemolytic toxicity of LAP was reduced when encapsulated into ZIF-8.

3.3. *In Vitro* Investigation of Cancer Activity

The cytotoxicity of LAP, ZIF-8 and LAP@ZIF-8 against SKBR-3 and MCF-7 cell lines, and consequently the potential of ZIF-8 used as drug carrier, were evaluated using the MTT assay (Figures 3.10 and 3.11).

It appears that the blank nanocarrier, ZIF-8, does not produce any cytotoxic effects on cancer cells. As shown in the Figure 3.10d and Figure 3.11d, ZIF-8 exhibited a limited effect on the proliferation of both cell lines. Although there was no significant difference, it was observed to be more lethal than SKBR-3 in MCF-7 cells. The fact that cell viability remained above 60% even at the highest concentration tested (100 µg/mL) for two cell lines in addition to almost no cell death at concentrations below this concentration, indicates that ZIF-8 nanoparticles have low cytotoxicity and good biocompatibility. It has been shown in the literature that ZIF-8 has no significant cytotoxicity up to 30 µg/mL, and cytotoxicity above 30 µg/mL is due to the effect of released Zn²⁺ on mitochondrial ROS production (Hoop et al. 2018). When the results were examined, it was seen that ZIF-8 maintained its viability and was compatible with the literature (R. Singh et al. 2021).

The cytotoxic effect of free LAP and LAP@ZIF-8 was tested in SKBR-3 (Figure 3.10a,b,c) and MCF-7 (Figure 3.11a,b,c) cancer cells depending on the incubation time. As shown in Figures, both formulations showed typical time and concentration dependent cytotoxicity in cancer cells. It was observed that there was no statistically significant difference between LAP and LAP@ZIF-8 treatment in MCF-7 cells within the investigated time periods. In fact, it is possible to say the same for SKBR-3 cells.

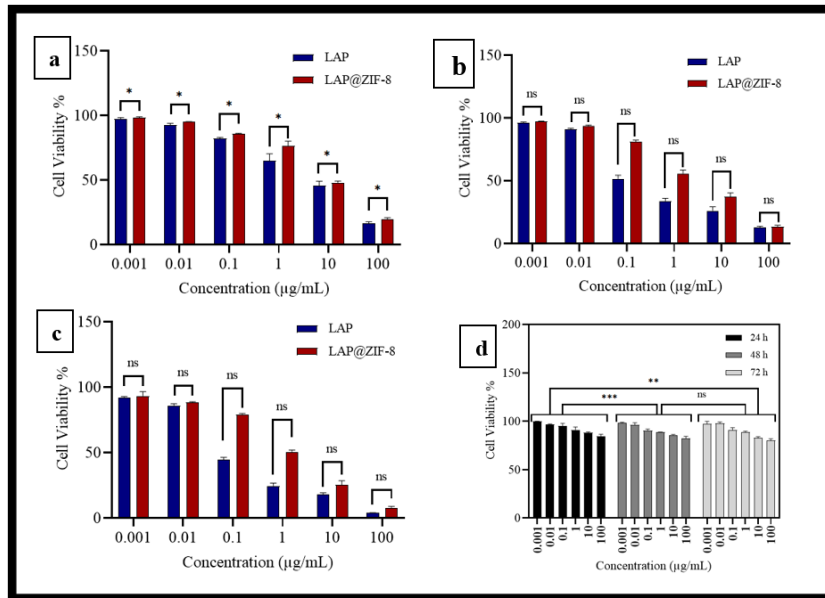


Figure 3.10. In vitro cytotoxicity profile of LAP, ZIF-8, LAP@ZIF-8 against SKBR-3 cell line at various concentrations. In vitro cytotoxicity profile of LAP and LAP@ZIF-8 after (a) 24 h, (b) 48 h and (c) 72 h incubation time as assayed by MTT. In vitro cytotoxicity profile of (d) ZIF-8. Significantly different data were indicated by asterisks (p-values: * <0.03 , ** <0.02 , *** <0.002 , **** <0.0001 , ns: non-significant)

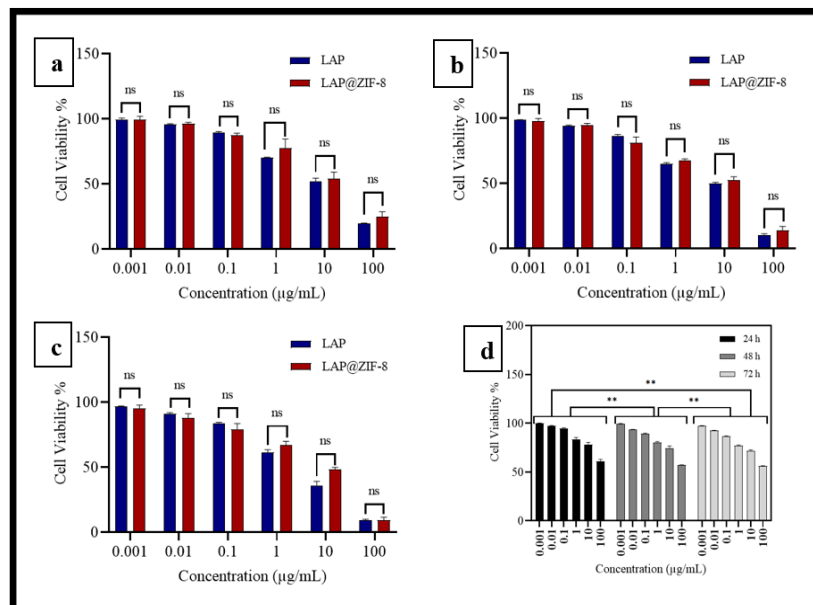


Figure 3.11. In vitro cytotoxicity profile of LAP, ZIF-8, LAP@ZIF-8 against MCF-7 cell line at various concentrations. In vitro cytotoxicity profile of LAP and LAP@ZIF-8 after (a) 24 h, (b) 48 h and (c) 72 h incubation time as assayed by MTT. In vitro cytotoxicity profile of (d) ZIF-8. Significantly different data were indicated by asterisks (p-values: * <0.03 , ** <0.02 , *** <0.002 , **** <0.0001 , ns: non-significant)

The IC₂₅ (concentration of inhibitor which causes 25% inhibition) and IC₇₅ (concentration of inhibitor which causes 75% inhibition) values (Table 3.3) and IC₅₀ values (Table 3.4) were calculated and shown as a result of 24, 48 and 72 hours of treatment of samples in SKBR-3 and MCF-7 cell lines.

Table 3.3. The IC₂₅ and IC₇₅ values of LAP, ZIF-8, and LAP@ZIF-8 for SKBR-3 and MCF-7 cell lines

Cell Line		IC ₂₅ (µg/mL)						IC ₇₅ (µg/mL)					
		SKBR-3			MCF-7			SKBR-3			MCF-7		
		LAP	ZIF-8	LAP@ZIF-8	LAP	ZIF-8	LAP@ZIF-8	LAP	ZIF-8	LAP@ZIF-8	LAP	ZIF-8	LAP@ZIF-8
Incubation Time	Sample	0.47	>100	1.50	0.78	26.95	1.94	73.53	>100	82.57	84.94	>100	>100
24 h		0.05	>100	0.31	0.59	10.36	0.52	18.22	>100	56.25	67.00	>100	74.52
48 h		0.03	>100	0.24	0.46	4.32	0.41	0.98	>100	11.38	47.15	>100	63.72
72 h													

Table 3.4. The IC₅₀ values of LAP, ZIF-8, and LAP@ZIF-8 for SKBR-3 and MCF-7 cell lines

Cell Line		IC ₅₀ (µg/mL)					
		SKBR-3			MCF-7		
		LAP	ZIF-8	LAP@ZIF-8	LAP	ZIF-8	LAP@ZIF-8
Incubation Time	Sample	7.96	>100	9.38	14.99	>100	22.05
24 h		0.19	>100	3.81	9.98	>100	16.13
48 h		0.09	>100	1.20	5.04	>100	9.14
72 h							

According to IC₅₀ values, LAP was much more toxic on SKBR-3 cells than on the MCF-7 cell line in the concentration range examined. In addition, LAP@ZIF-8 was significantly more toxic on SKBR-3 (HER2-positive) cells than on the MCF-7 (HER2-negative) cell line over the concentration range investigated. This demonstrated the effectiveness of LAP@ZIF in targeting in SKBR-3 cells where HER2 was overexpressed. The IC₅₀ values for compounds LAP, ZIF-8 and LAP@ZIF-8 are listed and indicate that in both SKBR-3 and MCF-7 cell lines the IC₅₀ value of ZIF-8 exceeded 100 µg/mL in all incubation times. After LAP was loaded onto ZIF-8 in SKBR-3 cell line, the IC₅₀ value of LAP@ZIF-8 was 9.38, 3.81, and 1.20 µg/mL after 24 h, 48 h, and 72 h incubation time,

respectively. After LAP was loaded onto ZIF-8 in MCF-7 cell line, the IC₅₀ value of LAP@ZIF-8 was 22.05, 16.13, and 9.14 µg/mL after 24 h, 48 h, and 72 h incubation time, respectively. Overall, a comparison of IC₅₀ values of LAP@ZIF-8 compound with LAP revealed that the LAP@ZIF-8 showed IC₅₀ value close to the IC₅₀ value of LAP in both SKBR-3 and MCF-7 cell lines. The lower cytotoxicity of LAP@ZIF-8 compared to LAP can be explained by the slow release of the drug.

The situation encountered as a result of the experiment is supported by similar results in the literature and explained by similar reasons such as drug release, encapsulation and loading. In one study, the cytotoxicity of DOXO (doxorubicin), ZIF-8 and DOXO-ZIF-8 complex determined by MTT assay were evaluated. It was observed that the DOXO-ZIF-8 complex had a higher IC₅₀ value than free DOXO. It has been mentioned that the weaker cytotoxicity of DOXO-ZIF-8 compared to DOXO can be explained by the slow release of the drug (Vasconcelos et al. 2012). In another study, the cytotoxicity of ZIF-8, DOX and DOX@ZIF-8 against HepG-2 and MCF-7 cell lines was evaluated. It was observed that DOX@ZIF-8 had a higher IC₅₀ value than DOX, thus the cytotoxicity of DOX@ZIF-8 was weaker compared to DOX. Although a small amount of DOX was loaded into DOX@ZIF-8; it was observed that the IC₅₀ values were close to the IC₅₀ values of free DOX in both cell lines. It is also said that these results confirm that a high amount of nanoparticles can be internalized into cancer cells and increase the efficiency of the drug. In addition, it is added that since the pH value of endosomes and lysosomes is acidic, the adopted DOX@ZIF-8 nanoparticles are predicted to release DOX quickly and abundantly into the cell (El-Bindary et al. 2020). In a study in which lapatinib was encapsulated in lipoprotein-like nanoparticles, it was noted that lipoprotein-like nanoparticles (LTNPs) incorporated with lapatinib resulted in lower cytotoxicity compared to free lapatinib (lapatinib suspension (LTS)) in the BT-474 breast cancer cell line (H. Gao et al. 2013). These results suggest that considering that only 6.55% of LAP@ZIF-8 used in the experiment was LAP, a high amount of nanoparticles could be taken up by cancer cells and the efficiency of LAP could be increased. The goal of anti-cancer drug delivery, such as protection of lapatinib from plasma proteins and early clearance from the bloodstream (Mobasseri et al. 2017), appears to have been achieved by using ZIF-8 as a nanocarrier in this study. In the study, ZIF-8 nanoparticles, which served as lapatinib carriers, retained its activity.

3.3.1. Coefficient of Variation for Cell Viability

The coefficient of variation is a dimensionless statistical tool that shows the relationship between the mean and distribution of data and allows variables to be compared independently of scale effects. It is used to express the precision and repeatability of an assay. It is defined as the ratio of the standard deviation to the mean and often expressed as a percentage. A coefficient of variation above about 30% is considered an indication that there is a problem with the data or that the experiment is out of control (Brown 1998). The coefficient of variation is also known as the relative standard deviation (Ospina and Marmolejo-Ramos 2019). The lower the coefficient of variation values, the smaller the spread of results and the higher the precision, while the higher the coefficient of variation values, the larger the spread of results and the lower the precision.

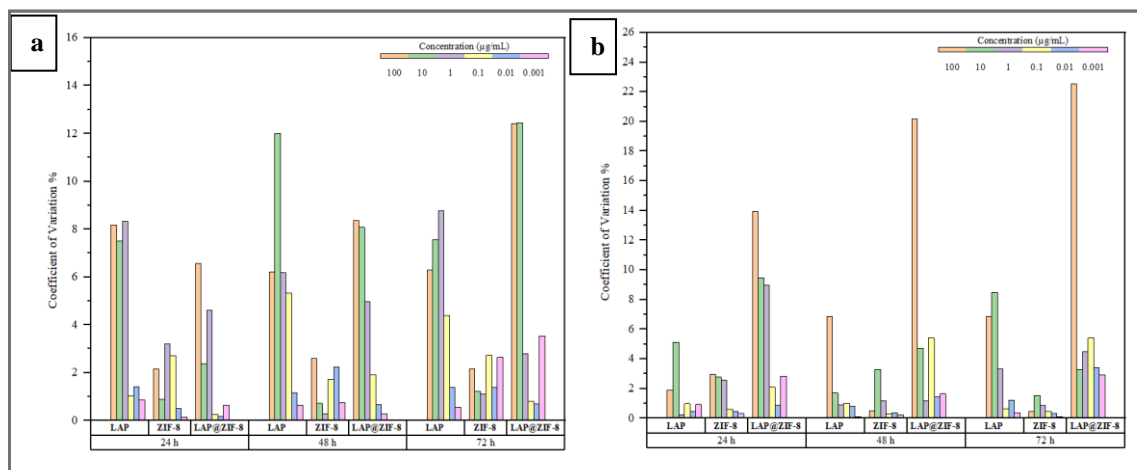


Figure 3.12. Coefficient of variation of average cell viabilities for different concentrations and incubation times of samples in (a) SKBR-3 and (b) MCF-7 cell lines

When the results were evaluated, it was seen that the coefficient of variation values did not exceed 30% in both cell lines, as seen in the graphs in Figure 3.12. These results show that there are no problems with the data set or experiment, as well as the consistency, precision, and reproducibility of the data.

CHAPTER 4

CONCLUSION

In conclusion, the cancer drug LAP was developed by one-pot synthesis as an effective drug delivery system by encapsulating it into ZIF-8. The synthesized LAP@ZIF-8 exhibited high encapsulation efficiency of 72.42% and drug loading capacity of 6.55%. Moreover, as a result of biocompatibility studies, the nanoparticle, characterized using SEM, EDX, DLS, zeta potential, FTIR, XRD and TGA, exhibited good biocompatibility and stability, making it an ideal candidate carrier for the delivery of drugs. As a result of the in vitro drug release experiment, it was found that the drug release behavior of LAP@ZIF-8 was higher in acidic environment (pH 5.5) compared to physiological environment (pH 7.4).

In vitro cytotoxicity findings showed that LAP@ZIF-8 had similar therapeutic effect to free LAP on breast cancer cell lines. The LAP@ZIF-8 system was shown to be internalized by cancer cells and exhibited lower cytotoxicity compared to LAP, probably due to its slow release from ZIF-8. In addition, the effect of LAP, a HER2 inhibitor used to treat HER2-positive breast cancer, and synthesized LAP@ZIF-8 on MCF-7, a HER2-negative breast cancer cell line, was observed in vitro. The results showed that LAP and LAP@ZIF-8 were also effective in HER2-negative breast cancer cell lines, suggesting that they could also be used therapeutically in HER2-negative breast cancer cell lines.

LAP@ZIF-8, a nanoparticle with a convenient synthesis procedure, was experimentally characterized, exhibited good release and biocompatibility abilities, and was shown to have promising anti-tumor effects in breast cancer cell lines. For the treatment to be successful, various limitations of chemotherapeutics used in cancer treatment must be resolved. Since both substances (LAP and ZIF-8) are hydrophobic, their solubility in water is quite limited. During the experiments, the solubility of synthesized LAP@ZIF-8 was visibly better than the solubility of its components. It has been shown that this observation result is reflected in the results of the experiments and that this statement is correct. The use of ZIF-8 as a carrier may increase the therapeutic efficacy of lapatinib while reducing possible side effects. Considering its potential capabilities and experimental results, LAP@ZIF-8 can be continued to be studied as a

drug carrier system in the development of pharmaceutical applications. In the future, such nanoparticles could potentially lead to studies that could be used for other chemotherapeutics, overcoming many limitations in the treatment of several cancers. More comprehensive studies will be useful in understanding the biological effects of these nanoparticles and their possible use as drug delivery vehicles in future clinical trials.

REFERENCES

- Abánades Lázaro, Isabel, Connor J. R. Wells, and Ross S. Forgan. 2020. "Multivariate Modulation of the Zr MOF UiO-66 for Defect-Controlled Combination Anticancer Drug Delivery." *Angewandte Chemie International Edition* 59 (13): 5211–17. doi:10.1002/anie.201915848.
- Abdelhamid, Hani Nasser, Zhehao Huang, Ahmed M. El-Zohry, Haoquan Zheng, and Xiaodong Zou. 2017. "A Fast and Scalable Approach for Synthesis of Hierarchical Porous Zeolitic Imidazolate Frameworks and One-Pot Encapsulation of Target Molecules." *Inorganic Chemistry* 56 (15): 9139–46. doi:10.1021/acs.inorgchem.7b01191.
- Adhikari, Chandan, Anupam Das, and Anjan Chakraborty. 2015. "Zeolitic Imidazole Framework (ZIF) Nanospheres for Easy Encapsulation and Controlled Release of an Anticancer Drug Doxorubicin under Different External Stimuli: A Way toward Smart Drug Delivery System." *Molecular Pharmaceutics* 12 (9): 3158–66. doi:10.1021/acs.molpharmaceut.5b00043.
- Ahn, Eugene R., and Charles L. Vogel. 2012. "Dual HER2-Targeted Approaches in HER2-Positive Breast Cancer." *Breast Cancer Research and Treatment* 131 (2): 371–83. doi:10.1007/s10549-011-1781-y.
- Alshawwa, Samar Zuhair, Abeer Ahmed Kassem, Ragwa Mohamed Farid, Shaimaa Khamis Mostafa, and Gihan Salah Labib. 2022. "Nanocarrier Drug Delivery Systems: Characterization, Limitations, Future Perspectives and Implementation of Artificial Intelligence." *Pharmaceutics* 14 (4): 883. doi:10.3390/pharmaceutics14040883.
- Anand, Uttpal, Abhijit Dey, Arvind K. Singh Chandel, Rupa Sanyal, Amarnath Mishra, Devendra Kumar Pandey, Valentina De Falco, et al. 2022. "Cancer Chemotherapy and beyond: Current Status, Drug Candidates, Associated Risks and Progress in Targeted Therapeutics." *Genes & Diseases*, March.

doi:10.1016/j.gendis.2022.02.007.

Anastasiadi, Zoi, Georgios D. Lianos, Eleftheria Ignatiadou, Haralampos V. Harissis, and Michail Mitsis. 2017. “Breast Cancer in Young Women: An Overview.” *Updates in Surgery* 69 (3): 313–17. doi:10.1007/s13304-017-0424-1.

Angelos, Sarah, Niveen M. Khashab, Ying-Wei Yang, Ali Trabolsi, Hussam A. Khatib, J. Fraser Stoddart, and Jeffrey I. Zink. 2009. “pH Clock-Operated Mechanized Nanoparticles.” *Journal of the American Chemical Society* 131 (36): 12912–14. doi:10.1021/ja9010157.

Antoniuk, Iurii, and Catherine Amiel. 2016. “Cyclodextrin-Mediated Hierarchical Self-Assembly and Its Potential in Drug Delivery Applications.” *Journal of Pharmaceutical Sciences* 105 (9): 2570–88. doi:10.1016/j.xphs.2016.05.010.

Arnold, Melina, Eileen Morgan, Harriet Rumgay, Allini Mafra, Deependra Singh, Mathieu Laversanne, Jerome Vignat, et al. 2022. “Current and Future Burden of Breast Cancer: Global Statistics for 2020 and 2040.” *The Breast* 66 (December): 15–23. doi:10.1016/j.breast.2022.08.010.

Arruebo, Manuel, Nuria Vilaboa, Berta Sáez-Gutierrez, Julio Lambea, Alejandro Tres, Mónica Valladares, and África González-Fernández. 2011. “Assessment of the Evolution of Cancer Treatment Therapies.” *Cancers* 3 (3): 3279–3330. doi:10.3390/cancers3033279.

Ateş, Mehmet. 2018. “Nanoparçacıkların Ölçme ve İnceleme Teknikleri.” *Türk Bilimsel Derlemeler Dergisi* 11 (1). Nobel Bilim ve Araştırma Merkezi Limited: 63–69.

Awasthi, Gaurav, Sahil Shivgotra, Shibyendu Nikhar, Subramanian Sundarrajan, Seeram Ramakrishna, and Pawan Kumar. 2022. “Progressive Trends on the Biomedical Applications of Metal Organic Frameworks.” *Polymers* 14 (21): 4710. doi:10.3390/polym14214710.

Basuli, Falguni, Haitao Wu, Changhui Li, Zhen-Dan Shi, Agnieszka Sulima, and Gary L.

- Griffiths. 2011. "A First Synthesis of ^{18}F -radiolabeled Lapatinib: A Potential Tracer for Positron Emission Tomographic Imaging of ErbB1/ErbB2 Tyrosine Kinase Activity." *Journal of Labelled Compounds and Radiopharmaceuticals* 54 (9): 633–36. doi:10.1002/jlcr.1898.
- Belgemen, Tuğba, and Nejat Akar. 2004. "Çinkonun Yaşamsal Fonksiyonları ve Çinko Metabolizması ile ilişkili Genler." *Ankara Üniversitesi Tıp Fakültesi Mecmuası* 57 (3): 1. doi:10.1501/Tipfak_0000000108.
- Bengtsson, Ylva, Kamil Demircan, Ann H. Rosendahl, Signe Borgquist, Malte Sandsveden, and Jonas Manjer. 2022. "Zinc and Breast Cancer Survival: A Prospective Cohort Study of Dietary Intake and Serum Levels." *Nutrients* 14 (13): 2575. doi:10.3390/nu14132575.
- Blair, Jimmy A, Daniel Rauh, Charles Kung, Cai-Hong Yun, Qi-Wen Fan, Haridas Rode, Chao Zhang, Michael J Eck, William A Weiss, and Kevan M Shokat. 2007. "Structure-Guided Development of Affinity Probes for Tyrosine Kinases Using Chemical Genetics." *Nature Chemical Biology* 3 (4): 229–38. doi:10.1038/nchembio866.
- Bonde, Gunjan Vasant, Gufran Ajmal, Sarita Kumari Yadav, Pooja Mittal, Juhi Singh, Bharati V. Bakde, and Brahmeshwar Mishra. 2020. "Assessing the Viability of Soluplus® Self-Assembled Nanocolloids for Sustained Delivery of Highly Hydrophobic Lapatinib (Anticancer Agent): Optimisation and in-Vitro Characterisation." *Colloids and Surfaces B: Biointerfaces* 185 (January): 110611. doi:10.1016/j.colsurfb.2019.110611.
- Bonde, Gunjan Vasant, Sarita Kumari Yadav, Sheetal Chauhan, Pooja Mittal, Gufran Ajmal, Sathish Thokala, and Brahmeshwar Mishra. 2018. "Lapatinib Nano-Delivery Systems: A Promising Future for Breast Cancer Treatment." *Expert Opinion on Drug Delivery* 15 (5): 495–507. doi:10.1080/17425247.2018.1449832.
- Brown, Charles E. 1998. "Coefficient of Variation." In *Applied Multivariate Statistics in Geohydrology and Related Sciences*, 155–57. Berlin, Heidelberg: Springer Berlin

Heidelberg. doi:10.1007/978-3-642-80328-4_13.

Bruneau, Marion, Simona Bennici, Jocelyne Brendle, Patrick Dutournie, Lionel Limousy, and Sylvain Pluchon. 2019. "Systems for Stimuli-Controlled Release: Materials and Applications." *Journal of Controlled Release* 294 (January): 355–71. doi:10.1016/j.jconrel.2018.12.038.

Cai, Hong, Yong-Liang Huang, and Dan Li. 2019. "Biological Metal–Organic Frameworks: Structures, Host–Guest Chemistry and Bio-Applications." *Coordination Chemistry Reviews* 378 (January): 207–21. doi:10.1016/j.ccr.2017.12.003.

Cai, Wen, Junqing Wang, Chengchao Chu, Wei Chen, Chunsheng Wu, and Gang Liu. 2019. "Metal-Organic Framework-Based Stimuli-Responsive Systems for Drug Delivery." *Advanced Science* 6 (1): 1801526. doi:10.1002/advs.201801526.

Carey, Lisa A., Charles M. Perou, Chad A. Livasy, Lynn G. Dressler, David Cowan, Kathleen Conway, Gamze Karaca, et al. 2006. "Race, Breast Cancer Subtypes, and Survival in the Carolina Breast Cancer Study." *JAMA* 295 (21): 2492. doi:10.1001/jama.295.21.2492.

Chen, Suning, Xingmei Zhu, Hongyu Qiao, Mingxiang Ye, Xiaofeng Lai, Shentong Yu, Likun Ding, Aidong Wen, and Jian Zhang. 2016. "Protective Autophagy Promotes the Resistance of HER2-Positive Breast Cancer Cells to Lapatinib." *Tumor Biology* 37 (2): 2321–31. doi:10.1007/s13277-015-3800-9.

Chen, Xuerui, Rongliang Tong, Zheqi Shi, Beng Yang, Hua Liu, Shiping Ding, Xu Wang, Qunfang Lei, Jian Wu, and Wenjun Fang. 2018. "MOF Nanoparticles with Encapsulated Autophagy Inhibitor in Controlled Drug Delivery System for Antitumor." *ACS Applied Materials & Interfaces* 10 (3): 2328–37. doi:10.1021/acsami.7b16522.

Chhikara, Bhupender S, and Keykavous Parang. 2022. "Global Cancer Statistics 2022: The Trends Projection Analysis." *Chemical Biology Letters* 10 (1): 451.

<https://pubs.thesciencein.org/journal/index.php/cbl/article/view/451>.

- Chintalaramulu, Naveen, Raja Vadivelu, Nam-Trung Nguyen, and Ian Edwin Cock. 2020. "Lapatinib Inhibits Doxorubicin Induced Migration of HER2-Positive Breast Cancer Cells." *Inflammopharmacology* 28 (5): 1375–86. doi:10.1007/s10787-020-00711-9.
- Cho, Kwangjae, Xu Wang, Shuming Nie, Zhuo (Georgia) Chen, and Dong M. Shin. 2008. "Therapeutic Nanoparticles for Drug Delivery in Cancer." *Clinical Cancer Research* 14 (5): 1310–16. doi:10.1158/1078-0432.CCR-07-1441.
- Cole, Adam J., Allan E. David, Jianxin Wang, Craig J. Galbán, Hannah L. Hill, and Victor C. Yang. 2011. "Polyethylene Glycol Modified, Cross-Linked Starch-Coated Iron Oxide Nanoparticles for Enhanced Magnetic Tumor Targeting." *Biomaterials* 32 (8): 2183–93. doi:10.1016/j.biomaterials.2010.11.040.
- Creighton, Chad. 2012. "The Molecular Profile of Luminal B Breast Cancer." *Biologics: Targets and Therapy*, August, 289. doi:10.2147/BTT.S29923.
- Değirmenci, Nurdan Sena, Merve Uslu, Oğuz Kaan Kırbaş, Fikrettin Şahin, and Evren Önay Uçar. 2022. "Lapatinib Loaded Exosomes as a Drug Delivery System in Breast Cancer." *Journal of Drug Delivery Science and Technology* 75 (September): 103584. doi:10.1016/j.jddst.2022.103584.
- Denizot, François, and Rita Lang. 1986. "Rapid Colorimetric Assay for Cell Growth and Survival." *Journal of Immunological Methods* 89 (2): 271–77. doi:10.1016/0022-1759(86)90368-6.
- Din, Fakhar ud, Waqar Aman, Izhar Ullah, Omer Salman Qureshi, Omer Mustapha, Shumaila Shafique, and Alam Zeb. 2017. "Effective Use of Nanocarriers as Drug Delivery Systems for the Treatment of Selected Tumors." *International Journal of Nanomedicine* Volume 12 (October): 7291–7309. doi:10.2147/IJN.S146315.
- Ding, Mengli, Wenbo Liu, and Ruxandra Gref. 2022. "Nanoscale MOFs: From Synthesis

- to Drug Delivery and Theranostics Applications.” *Advanced Drug Delivery Reviews* 190 (November): 114496. doi:10.1016/j.addr.2022.114496.
- Duan, Yan, Fanggui Ye, Yuanlin Huang, Yuemei Qin, Caimei He, and Shulin Zhao. 2018. “One-Pot Synthesis of a Metal–Organic Framework-Based Drug Carrier for Intelligent Glucose-Responsive Insulin Delivery.” *Chemical Communications* 54 (42): 5377–80. doi:10.1039/C8CC02708K.
- El-Bindary, Ashraf A., Elshahat A. Toson, Kamel R. Shoueir, Hind A. Aljohani, and Magy M. Abo-Ser. 2020. “Metal–Organic Frameworks as Efficient Materials for Drug Delivery: Synthesis, Characterization, Antioxidant, Anticancer, Antibacterial and Molecular Docking Investigation.” *Applied Organometallic Chemistry* 34 (11). doi:10.1002/aoc.5905.
- Eljack, Sahar, Stephanie David, Igor Chourpa, Areeg Faggad, and Emilie Allard-Vannier. 2022. “Formulation of Lipid-Based Nanoparticles for Simultaneous Delivery of Lapatinib and Anti-Survivin SiRNA for HER2+ Breast Cancer Treatment.” *Pharmaceuticals* 15 (12): 1452. doi:10.3390/ph15121452.
- Ettliger, Romy, Ulrich Lächelt, Ruxandra Gref, Patricia Horcajada, Twan Lammers, Christian Serre, Patrick Couvreur, Russell E. Morris, and Stefan Wuttke. 2022. “Toxicity of Metal–Organic Framework Nanoparticles: From Essential Analyses to Potential Applications.” *Chemical Society Reviews* 51 (2): 464–84. doi:10.1039/D1CS00918D.
- Fedorova, Olga, Alexandra Daks, Oleg Shuvalov, Alena Kizenko, Alexey Petukhov, Yulia Gnennaya, and Nikolai Barlev. 2020. “Attenuation of P53 Mutant as an Approach for Treatment Her2-Positive Cancer.” *Cell Death Discovery* 6 (1): 100. doi:10.1038/s41420-020-00337-4.
- Feng, Simin, Xiaoli Zhang, Dunnyun Shi, and Zheng Wang. 2021. “Zeolitic Imidazolate Framework-8 (ZIF-8) for Drug Delivery: A Critical Review.” *Frontiers of Chemical Science and Engineering* 15 (2): 221–37. doi:10.1007/s11705-020-1927-8.

- Feng, Xin, Mingjun Li, Jianming Wang, Xianrui Zou, Hongshui Wang, Donghui Wang, Huan Zhou, Lei Yang, Wei Gao, and Chunyong Liang. 2022. "MXene Quantum Dot/Zeolitic Imidazolate Framework Nanocarriers for Dual Stimulus Triggered Tumor Chemo-Phototherapy." *Materials* 15 (13): 4543. doi:10.3390/ma15134543.
- Feng, Yixiao, Mia Spezia, Shifeng Huang, Chengfu Yuan, Zongyue Zeng, Linghuan Zhang, Xiaojuan Ji, et al. 2018. "Breast Cancer Development and Progression: Risk Factors, Cancer Stem Cells, Signaling Pathways, Genomics, and Molecular Pathogenesis." *Genes & Diseases* 5 (2): 77–106. doi:10.1016/j.gendis.2018.05.001.
- Furukawa, Hiroyasu, Kyle E. Cordova, Michael O’Keeffe, and Omar M. Yaghi. 2013. "The Chemistry and Applications of Metal-Organic Frameworks." *Science* 341 (6149). doi:10.1126/science.1230444.
- Gabos, Zsolt, Richie Sinha, John Hanson, Nitin Chauhan, Judith Hugh, John R. Mackey, and Bassam Abdulkarim. 2006. "Prognostic Significance of Human Epidermal Growth Factor Receptor Positivity for the Development of Brain Metastasis After Newly Diagnosed Breast Cancer." *Journal of Clinical Oncology* 24 (36): 5658–63. doi:10.1200/JCO.2006.07.0250.
- Ganta, Srinivas, Harikrishna Devalapally, Aliasgar Shahiwala, and Mansoor Amiji. 2008. "A Review of Stimuli-Responsive Nanocarriers for Drug and Gene Delivery." *Journal of Controlled Release* 126 (3): 187–204. doi:10.1016/j.jconrel.2007.12.017.
- Gao, Huile, Shilei Cao, Chen Chen, Shijie Cao, Zhi Yang, Zhiqing Pang, Zhangjie Xi, Shuaiqi Pan, Qizhi Zhang, and Xinguo Jiang. 2013. "Incorporation of Lapatinib Into Lipoprotein-Like Nanoparticles with Enhanced Water Solubility and Anti-Tumor Effect in Breast Cancer." *Nanomedicine* 8 (9): 1429–42. doi:10.2217/nnm.12.180.
- Gao, Huile, Chen Chen, Zhangjie Xi, Jun Chen, Qizhi Zhang, Shilei Cao, and Xinguo Jiang. 2014. "In Vivo Behavior and Safety of Lapatinib-Incorporated Lipid Nanoparticles." *Current Pharmaceutical Biotechnology* 14 (12): 1062–71. doi:10.2174/1389201015666140113110746.

- Gao, Huile, Yuchen Wang, Chen Chen, Jun Chen, Yan Wei, Shilei Cao, and Xinguo Jiang. 2014. "Incorporation of Lapatinib into Core–Shell Nanoparticles Improves Both the Solubility and Anti-Glioma Effects of the Drug." *International Journal of Pharmaceutics* 461 (1–2): 478–88. doi:10.1016/j.ijpharm.2013.12.016.
- Gao, Lihua, Qing Chen, Tingting Gong, Jianhua Liu, and Chunxia Li. 2019. "Recent Advancement of Imidazolate Framework (ZIF-8) Based Nanoformulations for Synergistic Tumor Therapy." *Nanoscale* 11 (44): 21030–45. doi:10.1039/C9NR06558J.
- Gómez-Lázaro, Laura, Cristina Martín-Sabroso, Juan Aparicio-Blanco, and Ana Isabel Torres-Suárez. 2024. "Assessment of In Vitro Release Testing Methods for Colloidal Drug Carriers: The Lack of Standardized Protocols." *Pharmaceutics* 16 (1): 103. doi:10.3390/pharmaceutics16010103.
- Gross, Adam F., Elena Sherman, and John J. Vajo. 2012. "Aqueous Room Temperature Synthesis of Cobalt and Zinc Sodalite Zeolitic Imidizolate Frameworks." *Dalton Transactions* 41 (18): 5458. doi:10.1039/c2dt30174a.
- Gunjan Vasant, Bonde, Ajmal Gufran, Yadav Sarita Kumari, Mittal Pooja, and Mishra Brahmeshwar. 2020. "Lapatinib-Loaded Nanocolloidal Polymeric Micelles for the Efficient Treatment of Breast Cancer." *Journal of Applied Pharmaceutical Science*, September. doi:10.7324/JAPS.2020.10903.
- Hao, Jessica, Ivana Stavljenić Milašin, Zeynep Batu Eken, Marinka Mravak-Stipetic, Krešimir Pavelić, and Fusun Ozer. 2021. "Effects of Zeolite as a Drug Delivery System on Cancer Therapy: A Systematic Review." *Molecules* 26 (20): 6196. doi:10.3390/molecules26206196.
- Hassanpour, Seyed Hossein, and Mohammadamin Dehghani. 2017. "Review of Cancer from Perspective of Molecular." *Journal of Cancer Research and Practice* 4 (4): 127–29. doi:10.1016/j.jcrpr.2017.07.001.
- Helmlinger, Gabriel, Fan Yuan, Marc Dellian, and Rakesh K. Jain. 1997. "Interstitial pH

- and pO₂ Gradients in Solid Tumors in Vivo: High-Resolution Measurements Reveal a Lack of Correlation.” *Nature Medicine* 3 (2): 177–82. doi:10.1038/nm0297-177.
- Honary, S, and F Zahir. 2013. “Effect of Zeta Potential on the Properties of Nano-Drug Delivery Systems - A Review (Part 1).” *Tropical Journal of Pharmaceutical Research* 12 (2). doi:10.4314/tjpr.v12i2.19.
- Hoop, Marcus, Claudio F. Walde, Raffaele Riccò, Fajer Mushtaq, Anastasia Terzopoulou, Xiang-Zhong Chen, Andrew J. deMello, et al. 2018. “Biocompatibility Characteristics of the Metal Organic Framework ZIF-8 for Therapeutical Applications.” *Applied Materials Today* 11 (June): 13–21. doi:10.1016/j.apmt.2017.12.014.
- Hoskins, Bernard F., and Richard Robson. 1989. “Infinite Polymeric Frameworks Consisting of Three Dimensionally Linked Rod-like Segments.” *Journal of the American Chemical Society* 111 (15): 5962–64. doi:10.1021/ja00197a079.
- Huo, Zhi-Jun, Shi-Jiang Wang, Zhi-Qi Wang, Wen-Shu Zuo, Ping Liu, Bo Pang, and Kai Liu. 2015. “Novel Nanosystem to Enhance the Antitumor Activity of Lapatinib in Breast Cancer Treatment: Therapeutic Efficacy Evaluation.” *Cancer Science* 106 (10): 1429–37. doi:10.1111/cas.12737.
- Huxford, Rachel C, Joseph Della Rocca, and Wenbin Lin. 2010. “Metal–Organic Frameworks as Potential Drug Carriers.” *Current Opinion in Chemical Biology* 14 (2): 262–68. doi:10.1016/j.cbpa.2009.12.012.
- Iqbal, Nida, and Naveed Iqbal. 2014. “Human Epidermal Growth Factor Receptor 2 (HER2) in Cancers: Overexpression and Therapeutic Implications.” *Molecular Biology International* 2014 (September): 1–9. doi:10.1155/2014/852748.
- Januškevičienė, Indrė, and Vilma Petrikaitė. 2019. “Heterogeneity of Breast Cancer: The Importance of Interaction between Different Tumor Cell Populations.” *Life Sciences* 239 (December): 117009. doi:10.1016/j.lfs.2019.117009.

- Jiang, Wei, Huiyuan Zhang, Jilian Wu, Guangxi Zhai, Zhonghao Li, Yuxia Luan, and Sanjay Garg. 2018. "CuS@MOF-Based Well-Designed Quercetin Delivery System for Chemo-Photothermal Therapy." *ACS Applied Materials & Interfaces* 10 (40): 34513–23. doi:10.1021/acsami.8b13487.
- Jongert, Tristan K., Ian A. Slowinski, Benjamin Dao, Victor H. Cortez, Thomas Gredig, Nestor D. Plascencia, and Fangyuan Tian. 2024. "Zeta Potential and Size Analysis of Zeolitic Imidazolate Framework-8 Nanocrystals Prepared by Surfactant-Assisted Synthesis." *Langmuir* 40 (12): 6138–48. doi:10.1021/acs.langmuir.3c03193.
- Kaczmarek, Katarzyna, Anna Jakubowska, Grzegorz Sukiennicki, Magdalena Muszyńska, Katarzyna Jaworska-Bieniek, Katarzyna Durda, Tomasz Huzarski, et al. 2012. "Zinc and Breast Cancer Risk." *Hereditary Cancer in Clinical Practice* 10 (Suppl 4): A6. doi:10.1186/1897-4287-10-S4-A6.
- Kaneti, Yusuf Valentino, Saikat Dutta, Md. S. A. Hossain, Muhammad J. A. Shiddiky, Kuo-Lun Tung, Fa-Kuen Shieh, Chia-Kuang Tsung, Kevin C.-W. Wu, and Yusuke Yamauchi. 2017. "Strategies for Improving the Functionality of Zeolitic Imidazolate Frameworks: Tailoring Nanoarchitectures for Functional Applications." *Advanced Materials* 29 (38): 1700213. doi:10.1002/adma.201700213.
- Kaur, Harpreet, Girish C. Mohanta, Vandana Gupta, Deepak Kukkar, and Sachin Tyagi. 2017. "Synthesis and Characterization of ZIF-8 Nanoparticles for Controlled Release of 6-Mercaptopurine Drug." *Journal of Drug Delivery Science and Technology* 41 (October): 106–12. doi:10.1016/j.jddst.2017.07.004.
- Khan, Abdullah, S Roshan, K Anandarajagopal, and B Tazneem. 2021. "Development and Evaluation of Lapatinib Ditosylate Self-Nanoemulsifying Drug Delivery Systems." *International Journal of Pharmaceutical Sciences and Research* 12 (4). doi:10.13040/IJPSR.0975-8232.12(4).2492-99.
- Kim, Young Jin, Min-Zy Kim, Syed Fakhar Alam, Aafaq ur Rehman, Arepalli Devipriyanka, Pankaj Sharma, Hye Ryeon Lee, and Churl-Hee Cho. 2021. "Polarity-Dependent Particle Size of Zeolitic Imidazolate Framework Synthesized in Various

- Solvents.” *Materials Chemistry and Physics* 259 (February): 124021. doi:10.1016/j.matchemphys.2020.124021.
- Kim, Yu-Mee, William Reed, Weidong Wu, Philip A. Bromberg, Lee M. Graves, and James M. Samet. 2006. “Zn²⁺-Induced IL-8 Expression Involves AP-1, JNK, and ERK Activities in Human Airway Epithelial Cells.” *American Journal of Physiology-Lung Cellular and Molecular Physiology* 290 (5): L1028–35. doi:10.1152/ajplung.00479.2005.
- Lee, A. V., S. Oesterreich, and N. E. Davidson. 2015. “MCF-7 Cells--Changing the Course of Breast Cancer Research and Care for 45 Years.” *JNCI Journal of the National Cancer Institute* 107 (7): djv073–djv073. doi:10.1093/jnci/djv073.
- Lee, Song Yi, and Hyun-Jong Cho. 2019. “Mitochondria Targeting and Destabilizing Hyaluronic Acid Derivative-Based Nanoparticles for the Delivery of Lapatinib to Triple-Negative Breast Cancer.” *Biomacromolecules* 20 (2): 835–45. doi:10.1021/acs.biomac.8b01449.
- Lee, Yu-Ri, Min-Seok Jang, Hye-Young Cho, Hee-Jin Kwon, Sangho Kim, and Wha-Seung Ahn. 2015. “ZIF-8: A Comparison of Synthesis Methods.” *Chemical Engineering Journal* 271 (July): 276–80. doi:10.1016/j.cej.2015.02.094.
- Levit, Shani L., Hu Yang, and Christina Tang. 2020. “Rapid Self-Assembly of Polymer Nanoparticles for Synergistic Codelivery of Paclitaxel and Lapatinib via Flash NanoPrecipitation.” *Nanomaterials* 10 (3): 561. doi:10.3390/nano10030561.
- Li, Xue, Marianna Porcino, Jingwen Qiu, Doru Constantin, Charlotte Martineau-Corcus, and Ruxandra Gref. 2021. “Doxorubicin-Loaded Metal-Organic Frameworks Nanoparticles with Engineered Cyclodextrin Coatings: Insights on Drug Location by Solid State NMR Spectroscopy.” *Nanomaterials* 11 (4): 945. doi:10.3390/nano11040945.
- Li, Yawei, Na Xu, Wenhe Zhu, Lei Wang, Bin Liu, Jianxu Zhang, Zhigang Xie, and Wensen Liu. 2018. “Nanoscale Melittin@Zeolitic Imidazolate Frameworks for

- Enhanced Anticancer Activity and Mechanism Analysis.” *ACS Applied Materials & Interfaces* 10 (27): 22974–84. doi:10.1021/acsami.8b06125.
- Liang, Weibin, Raffaele Ricco, Natasha K. Maddigan, Robert P. Dickinson, Huoshu Xu, Qiaowei Li, Christopher J. Sumby, Stephen G. Bell, Paolo Falcaro, and Christian J. Doonan. 2018. “Control of Structure Topology and Spatial Distribution of Biomacromolecules in Protein@ZIF-8 Biocomposites.” *Chemistry of Materials* 30 (3): 1069–77. doi:10.1021/acs.chemmater.7b04977.
- Liédana, Nuria, Alejandro Galve, César Rubio, Carlos Téllez, and Joaquín Coronas. 2012. “CAF@ZIF-8: One-Step Encapsulation of Caffeine in MOF.” *ACS Applied Materials & Interfaces* 4 (9): 5016–21. doi:10.1021/am301365h.
- Liu, Juan, Yuran Huang, Anil Kumar, Aaron Tan, Shubin Jin, Anbu Mozhi, and Xing-Jie Liang. 2014. “pH-Sensitive Nano-Systems for Drug Delivery in Cancer Therapy.” *Biotechnology Advances* 32 (4): 693–710. doi:10.1016/j.biotechadv.2013.11.009.
- Liu, Shuang, Zhonghua Xiang, Zan Hu, Xiaoping Zheng, and Dapeng Cao. 2011. “Zeolitic Imidazolate Framework-8 as a Luminescent Material for the Sensing of Metal Ions and Small Molecules.” *Journal of Materials Chemistry* 21 (18): 6649. doi:10.1039/c1jm10166h.
- Liyanage, Piumi Y, Sajini D Hettiarachchi, Yiqun Zhou, Allal Ouhtit, Elif S Seven, Cagri Y Oztan, Emrah Celik, and Roger M Leblanc. 2019. “Nanoparticle-Mediated Targeted Drug Delivery for Breast Cancer Treatment.” *Biochimica et Biophysica Acta. Reviews on Cancer* 1871 (2): 419–33. doi:10.1016/j.bbcan.2019.04.006.
- Lu, Jialin, Xiaohui Zhu, Mingxia Li, Cuiping Fu, Yong Li, Jing Zhang, Jinliang Liu, and Yong Zhang. 2021. “Engineering Near-Infrared-Excitable Metal–Organic Framework for Tumor Microenvironment Responsive Therapy.” *ACS Applied Bio Materials* 4 (8): 6316–25. doi:10.1021/acsabm.1c00573.
- Lu, Kuangda, Theint Aung, Nining Guo, Ralph Weichselbaum, and Wenbin Lin. 2018. “Nanoscale Metal-Organic Frameworks for Therapeutic, Imaging, and Sensing

- Applications.” *Advanced Materials* 30 (37): 1707634. doi:10.1002/adma.201707634.
- Majumder, Joydeb, Oleh Taratula, and Tamara Minko. 2019. “Nanocarrier-Based Systems for Targeted and Site Specific Therapeutic Delivery.” *Advanced Drug Delivery Reviews* 144 (April): 57–77. doi:10.1016/j.addr.2019.07.010.
- Malehmir, Shirin, Mohammad Ali Esmaili, M. Khaksary Mahabady, Ali Sobhani-Nasab, Amir Atapour, Mohammad Reza Ganjali, Ali Ghasemi, and Amin Moradi Hasan-Abad. 2023. “A Review: Hemocompatibility of Magnetic Nanoparticles and Their Regenerative Medicine, Cancer Therapy, Drug Delivery, and Bioimaging Applications.” *Frontiers in Chemistry* 11 (August). doi:10.3389/fchem.2023.1249134.
- Maleki, Aziz, Mohammad-Ali Shahbazi, Vajiheh Alinezhad, and Hélder A. Santos. 2020. “The Progress and Prospect of Zeolitic Imidazolate Frameworks in Cancer Therapy, Antibacterial Activity, and Biomineralization.” *Advanced Healthcare Materials* 9 (12): 2000248. doi:10.1002/adhm.202000248.
- Mane, Preeti Tanaji, Balaji Sopanrao Wakure, and Pravin Shridhar Wakte. 2022. “Binary and Ternary Inclusion Complexation of Lapatinib Ditosylate with β -Cyclodextrin: Preparation, Evaluation and in Vitro Anticancer Activity.” *Beni-Suef University Journal of Basic and Applied Sciences* 11 (1): 150. doi:10.1186/s43088-022-00332-x.
- Martinez, Diego Stéfani T., Amauri J. Paula, Leandro C. Fonseca, Luis Augusto V. Luna, Camila P. Silveira, Nelson Durán, and Oswaldo L. Alves. 2015. “Monitoring the Hemolytic Effect of Mesoporous Silica Nanoparticles after Human Blood Protein Corona Formation.” *European Journal of Inorganic Chemistry* 2015 (27): 4595–4602. doi:10.1002/ejic.201500573.
- Matsumura, Y, and H Maeda. 1986. “A New Concept for Macromolecular Therapeutics in Cancer Chemotherapy: Mechanism of Tumorotropic Accumulation of Proteins and the Antitumor Agent Smancs.” *Cancer Research* 46 (12 Pt 1): 6387–92.

- McArthur, Heather. 2009. "An Overview of HER-Targeted Therapy with Lapatinib in Breast Cancer." *Advances in Therapy* 26 (3): 263–71. doi:10.1007/s12325-009-0012-y.
- "MCF7 - HTB-22." n.d. *ATCC*. Accessed June 7, 2024. <https://www.atcc.org/products/htb-22#detailed-product-images>.
- McIlwain, D. R., T. Berger, and T. W. Mak. 2013. "Caspase Functions in Cell Death and Disease." *Cold Spring Harbor Perspectives in Biology* 5 (4): a008656–a008656. doi:10.1101/cshperspect.a008656.
- Meacham, Corbin E., and Sean J. Morrison. 2013. "Tumour Heterogeneity and Cancer Cell Plasticity." *Nature* 501 (7467): 328–37. doi:10.1038/nature12624.
- Medina, P, and S Goodin. 2008. "Lapatinib: A Dual Inhibitor of Human Epidermal Growth Factor Receptor Tyrosine Kinases." *Clinical Therapeutics* 30 (8): 1426–47. doi:10.1016/j.clinthera.2008.08.008.
- Meerlo, Johan van, Gertjan J. L. Kaspers, and Jacqueline Cloos. 2011. "Cell Sensitivity Assays: The MTT Assay." In , 237–45. doi:10.1007/978-1-61779-080-5_20.
- Mi, Xiao, Meigeng Hu, Mingran Dong, Zhihong Yang, Xia Zhan, Xinyue Chang, Juan Lu, and Xi Chen. 2021. "Folic Acid Decorated Zeolitic Imidazolate Framework (ZIF-8) Loaded with Baicalin as a Nano-Drug Delivery System for Breast Cancer Therapy." *International Journal of Nanomedicine* Volume 16 (December): 8337–52. doi:10.2147/IJN.S340764.
- Mishra, B., Bhavesh B. Patel, and Sanjay Tiwari. 2010. "Colloidal Nanocarriers: A Review on Formulation Technology, Types and Applications toward Targeted Drug Delivery." *Nanomedicine: Nanotechnology, Biology and Medicine* 6 (1): 9–24. doi:10.1016/j.nano.2009.04.008.
- Mitchell, Michael J., Margaret M. Billingsley, Rebecca M. Haley, Marissa E. Wechsler, Nicholas A. Peppas, and Robert Langer. 2021. "Engineering Precision Nanoparticles

- for Drug Delivery.” *Nature Reviews Drug Discovery* 20 (2): 101–24. doi:10.1038/s41573-020-0090-8.
- Mo, Ran, and Zhen Gu. 2016. “Tumor Microenvironment and Intracellular Signal-Activated Nanomaterials for Anticancer Drug Delivery.” *Materials Today* 19 (5): 274–83. doi:10.1016/j.mattod.2015.11.025.
- Mobasser, Rezvan, Mahdi Karimi, Lingling Tian, Hossein Naderi-Manesh, and Seeram Ramakrishna. 2017. “Hydrophobic Lapatinib Encapsulated Dextran-Chitosan Nanoparticles Using a Toxic Solvent Free Method: Fabrication, Release Property & in Vitro Anti-Cancer Activity.” *Materials Science and Engineering: C* 74 (May): 413–21. doi:10.1016/j.msec.2016.12.027.
- Mohanraj, V J, and Y Chen. 2007. “Nanoparticles - A Review.” *Tropical Journal of Pharmaceutical Research* 5 (1). doi:10.4314/tjpr.v5i1.14634.
- Mosmann, Tim. 1983. “Rapid Colorimetric Assay for Cellular Growth and Survival: Application to Proliferation and Cytotoxicity Assays.” *Journal of Immunological Methods* 65 (1–2): 55–63. doi:10.1016/0022-1759(83)90303-4.
- Moura Ferraz, Leslie Raphael de, Alinne Élide Gonçalves Alves Tabosa, Débora Dolores Souza da Silva Nascimento, Aline Silva Ferreira, Victor de Albuquerque Wanderley Sales, José Yago Rodrigues Silva, Severino Alves Júnior, Larissa Araújo Rolim, Jorge José de Souza Pereira, and Pedro José Rolim-Neto. 2020. “ZIF-8 as a Promising Drug Delivery System for Benzimidazole: Development, Characterization, in Vitro Dialysis Release and Cytotoxicity.” *Scientific Reports* 10 (1): 16815. doi:10.1038/s41598-020-73848-w.
- Mura, Simona, Julien Nicolas, and Patrick Couvreur. 2013. “Stimuli-Responsive Nanocarriers for Drug Delivery.” *Nature Materials* 12 (11): 991–1003. doi:10.1038/nmat3776.
- Nattestad, Maria, Sara Goodwin, Karen Ng, Timour Baslan, Fritz J. Sedlazeck, Philipp Rescheneder, Tyler Garvin, et al. 2018. “Complex Rearrangements and Oncogene

- Amplifications Revealed by Long-Read DNA and RNA Sequencing of a Breast Cancer Cell Line.” *Genome Research* 28 (8): 1126–35. doi:10.1101/gr.231100.117.
- Nunzio, Maria Rosaria di, Valentina Agostoni, Boiko Cohen, Ruxandra Gref, and Abderrazzak Douhal. 2014. “A ‘Ship in a Bottle’ Strategy To Load a Hydrophilic Anticancer Drug in Porous Metal Organic Framework Nanoparticles: Efficient Encapsulation, Matrix Stabilization, and Photodelivery.” *Journal of Medicinal Chemistry* 57 (2): 411–20. doi:10.1021/jm4017202.
- Oh, Sojin, Sujeong Lee, Gihyun Lee, and Moonhyun Oh. 2023. “Enhanced Adsorption Capacity of ZIF-8 for Chemical Warfare Agent Simulants Caused by Its Morphology and Surface Charge.” *Scientific Reports* 13 (1): 12250. doi:10.1038/s41598-023-39507-6.
- Opdam, Frans L., Henk-Jan Guchelaar, Jos H. Beijnen, and Jan H.M. Schellens. 2012. “Lapatinib for Advanced or Metastatic Breast Cancer.” *The Oncologist* 17 (4): 536–42. doi:10.1634/theoncologist.2011-0461.
- Ospina, Raydonal, and Fernando Marmolejo-Ramos. 2019. “Performance of Some Estimators of Relative Variability.” *Frontiers in Applied Mathematics and Statistics* 5 (August). doi:10.3389/fams.2019.00043.
- Padhy, Lakshmi Charan, Chiaho Shih, Deborah Cowing, Robert Finkelstein, and Robert A. Weinberg. 1982. “Identification of a Phosphoprotein Specifically Induced by the Transforming DNA of Rat Neuroblastomas.” *Cell* 28 (4): 865–71. doi:10.1016/0092-8674(82)90065-4.
- Pan, Yichang, Yunyang Liu, Gaofeng Zeng, Lan Zhao, and Zhiping Lai. 2011. “Rapid Synthesis of Zeolitic Imidazolate Framework-8 (ZIF-8) Nanocrystals in an Aqueous System.” *Chemical Communications* 47 (7): 2071. doi:10.1039/c0cc05002d.
- Pang, Yichuan, Yao Fu, Chen Li, Zuoxing Wu, Weicheng Cao, Xi Hu, Xiaochen Sun, et al. 2020. “Metal–Organic Framework Nanoparticles for Ameliorating Breast Cancer-Associated Osteolysis.” *Nano Letters* 20 (2): 829–40.

doi:10.1021/acs.nanolett.9b02916.

- Papaioannou, Ligeri, Argiris Kolokithas-Ntoukas, Lito Karkaletsou, Stylianos Didaskalou, Maria D. Koffa, and Konstantinos Avgoustakis. 2023. “NIR-Responsive, Lapatinib-Loaded Gold Nanorods for Combined Photothermal and Pharmacological Treatment of HER2 Positive Breast Cancer: In Vitro Evaluation and Cell Studies.” *Journal of Drug Delivery Science and Technology* 82 (April): 104347. doi:10.1016/j.jddst.2023.104347.
- Park, K, S Han, H J Kim, J Kim, and E Shin. 2006. “HER2 Status in Pure Ductal Carcinoma in Situ and in the Intraductal and Invasive Components of Invasive Ductal Carcinoma Determined by Fluorescence in Situ Hybridization and Immunohistochemistry.” *Histopathology* 48 (6): 702–7. doi:10.1111/j.1365-2559.2006.02403.x.
- Park, Kyo Sung, Zheng Ni, Adrien P. Côté, Jae Yong Choi, Rudan Huang, Fernando J. Uribe-Romo, Hee K. Chae, Michael O’Keeffe, and Omar M. Yaghi. 2006. “Exceptional Chemical and Thermal Stability of Zeolitic Imidazolate Frameworks.” *Proceedings of the National Academy of Sciences* 103 (27): 10186–91. doi:10.1073/pnas.0602439103.
- Parveen, Suphiya, Ranjita Misra, and Sanjeeb K. Sahoo. 2012. “Nanoparticles: A Boon to Drug Delivery, Therapeutics, Diagnostics and Imaging.” *Nanomedicine: Nanotechnology, Biology and Medicine* 8 (2): 147–66. doi:10.1016/j.nano.2011.05.016.
- Paseta, Lorena, Grégory Potier, Steven Abbott, and Joaquín Coronas. 2015. “Using Hansen Solubility Parameters to Study the Encapsulation of Caffeine in MOFs.” *Organic & Biomolecular Chemistry* 13 (6): 1724–31. doi:10.1039/C4OB01898B.
- Patra, Jayanta Kumar, Gitishree Das, Leonardo Fernandes Fraceto, Estefania Vangelie Ramos Campos, Maria del Pilar Rodriguez-Torres, Laura Susana Acosta-Torres, Luis Armando Diaz-Torres, et al. 2018. “Nano Based Drug Delivery Systems: Recent Developments and Future Prospects.” *Journal of Nanobiotechnology* 16 (1):

71. doi:10.1186/s12951-018-0392-8.

Pitchika, Subrahmanyam, and Suwendu Kumar Sahoo. 2022. "Paclitaxel and Lapatinib Dual Loaded Chitosan-Coated PLGA Nanoparticles Enhance Cytotoxicity by Circumventing MDR1-Mediated Trastuzumab Resistance in HER2 Positive Breast Cancers: In-Vitro and in-Vivo Studies." *Journal of Drug Delivery Science and Technology* 73 (July): 103445. doi:10.1016/j.jddst.2022.103445.

Poon, Song, John R McPherson, Patrick Tan, Bin Teh, and Steven G Rozen. 2014. "Mutation Signatures of Carcinogen Exposure: Genome-Wide Detection and New Opportunities for Cancer Prevention." *Genome Medicine* 6 (3): 24. doi:10.1186/gm541.

Prabhu, Pavithra P., Prathvi, Tanvi V. Gujaraan, Chetan H. Mehta, Akhil Suresh, K.B. Koteswara, K Girish Pai, and Usha Y. Nayak. 2021. "Development of Lapatinib Nanosponges for Enhancing Bioavailability." *Journal of Drug Delivery Science and Technology* 65 (October): 102684. doi:10.1016/j.jddst.2021.102684.

Qiu, Jingwen, Xue Li, Mahsa Rezaei, Gilles Patriarche, Juan M. Casas-Solvas, Borja Moreira-Alvarez, Jose Manuel Costa Fernandez, et al. 2021. "Porous Nanoparticles with Engineered Shells Release Their Drug Cargo in Cancer Cells." *International Journal of Pharmaceutics* 610 (December): 121230. doi:10.1016/j.ijpharm.2021.121230.

"Quest Calculate™ PBS (Phosphate Buffered Saline) (1X, pH 7.4) Preparation and Recipe." n.d. *AAT Bioquest*. Accessed June 7, 2024. <https://www.aatbio.com/resources/buffer-preparations-and-recipes/pbs-phosphate-buffered-saline>.

Rami, J.M., C.D. Patel, C.M. Patel, and M.V. Patel. 2021. "Thermogravimetric Analysis (TGA) of Some Synthesized Metal Oxide Nanoparticles." *Materials Today: Proceedings* 43: 655–59. doi:10.1016/j.matpr.2020.12.554.

Rana, Punam, and Srikala S. Sridhar. 2012. "Efficacy and Tolerability of Lapatinib in the

- Management of Breast Cancer.” *Breast Cancer: Basic and Clinical Research* 6 (January): BCBCR.S6374. doi:10.4137/BCBCR.S6374.
- Ren, Hong, Lingyu Zhang, Jiping An, Tingting Wang, Lu Li, Xiaoyan Si, Liu He, Xiaotong Wu, Chungang Wang, and Zhongmin Su. 2014. “Polyacrylic Acid@zeolitic Imidazolate Framework-8 Nanoparticles with Ultrahigh Drug Loading Capability for pH-Sensitive Drug Release.” *Chem. Commun.* 50 (8): 1000–1002. doi:10.1039/C3CC47666A.
- Rizvi, Syed A.A., and Ayman M. Saleh. 2018. “Applications of Nanoparticle Systems in Drug Delivery Technology.” *Saudi Pharmaceutical Journal* 26 (1): 64–70. doi:10.1016/j.jsps.2017.10.012.
- Rusnak, D W, K Lackey, K Affleck, E R Wood, K J Alligood, N Rhodes, B R Keith, et al. 2001. “The Effects of the Novel, Reversible Epidermal Growth Factor Receptor/ErbB-2 Tyrosine Kinase Inhibitor, GW2016, on the Growth of Human Normal and Tumor-Derived Cell Lines in Vitro and in Vivo.” *Molecular Cancer Therapeutics* 1 (2): 85–94.
- Sanità, Gennaro, Barbara Carrese, and Annalisa Lamberti. 2020. “Nanoparticle Surface Functionalization: How to Improve Biocompatibility and Cellular Internalization.” *Frontiers in Molecular Biosciences* 7 (November). doi:10.3389/fmolb.2020.587012.
- Sava Gallis, Dorina F., Kimberly S. Butler, Jacob O. Agola, Charles J. Pearce, and Amber A. McBride. 2019. “Antibacterial Countermeasures via Metal–Organic Framework-Supported Sustained Therapeutic Release.” *ACS Applied Materials & Interfaces* 11 (8): 7782–91. doi:10.1021/acsami.8b21698.
- Schaeper, Ute, and Katja S. Grossmann. n.d. “Tyrosine Kinases.” In *Encyclopedic Reference of Genomics and Proteomics in Molecular Medicine*, 1951–59. Springer Berlin Heidelberg. doi:10.1007/3-540-29623-9_3120.
- Schechter, Alan L., David F. Stern, Lalitha Vaidyanathan, Stuart J. Decker, Jeffrey A. Drebin, Mark I. Greene, and Robert A. Weinberg. 1984. “The Neu Oncogene: An

- Erb-B-Related Gene Encoding a 185,000-Mr Tumour Antigen.” *Nature* 312 (5994): 513–16. doi:10.1038/312513a0.
- Schejn, Aleksandra, Lavinia Balan, Véronique Falk, Lionel Aranda, Ghouti Medjahdi, and Raphaël Schneider. 2014. “Controlling ZIF-8 Nano- and Microcrystal Formation and Reactivity through Zinc Salt Variations.” *CrystEngComm* 16 (21): 4493–4500. doi:10.1039/C3CE42485E.
- Schlam, Ilana, and Sandra M. Swain. 2021. “HER2-Positive Breast Cancer and Tyrosine Kinase Inhibitors: The Time Is Now.” *Npj Breast Cancer* 7 (1): 56. doi:10.1038/s41523-021-00265-1.
- Scimeca, Manuel, Simone Bischetti, Harpreet Kaur Lamsira, Rita Bonfiglio, and Elena Bonanno. 2018. “Energy Dispersive X-Ray (EDX) Microanalysis: A Powerful Tool in Biomedical Research and Diagnosis.” *European Journal of Histochemistry*, March. doi:10.4081/ejh.2018.2841.
- Semete, Boitumelo, Laetitia Booysen, Lonji Kalombo, Bathabile Ramalapa, Rose Hayeshi, and Hulda S. Swai. 2012. “Effects of Protein Binding on the Biodistribution of PEGylated PLGA Nanoparticles Post Oral Administration.” *International Journal of Pharmaceutics* 424 (1–2): 115–20. doi:10.1016/j.ijpharm.2011.12.043.
- Senapati, Sudipta, Arun Kumar Mahanta, Sunil Kumar, and Pralay Maiti. 2018. “Controlled Drug Delivery Vehicles for Cancer Treatment and Their Performance.” *Signal Transduction and Targeted Therapy* 3 (1): 7. doi:10.1038/s41392-017-0004-3.
- Shprakh, Zoya S., Yana A. Poskedova, and Galina V. Ramenskaya. 2022. “Modern Instrumental Methods for Qualitative and Quantitative Analysis of Lapatinib in Biological Fluids and Dosage Forms (Review).” *International Journal of Applied Pharmaceutics*, January, 7–12. doi:10.22159/ijap.2022v14i1.42992.
- Siddiqui, Sharmin, Faisal Ameen, Sayeed ur Rehman, Tarique Sarwar, and Mohammad

- Tabish. 2021. "Studying the Interaction of Drug/Ligand with Serum Albumin." *Journal of Molecular Liquids* 336 (August): 116200. doi:10.1016/j.molliq.2021.116200.
- Singh, Namita, Somayah Qutub, and Niveen M. Khashab. 2021. "Biocompatibility and Biodegradability of Metal Organic Frameworks for Biomedical Applications." *Journal of Materials Chemistry B* 9 (30): 5925–34. doi:10.1039/D1TB01044A.
- Singh, Ragini, Binayak Kumar, Ram Krishna Sahu, Soni Kumari, Chandan Bhogendra Jha, Nahar Singh, Rashi Mathur, and Suresh T. Hedau. 2021. "Development of a pH-Sensitive Functionalized Metal Organic Framework: *In Vitro* Study for Simultaneous Delivery of Doxorubicin and Cyclophosphamide in Breast Cancer." *RSC Advances* 11 (53): 33723–33. doi:10.1039/D1RA04591A.
- Sinha, Rajni, Gloria J. Kim, Shuming Nie, and Dong M. Shin. 2006. "Nanotechnology in Cancer Therapeutics: Bioconjugated Nanoparticles for Drug Delivery." *Molecular Cancer Therapeutics* 5 (8): 1909–17. doi:10.1158/1535-7163.MCT-06-0141.
- "SK-BR-3 [SKBR3] - HTB-30." n.d. *ATCC*. Accessed June 7, 2024. <https://www.atcc.org/products/htb-30#detailed-product-images>.
- Slamon, Dennis J., Brian Leyland-Jones, Steven Shak, Hank Fuchs, Virginia Paton, Alex Bajamonde, Thomas Fleming, et al. 2001. "Use of Chemotherapy plus a Monoclonal Antibody against HER2 for Metastatic Breast Cancer That Overexpresses HER2." *New England Journal of Medicine* 344 (11): 783–92. doi:10.1056/NEJM200103153441101.
- Soomro, Najaf Ali, Qiao Wu, Safdar Ali Amur, Hao Liang, Aziz Ur Rahman, Qeping Yuan, and Yun Wei. 2019. "Natural Drug Physcion Encapsulated Zeolitic Imidazolate Framework, and Their Application as Antimicrobial Agent." *Colloids and Surfaces B: Biointerfaces* 182 (October): 110364. doi:10.1016/j.colsurfb.2019.110364.
- Sun, Chun-Yi, Chao Qin, Xin-Long Wang, Guang-Sheng Yang, Kui-Zhan Shao, Ya-Qian

- Lan, Zhong-Min Su, Peng Huang, Chun-Gang Wang, and En-Bo Wang. 2012. “Zeolitic Imidazolate Framework-8 as Efficient pH-Sensitive Drug Delivery Vehicle.” *Dalton Transactions* 41 (23): 6906. doi:10.1039/c2dt30357d.
- Sung, Hyuna, Jacques Ferlay, Rebecca L. Siegel, Mathieu Laversanne, Isabelle Soerjomataram, Ahmedi Jemal, and Freddie Bray. 2021. “Global Cancer Statistics 2020: GLOBOCAN Estimates of Incidence and Mortality Worldwide for 36 Cancers in 185 Countries.” *CA: A Cancer Journal for Clinicians* 71 (3): 209–49. doi:10.3322/caac.21660.
- Swain, Sandra M., Mythili Shastry, and Erika Hamilton. 2023. “Targeting HER2-Positive Breast Cancer: Advances and Future Directions.” *Nature Reviews Drug Discovery* 22 (2): 101–26. doi:10.1038/s41573-022-00579-0.
- Tanaka, Shunsuke, Koji Kida, Takuya Nagaoka, Takehiro Ota, and Yoshikazu Miyake. 2013. “Mechanochemical Dry Conversion of Zinc Oxide to Zeolitic Imidazolate Framework.” *Chemical Communications* 49 (72): 7884. doi:10.1039/c3cc43028f.
- Taskar, Kunal S., Vinay Rudraraju, Rajendar K. Mittapalli, Ramakrishna Samala, Helen R. Thorsheim, Julie Lockman, Brunilde Gril, et al. 2012. “Lapatinib Distribution in HER2 Overexpressing Experimental Brain Metastases of Breast Cancer.” *Pharmaceutical Research* 29 (3): 770–81. doi:10.1007/s11095-011-0601-8.
- Tevaarwerk, Amye J., and Jill M. Kolesar. 2009. “Lapatinib: A Small-Molecule Inhibitor of Epidermal Growth Factor Receptor and Human Epidermal Growth Factor Receptor—2 Tyrosine Kinases Used in the Treatment of Breast Cancer.” *Clinical Therapeutics* 31 (January): 2332–48. doi:10.1016/j.clinthera.2009.11.029.
- Tran, Vy Anh, Van Thuan Le, Van Dat Doan, and Giang N. L. Vo. 2023. “Utilization of Functionalized Metal–Organic Framework Nanoparticle as Targeted Drug Delivery System for Cancer Therapy.” *Pharmaceutics* 15 (3): 931. doi:10.3390/pharmaceutics15030931.
- Vasconcelos, Iane B., Teresinha G. da Silva, Gardenia C. G. Militão, Thereza A. Soares,

- Nailton M. Rodrigues, Marcelo O. Rodrigues, Nivan B. da Costa, Ricardo O. Freire, and Severino A. Junior. 2012. "Cytotoxicity and Slow Release of the Anti-Cancer Drug Doxorubicin from ZIF-8." *RSC Advances* 2 (25): 9437. doi:10.1039/c2ra21087h.
- Vasić, Katja, Željko Knez, Elizaveta A. Konstantinova, Alexander I. Kokorin, Sašo Gyergyek, and Maja Leitgeb. 2020. "Structural and Magnetic Characteristics of Carboxymethyl Dextran Coated Magnetic Nanoparticles: From Characterization to Immobilization Application." *Reactive and Functional Polymers* 148 (March): 104481. doi:10.1016/j.reactfunctpolym.2020.104481.
- Vasir, Jaspreet K., and Vinod Labhsetwar. 2005. "Targeted Drug Delivery in Cancer Therapy." *Technology in Cancer Research & Treatment* 4 (4): 363–74. doi:10.1177/153303460500400405.
- Velásquez-Hernández, Miriam de J., Mercedes Linares-Moreau, Efwita Astria, Francesco Carraro, Mram Z. Alyami, Niveen M. Khashab, Christopher J. Sumby, Christian J. Doonan, and Paolo Falcaro. 2021. "Towards Applications of Bioentities@MOFs in Biomedicine." *Coordination Chemistry Reviews* 429 (February): 213651. doi:10.1016/j.ccr.2020.213651.
- Velásquez-Hernández, Miriam de J., Raffaele Ricco, Francesco Carraro, F. Ted Limpoco, Mercedes Linares-Moreau, Erich Leitner, Helmar Wiltsche, et al. 2019. "Degradation of ZIF-8 in Phosphate Buffered Saline Media." *CrystEngComm* 21 (31): 4538–44. doi:10.1039/C9CE00757A.
- Velázquez-Delgado, Elih M., and Jeanne A. Hardy. 2012. "Zinc-Mediated Allosteric Inhibition of Caspase-6." *Journal of Biological Chemistry* 287 (43): 36000–11. doi:10.1074/jbc.M112.397752.
- Wan, Xu, Xiaoyao Zheng, Xiaoyin Pang, Zhiqing Pang, Jingjing Zhao, Zheming Zhang, Tao Jiang, Wei Xu, Qizhi Zhang, and Xinguo Jiang. 2016. "Lapatinib-Loaded Human Serum Albumin Nanoparticles for the Prevention and Treatment of Triple-Negative Breast Cancer Metastasis to the Brain." *Oncotarget* 7 (23): 34038–51.

doi:10.18632/oncotarget.8697.

Wang, Miao Chen, Fan Li, Tingwei Lu, Ruoyi Wu, Shengbing Yang, and Wantao Chen. 2022. “Photodynamic and Ferroptotic Ce6@ZIF-8@ssPDA for Head and Neck Cancer Treatment.” *Materials & Design* 224 (December): 111403. doi:10.1016/j.matdes.2022.111403.

Wang, Na, Yifan Li, Fei He, Susu Liu, Yuan Liu, Jinting Peng, Jiahui Liu, Changyuan Yu, and Shihui Wang. 2022. “Assembly of Celastrol to Zeolitic Imidazolate Framework-8 by Coordination as a Novel Drug Delivery Strategy for Cancer Therapy.” *Pharmaceuticals* 15 (9): 1076. doi:10.3390/ph15091076.

Wang, Qiuxiang, Yue Sun, Shangfei Li, Pingping Zhang, and Qingqiang Yao. 2020. “Synthesis and Modification of ZIF-8 and Its Application in Drug Delivery and Tumor Therapy.” *RSC Advances* 10 (62): 37600–620. doi:10.1039/D0RA07950B.

Williams, Ryan M., Shi Chen, Rachel E. Langenbacher, Thomas V. Galassi, Jackson D. Harvey, Prakrit V. Jena, Januka Budhathoki-Uprety, Minkui Luo, and Daniel A. Heller. 2021. “Harnessing Nanotechnology to Expand the Toolbox of Chemical Biology.” *Nature Chemical Biology* 17 (2): 129–37. doi:10.1038/s41589-020-00690-6.

Xia, Wenle, Robert J Mullin, Barry R Keith, Lei-Hua Liu, Hong Ma, David W Rusnak, Gary Owens, Krystal J Alligood, and Neil L Spector. 2002. “Anti-Tumor Activity of GW572016: A Dual Tyrosine Kinase Inhibitor Blocks EGF Activation of EGFR/ErbB2 and Downstream Erk1/2 and AKT Pathways.” *Oncogene* 21 (41): 6255–63. doi:10.1038/sj.onc.1205794.

Xie, Hongxin, Xinyu Liu, Zhengrong Huang, Liexi Xu, Rui Bai, Fajian He, Mengqin Wang, et al. 2022. “Nanoscale Zeolitic Imidazolate Framework (ZIF)–8 in Cancer Theranostics: Current Challenges and Prospects.” *Cancers* 14 (16): 3935. doi:10.3390/cancers14163935.

Xu, Dandan, Yongqiang You, Fanyu Zeng, Yong Wang, Chunyan Liang, Huanhuan

- Feng, and Xing Ma. 2018. "Disassembly of Hydrophobic Photosensitizer by Biodegradable Zeolitic Imidazolate Framework-8 for Photodynamic Cancer Therapy." *ACS Applied Materials & Interfaces* 10 (18): 15517–23. doi:10.1021/acsami.8b03831.
- Xuhong, Jun-Cheng, Xiao-Wei Qi, Yi Zhang, and Jun Jiang. 2019. "Mechanism, Safety and Efficacy of Three Tyrosine Kinase Inhibitors Lapatinib, Neratinib and Pyrotinib in HER2-Positive Breast Cancer." *American Journal of Cancer Research* 9 (10): 2103–19.
- Yallapu, Murali M., Neeraj Chauhan, Shadi F. Othman, Vahid Khalilzad-Sharghi, Mara C. Ebeling, Sheema Khan, Meena Jaggi, and Subhash C. Chauhan. 2015. "Implications of Protein Corona on Physico-Chemical and Biological Properties of Magnetic Nanoparticles." *Biomaterials* 46 (April): 1–12. doi:10.1016/j.biomaterials.2014.12.045.
- Yang, Peipei, Jia Tao, Fengfeng Chen, Yuying Chen, Jiaqi He, Kui Shen, Peng Zhao, and Yingwei Li. 2021. "Multienzyme-Mimic Ultrafine Alloyed Nanoparticles in Metal Organic Frameworks for Enhanced Chemodynamic Therapy." *Small* 17 (7): 2005865. doi:10.1002/sml.202005865.
- Yao, Jianfeng, Ming He, and Huanting Wang. 2015. "Strategies for Controlling Crystal Structure and Reducing Usage of Organic Ligand and Solvents in the Synthesis of Zeolitic Imidazolate Frameworks." *CrystEngComm* 17 (27): 4970–76. doi:10.1039/C5CE00663E.
- Yersal, Ozlem. 2014. "Biological Subtypes of Breast Cancer: Prognostic and Therapeutic Implications." *World Journal of Clinical Oncology* 5 (3): 412. doi:10.5306/wjco.v5.i3.412.
- Zhang, Cheng, Xuerui Wang, Miao Hou, Xiaoyang Li, Xiaoling Wu, and Jun Ge. 2017. "Immobilization on Metal–Organic Framework Engenders High Sensitivity for Enzymatic Electrochemical Detection." *ACS Applied Materials & Interfaces* 9 (16): 13831–36. doi:10.1021/acsami.7b02803.

- Zhang, Huijie, Wei Chen, Kai Gong, and Jinghua Chen. 2017. "Nanoscale Zeolitic Imidazolate Framework-8 as Efficient Vehicles for Enhanced Delivery of CpG Oligodeoxynucleotides." *ACS Applied Materials & Interfaces* 9 (37): 31519–25. doi:10.1021/acsami.7b09583.
- Zhang, Huiyuan, Qian Li, Ruiling Liu, Xinke Zhang, Zhonghao Li, and Yuxia Luan. 2018. "A Versatile Prodrug Strategy to In Situ Encapsulate Drugs in MOF Nanocarriers: A Case of Cytarabine-IR820 Prodrug Encapsulated ZIF-8 toward Chemo-Photothermal Therapy." *Advanced Functional Materials* 28 (35): 1802830. doi:10.1002/adfm.201802830.
- Zhang, Li, Gerile Oudeng, Feiqiu Wen, and Guangfu Liao. 2022. "Recent Advances in Near-Infrared-II Hollow Nanoplatfoms for Photothermal-Based Cancer Treatment." *Biomaterials Research* 26 (1): 61. doi:10.1186/s40824-022-00308-z.
- Zhang, Yongyong, Ying Jia, and Li'an Hou. 2018. "Synthesis of Zeolitic Imidazolate Framework-8 on Polyester Fiber for PM_{2.5} Removal." *RSC Advances* 8 (55): 31471–77. doi:10.1039/C8RA06414H.
- Zheng, Haoquan, Yuning Zhang, Leifeng Liu, Wei Wan, Peng Guo, Andreas M. Nyström, and Xiaodong Zou. 2016. "One-Pot Synthesis of Metal–Organic Frameworks with Encapsulated Target Molecules and Their Applications for Controlled Drug Delivery." *Journal of the American Chemical Society* 138 (3): 962–68. doi:10.1021/jacs.5b11720.
- Zheng, Min, Shi Liu, Xingang Guan, and Zhigang Xie. 2015. "One-Step Synthesis of Nanoscale Zeolitic Imidazolate Frameworks with High Curcumin Loading for Treatment of Cervical Cancer." *ACS Applied Materials & Interfaces* 7 (40): 22181–87. doi:10.1021/acsami.5b04315.
- Zhuang, Jia, Chun-Hong Kuo, Lien-Yang Chou, De-Yu Liu, Eranthie Weerapana, and Chia-Kuang Tsung. 2014. "Optimized Metal–Organic-Framework Nanospheres for Drug Delivery: Evaluation of Small-Molecule Encapsulation." *ACS Nano* 8 (3): 2812–19. doi:10.1021/nn406590q.

APPENDIX A

SOLUTIONS

PBS Preparation

Since it is not toxic to cells, PBS, which is used for washing cells and dilutions, is an isotonic buffer that can mimic the pH, osmolarity and ion concentrations of the human body.

To prepare 1X PBS, 8 g of sodium chloride (NaCl, 58.44 g/mol, Sigma Aldrich), 0.2 g of potassium chloride (KCl, 74.55 g/mol, Sigma Aldrich), 1.44 g of sodium phosphate dibasic (Na₂HPO₄, 141.96 g/mol, Sigma Aldrich) and 0.245 g of potassium phosphate monobasic (KH₂PO₄, 136.09 g/mol, Sigma Aldrich) were added to 800 mL of distilled water in a glass container. Distilled water was added until the volume was 1 liter (“Quest Calculate™ PBS (Phosphate Buffered Saline) (1X, pH 7.4) Preparation and Recipe,” n.d.) . The solution was adjusted to pH 7.4 using a pH meter (Hanna Edge pH Meter). Hydrochloric acid (HCl, Merck) was used to adjust PBS to pH 5.5. The solution was adjusted to pH 5.5 using a pH meter. The prepared solutions were autoclaved for sterilization and stored at 4°C.

MTT Preparation

To prepare the solution at a concentration of 5 mg/mL, 5 mg of MTT powder was weighed and dissolved in 1 mL of sterile PBS (pH 7.4). It was mixed by sonication. The solution was sterilized by filtering using a 0.22 µm sterile filter. It was divided into ependorfs to be used in the cell viability experiment and stored at -20°C.

APPENDIX B

ENCAPSULATION EFFICIENCY AND DRUG LOADING

According to the calibration curve of lapatinib, the equation is:

$$y = 0.0226x - 0.0459$$

The calculation of supernatant concentration: 165.48 $\mu\text{g/mL}$

The concentration of the prepared solution: 600 $\mu\text{g/mL}$

Amount of lapatinib encapsulated: 600 $\mu\text{g/mL}$ – 165.48 $\mu\text{g/mL}$ = 434.52 $\mu\text{g/mL}$

Thus, LAP@ZIF-8 was calculated to contain 434.52 μg of LAP, and the encapsulation efficiency can be calculated as:

$$\text{EE \%} = \frac{434.52 \mu\text{g/mL}}{600 \mu\text{g/mL}} \times 100 \% = 72.42 \%$$

Considering 3 mg of lapatinib in reaction medium and 72.42 %, the amount of encapsulated lapatinib in mg and the drug loading calculated as:

$$\text{Amount of lapatinib encapsulated (mg)} = \frac{3 \text{ mg} \times 72.42}{100} = 2.173 \text{ mg}$$

$$\text{DL \%} = \frac{2.173 \mu\text{g/mL}}{33.18 \mu\text{g/mL}} \times 100 \% = 6.55 \%$$